



**University of  
Leicester**

**System L amino acid transporters & their relation to  
cellular energy status & glucose**

Thesis submitted for the degree of

**Doctor of Philosophy**

**University of Leicester**

by

**Violeta Diez Beltran**

Department of Infection, Immunity and Inflammation

College of Medicine, Biological Sciences and Psychology

School of Medicine

University of Leicester

2017

## Abstract

---

### System L amino acid transporters & their relation to cellular energy status & glucose

Violeta Diez Beltran

Intracellular availability of the amino acid L-leucine in pancreatic  $\beta$  cells is thought to regulate cell growth and modulate D-glucose-induced insulin secretion (Data published in Cheng et al. 2016). System L amino acid transporters (LATs) control transport of L-leucine across the plasma membrane and may therefore influence intracellular L-leucine concentration. The aim of this project was to test the hypothesis that D-glucose supply to the cultured rat  $\beta$  cell line INS1E regulates leucine transport by acting on LATs.

Incubation of cells in medium containing 0 versus 5 mM (control) D-glucose for 6 hours increased L-[ $^3$ H]-leucine transport influx by 70% and increased intracellular L-leucine concentration by 150% in INS1E. In contrast, very variable responses were seen on exposure of INS1E to 25 mM D-glucose. Treating INS1E with the AMP-activated kinase (AMPK) agonist AICAR also increased L-[ $^3$ H]-leucine influx by 70% suggesting that D-glucose deprivation regulates transport by lowering energy status which then activates the energy status sensor AMPK. D-glucose deprivation increased mRNA expression for the LAT1 (SLC7A5) isoform of LAT transporter about 3.5-fold when assessed by RT-Q-PCR. The effect showed very variable magnitude and was not observed for LAT2 (SLC7A8) or LAT4 (SLC43A2) mRNA, which were also strongly expressed in INS1E. In spite of strong LAT2/4 expression, siRNA silencing of LAT1 mRNA by 85% was sufficient to decrease basal L-[ $^3$ H]-leucine influx by 35%. However, blockade of the LAT1 mRNA increase on D-glucose deprivation by treating with transcription inhibitor actinomycin-D failed to block the accompanying increase in L-[ $^3$ H]-leucine influx, suggesting that activation of LAT transporter proteins by low energy status was largely occurring through an additional non-transcriptional mechanism.

To test this, a human LAT1-eGFP-tagged cDNA construct completely lacking the normal LAT1 promoter sequence was transfected into HEK293A cells and successfully expressed eGFP fluorescence. Even though wild-type HEK293A showed high basal L-[ $^3$ H]-leucine influx and no stimulation of this flux by AICAR, and LAT1-eGFP transfection alone failed to give statistically significant stimulation of L-[ $^3$ H]-leucine influx, a significant 24% increase in transport was obtained in cells subjected to combined LAT1-eGFP transfection + AICAR. These results suggest that D-glucose starvation and AMPK activation in INS1E cells lead to a previously undescribed stimulation of L-leucine transport, which is similar in magnitude to that previously described for glucose transport in response to AMPK activation in muscle.

It is concluded that declining energy status sensed through AMPK activates LAT1 (and maybe other isoforms of LAT L-leucine transporters), possibly through an AMPK-dependent translocation of LAT proteins between sub-cellular pools analogous to that previously described for GLUT monosaccharide transporters in muscle.

## **Acknowledgements**

---

I would like to express my special appreciation and thanks to my supervisors Dr Alan Bevington and Dr Karen Molyneux who provided me the opportunity to join the renal group. For their keen supervision, guidance, support and for being a tremendous mentors for me. Their advice has been priceless, and without their precious support it would not be possible to successfully finish my research.

I would also like to thank my progress review panel members, Dr Cordula Stover and Dr Gary Willars; and Dr Terry Herbert who offered me the opportunity to join his team. And to Cheng Qi, Ghazi Alghanim and Abdusalam Elfowiris for the help during my first year of PhD.

I also want to acknowledge with sincere thanks all my colleagues in the renal group for their help and support, particularly Jeremy Brown, I greatly appreciate the time and patience he committed to help me. I am also grateful to Dr Emma Watson, Dr Izabella Pawluczyk, Dr Nima Abbasian, Ziyad Aldosari, Abdullah Alruwaili, Doug Gould, Tom O'Sullivan, Dina Nilasari, and all the renal group members. I also thank Antoine Maresca for the assistance during his MSc research project. I would like to express my sincere gratitude to Safia Blbas for all the support and encouragement. I extend my sincere thanks to Patricia Higgins for her support and for showing me beautiful places around Leicestershire.

A very special gratitude goes to Caroline Berry for helping me to start this long journey and to my Colombian family in Leicester Luis Alejandro Barbosa, Manuel Franco, and Guillermo Rangel. I would especially like to thank Ana Maria Pacheco and Karol Valderrama for all the unforgettable moments we spent together and the invaluable company they were. Also I want to thank all my friends from Colombia that I met during these years in Leicester that encourage me to strive towards my goals.

I am deeply indebted to my beloved mother who deserves all the credit for what I am today, her unwavering love and endless support are very important to me. Her prayer for me was what sustained me this far. I am also grateful to my father, my brother Mateo, my stepmother Clara, all my family in Colombia: aunts, uncles, cousins, my stepfather Dario and all of the friends who supported me during this long way. Words cannot express how grateful I am to my two grandmothers Blanca and Gilma that are now in their heavenly home and are my truly angels of grace. Finally, I am indebted to my fiancé Juan Camilo for being my inspiration, my support in the moments when there was no one to answer my queries. Thanks for the endless patience and for all the sacrifices made on my behalf. We have been together all the way through this extended journey hoping to have brighter future.

**Thanks for all your encouragement!**

## Table of contents

---

<b>Abstract</b> .....	i
<b>Acknowledgements</b> .....	ii
<b>Table of contents</b> .....	iii
<b>List of tables</b> .....	viii
<b>List of Figures</b> .....	ix
<b>List of abbreviations</b> .....	xi
<b>Chapter 1. General Introduction</b> .....	1
1.1. Introduction to diabetes .....	1
1.1.1 Type 1 diabetes (T1DM).....	2
1.1.2 Type 2 diabetes (T2DM).....	3
1.1.3 Clinical complications arising from diabetes .....	5
1.1.4 $\beta$ cell failure in T2DM and glucotoxicity .....	6
1.2. Pancreatic $\beta$ cells synthesize insulin to control blood glucose concentrations .....	8
1.2.1. The endocrine pancreas .....	9
1.2.2. Insulin .....	12
1.3. The role of leucine as essential amino acid in $\beta$ cell biology .....	13
1.4. The role of mTOR in the regulation of pancreatic $\beta$ cell mass and function .....	16
1.5. Upstream regulators of mTORC1 .....	17
1.6. Energy status, AMPK and mTORC1 .....	19
1.7. Downstream targets of mTORC1.....	21
1.8. Amino acid regulation of mTORC1.....	22
1.9. Amino acid transporters.....	24
1.10. SLC gene families.....	26
1.10.1. System L transporters .....	26
1.10.2. System $y^+$ L transporters .....	28
1.10.3. System $b^{0,+}$ transporters .....	29
1.10.4. Coupling between System L and active transporters .....	32
1.11. Physiological responses of System L amino acid transporters.....	33

1.12. Regulation of LAT1 expression in response to D-glucose .....	35
1.13. Hypothesis and aims of this study .....	36
<b>Chapter 2. Methods .....</b>	<b>38</b>
2.1. Culture.....	38
2.2. Isolation of rat islets of Langerhans .....	39
2.3. Culture of rat islets of Langerhans .....	40
2.4. LAT1 and CD98 cDNA construct design.....	40
2.5. Bacterial (competent cell) transformation.....	42
2.6. Transfection of HEK293A cells by calcium phosphate precipitation.....	44
2.7. Transport Assays.....	44
2.8. Folin protein assay .....	46
2.9. Cell viability test (MTT) .....	46
2.10. SDS-Polyacrylamide Gel Electrophoresis and Western Blot Analysis .....	46
2.11. Protein Assay (BioRad DC™ Protein Assay) .....	47
2.12. SDS-Polyacrylamide Gel Electrophoresis and Western Blot Analysis .....	47
2.13. Lipofectamine transfection for siRNA .....	48
2.14. RNA isolation for qRT-PCR.....	50
2.15. cDNA synthesis.....	50
2.16. Quantitative real-time polymerase chain reaction (qRT-PCR) .....	51
2.17. High-performance liquid chromatography (HPLC Analysis).....	52
2.18. Statistical Analysis .....	52
<b>Chapter 3. Characterization of L-leucine transport &amp; signalling in <math>\beta</math> cells.....</b>	<b>54</b>
3.1. Introduction .....	54
3.2. Results .....	55
3.1.1 BCH inhibits leucine-stimulated mTORC1 activation in rat islets of Langerhans and INS1E cells. ....	55
3.1.2 Blocking $\text{Ca}^{2+}$ channels, which are relevant for insulin secretion, has no impact on the effect of L-leucine on mTORC1 activation in INS1E cells.....	58
3.1.3 L-[ $^3\text{H}$ ]-leucine uptake increases in a concentration-dependent and saturable manner in INS1E cells .....	59
3.1.4 L-[ $^3\text{H}$ ]-leucine transport assay in INS1E cells and rat islets of Langerhans..	61

3.1.5	Expression of system L amino acid transporter (LAT) mRNAs in INS1E cells .....	63
3.3.	Discussion.....	65
3.3.1.	The role of L-leucine availability in the activation of mTORC1 in pancreatic β cells .....	65
3.3.2.	The uptake of L-leucine by LATs.....	66
3.3.3.	LAT1 expression in primary β cells.....	67
3.4.	Conclusion.....	68
<b>Chapter 4. Characterization of L-leucine transport &amp; signalling in β cells .....</b>		<b>69</b>
4.1.	Introduction .....	69
4.2.	Results.....	70
4.2.1.	The effect of aglycaemia and hyperglycaemia in the L-[ <sup>3</sup> H]-leucine transport in INS1E cells.....	70
4.2.2.	Blocking Ca <sup>2+</sup> channels with nifedipine does not affect the action of high D- glucose on L-[ <sup>3</sup> H]-leucine transport.....	73
4.2.3.	AMPK activation by AICAR and the absence of D-glucose activate L-[ <sup>3</sup> H]- leucine transport in INS1E cells .....	75
4.2.4.	D-glucose deprivation and AICAR effects on System A amino acid transport in INS1E cells and L6 myoblasts .....	78
4.2.5.	The effect of D-glucose starvation on AMPK phosphorylation in INS1E cells .....	80
4.2.6.	The effect of 4 hours of D-glucose starvation or the activation of AMPK with AICAR on LAT1-4 mRNA expression on INS1E cells .....	82
4.2.7.	The effect of D-glucose starvation or the activation of AMPK with AICAR on LAT1-4 mRNA expression in INS1E cells at 6 hours .....	85
4.2.8.	The effect of 4 hours of D-glucose starvation or the activation of AMPK with AICAR on LAT1 and LAT2 mRNA expression in mouse MIN6 cells.....	87
4.2.9.	The effect of D-glucose starvation on L-[ <sup>3</sup> H]-leucine transport is not affected by blocking transcription with actinomycin-D in INS1E cells .....	89
4.2.10.	Confirming blockade of transcription with actinomycin-D .....	90
4.2.11.	Effect of siRNA Silencing of LAT1 in Rat INS1E cells on expression of system	

L amino acid transporters (LATs).....	94
4.2.12. Effect of siRNA Silencing of LAT1 in Rat INS1E cells on L-[ <sup>3</sup> H]-leucine transport.....	96
4.2.13. Effect of D-glucose withdrawal in the absence and presence of AICAR on intracellular L-leucine concentration.....	98
4.3. Discussion.....	100
4.3.1. D-glucose starvation & AICAR activate System L-[ <sup>3</sup> H]-leucine transport in INS1E cells.....	100
4.3.2. Effects of D-glucose starvation and AICAR on L-leucine transport are not accompanied by stimulation of System A.....	102
4.3.3. The LAT1 transport activation under D-glucose removal is accompanied by increased expression of LAT1 mRNA but not the mRNA for other LATs....	103
4.3.4. Blockade of transcription with actinomycin-D may slightly blunt the stimulated L-[ <sup>3</sup> H]-leucine transport effect of D-glucose starvation but does not abolish it.....	104
4.3.5. siRNA silencing can suppress LAT1 mRNA expression in INS1E, and this can blunt basal (unstimulated) L-[ <sup>3</sup> H]-leucine transport .....	105
4.3.6. Intracellular concentrations of L-leucine increased under D-glucose deprivation.....	106
4.4. Conclusion.....	107
<b>Chapter 5. Cloning &amp; expression of a System L transporter in HEK293A cells.....</b>	<b>108</b>
5.1. Introduction .....	108
5.2. Results.....	109
5.2.1. Efficiency of transfection in HEK293A cells .....	109
5.2.2. The effect of LAT1 or CD98 cDNA constructs on L-[ <sup>3</sup> H]-leucine transport in HEK293A cells .....	110
5.2.3. Effect of AICAR on HEK293A cells overexpressing LAT1-eGFP.....	113
5.2.4. AICAR effect on the localisation of LAT1-eGFP in HEK293A cells .....	115
5.2.5. Analysis of the effect of AICAR on the localisation of LAT1-eGFP fluorescence .....	117
5.3. Discussion.....	118

5.4. Conclusion .....	120
<b>Chapter 6. General Discussion &amp; Future Work .....</b>	<b>121</b>
6.1. Biological significance of these findings .....	121
6.2. Studies of LAT1-eGFP location do not support a simple two-pool model of LAT1 distribution.....	122
6.3. Does LAT1 up-regulation in energy-depleted cells drive influx or efflux of L- leucine from the cell?.....	125
6.4. Future experiments to confirm and extend these findings .....	127
6.5. Relevance of these findings to $\beta$ cell function and glucotoxicity in T2DM .....	129
6.6. Possible relevance to cancer .....	131
6.7. Conclusion.....	131
<b>References.....</b>	<b>132</b>
<b>Appendix 1. DNA sequencing confirmation of the LAT1-eGFP cDNA construct ....</b>	<b>145</b>
<b>Appendix 2. DMEM preparation without L-leucine, L-glutamine and D-glucose..</b>	<b>146</b>
<b>Appendix 3. Lysis buffer for preparation of cell lysates for Western blotting .....</b>	<b>147</b>

## List of tables

---

Table 1.1. Cell types in the endocrine pancreas.....	10
Table 1.2. SLC gene families encoding proteins that transport L-leucine in humans.....	31
Table 2.1. Details of the pLEICS-29 and pLEICS-49 vectors shown in Figure 2.1 .....	42
Table 2.2. List of antibodies .....	48
Table 2.3. Silencing siRNA used for transfections.....	49
Table 2.4. Reagents used for Silencing siRNA transfections.....	49
Table 2.5. Reagents used for cDNA synthesis.....	51
Table 2.6. PCR primers Sequences.....	51
Table 2.7. PCR primers Sequences.....	51
Table 2.8. Thermal cycling for PCR reaction .....	52

## List of Figures

---

Figure 1.1. The role of environment and genetics in the development of T2DM.....	3
Figure 1.2. Long-term complications of T2DM.....	6
Figure 1.3. Islet $\beta$ cell failure and the natural history of T2DM.....	7
Figure 1.4. Anatomy of the pancreas .....	9
Figure 1.5. Pancreatic islet endocrine tissue surrounded by exocrine acini .....	10
Figure 1.6. Insulin structure.....	13
Figure 1.7. Composition of mTORC1 and mTORC2 .....	17
Figure 1.8. mTORC1 is activated by growth factors and amino acids. ....	19
Figure 1.9. AMPK pathway .....	21
Figure 1.10. Activation of mTORC1 via recruitment of L-leucine transporter to lysosomes .....	24
Figure 1.11. Model of the human 4F2hc/LAT1 heterodimer.....	27
Figure 1.12. Coupled SNAT2/LAT1 system .....	33
Figure 2.1. Plasmids with 3xFlag His4 (pLEICS-49) and EGFP (pLEICS-29).....	42
Figure 3.1. BCH inhibits leucine-stimulated mTORC1 activation in rat islets of Langerhans and INS1E cells.....	57
Figure 3.2. Effect of $Ca^{2+}$ channel blocker (nifedipine) on mTORC1 signalling in INS1E cells. ....	58
Figure 3.3. L-leucine transport dose-response experiment on INS1E cells.....	60
Figure 3.4. L-leucine transport analysis in INS1E cells and rat islets of Langerhans. ....	61
Figure 3.5. Expression of system L amino acid transporters (LATs) in INS1E cells.....	64
Figure 4.1. Effect of D-glucose concentration on L-[ $^3H$ ]-leucine transport in INS1E and HEK293A cells after 3 to 6 hours incubation .....	72
Figure 4.2. INS1E D-glucose/nifedipine effect on L-[ $^3H$ ]-leucine transport after 6 hours of incubation.....	74
Figure 4.3. INS1E, HEK293 and L6 cells D-glucose/AICAR effect on L-[ $^3H$ ]-leucine transport at 6 hours incubation.....	76
Figure 4.4. Effect of D-glucose and AICAR in INS1E and L6 myoblasts on $^{14}C$ -MeIAB (System A) transport.....	79
Figure 4.5. Effect of D-glucose starvation on Thr172 AMPK phosphorylation in INS1E cells	

.....	80
Figure 4.6. INS1E D-glucose/AICAR effect on relative expression of system L amino acid transporters (LATs).....	84
Figure 4.7. INS1E D-glucose/AICAR effect on relative expression of system L amino acid transport (LATs).....	86
Figure 4.8. MIN6 D-glucose/AICAR effect on relative expression of system L amino acid transporters (LATs).....	88
Figure 4.9. INS1E D-glucose/actinomycin-D effect on L-[ <sup>3</sup> H]-leucine transport after 6 hours incubation.....	89
Figure 4.10. INS1E D-glucose/actinomycin-D effect on LAT mRNA expression after 6 hours incubation.....	92
Figure 4.11. INS1E LAT1 siRNA effect on relative expression of system L amino acid transporters (LATs).....	95
Figure 4.12. INS1E LAT1 siRNA effect on L-[ <sup>3</sup> H]-leucine transport. ....	97
Figure 4.13. Effect of D-glucose availability and the presence of AICAR on intracellular L-leucine concentration in INS1E cells.....	99
Figure 5.1. Efficiency of transfection in HEK293A cells .....	109
Figure 5.2. Effect of transfection with LAT1-eGFP and CD98-FLAG on L-[ <sup>3</sup> H]-leucine transport and cell viability in HEK293A cells. ....	112
Figure 5.3. Effect of AICAR on L-[ <sup>3</sup> H]-leucine transport in HEK293A cells overexpressing LAT1-eGFP. ....	114
Figure 5.4. Effect of AICAR on fluorescence images of HEK293A cells overexpressing LAT1-eGFP .....	116
Figure 5.5. Analysis of the effect of AICAR on the localisation of LAT1-eGFP fluorescence in HEK293A cells. ....	117
Figure 6.1. Distribution of LAT1(SLC7A5)/4F2hc(SLC3A2) into 3 pools .....	125

## List of abbreviations

---

<i>4EBP</i>	Eukaryotic initiation factor 4E-binding protein
ADP	Adenosine diphosphate
AMP	Adenosine monophosphate
AMPK	AMP activated protein kinase
ATP	Adenosine triphosphate
BCAA	Branched-chain amino acid
BCH	2-aminobicyclo (2,2,1) heptane-2-carboxylic acid
BCKADH	Branched chain keto acid dehydrogenase
DEPTOR	DEP domain-containing mTOR-interacting protein
DMEM	Dulbecco's modified Eagle's medium
FFA	Free fatty acid
GAP	GTPase-activating protein
GDP	Guanosine diphosphate
GLUT2 or 4	Glucose transporter 2 or 4
GRP58	58kDa glucose-regulated protein
GSK3 $\beta$	Glycogen synthase kinase 3 $\beta$
GTP	Guanosine triphosphate
INS1E	Rat insulinoma cell line 1E
IPMK	Inositol polyphosphate multikinase
IRS1	Insulin receptor substrate protein 1
KRB	Krebs' Ringer bicarbonate buffer
LAT	L type amino acid transporter
MAP4K3	MAPK (mitogen-activated protein kinase) kinase kinase kinase kinase 3
mLST8	Mammalian orthologue of lethal with SEC13 protein 8 (G $\beta$ L)
mSIN1	Mammalian stress-activated MAP kinase-interacting protein 1, (MAPKAP1)
mTOR	Mechanistic target of rapamycin (formerly mammalian target of rapamycin)
p70S6K	70-kDa ribosomal S6 Kinase

PAT1/2	Proton-assisted amino acid transporters
PDK1	Phosphoinositide-dependent kinase 1
PI3K	Phosphoinositide 3-kinase
PIP2/3	Phosphatidylinositol 4,5-bisphosphate/3,4,5-triphosphate
PKB	Protein kinase B, also known as Akt
PRAS40	Pro-rich Akt substrate of 40 kDa, also known as AKT1S1
PROTOR	Protein observed with RICTOR
PTEN	Phosphatase and tensin homologue on chromosome 10
Rac1	Ras-related C3 botulinum toxin substrate 1
RAPTOR	Regulatory-associated protein of mTOR
Rheb	Ras homologue enriched in brain
RICTOR	Rapamycin-insensitive companion of mTOR
rpS6	Ribosomal protein S6
S6K	S6 kinase
SDS-PAGE	Sodium dodecyl sulphate – polyacrylamide gel electrophoresis
SLC	Solute-linked carrier
SNAT2	System A transporter encoded by SLC38A2
SNAT3	System N transporter encoded by SLC38A3
T1DM	Type-1 diabetes mellitus
T2DM	Type-2 diabetes mellitus
Tel2	Telomere maintenance 2
TSC1/2	Tuberous sclerosis 1/2, also known as hamartin
Tti1	Tel2 interacting protein 1
v-ATPase	Vacuolar H <sup>+</sup> -ATPase

### 1.1. Introduction to diabetes

Diabetes is a chronic progressive disease that occurs either when the pancreas cannot produce enough insulin to regulate the blood glucose levels, or when the body does not effectively use the insulin that it produces (Association 2014, Williams and Pickup 1999). Diabetes has become an increasing public health problem. Globally it is estimated that 422 million adults had been diagnosed with diabetes in 2014 compared with 108 million in 1980. In the UK the number of people with diabetes has risen from 1.4 to 3.5 million in the past 10 years. Globally, in 2012 diabetes caused 1.5 million deaths and higher than optimal glucose levels caused 2.2 million additional deaths by increasing the risk of cardiovascular and other diseases (WHO 2016). The increased prevalence is associated with a high economic impact on health systems. It has been estimated that the direct annual cost of diabetes to the world is more than US\$ 827 billion (Whiting et al. 2011, WHO 2016).

There are two main types of diabetes: Type 1 (T1DM) or insulin dependent diabetes is mainly diagnosed in childhood or adolescence. T1DM is characterized by deficient insulin production caused by autoimmune destruction of the pancreatic  $\beta$  cells and requires daily administration of insulin to regulate the blood glucose levels (Association 2014, Williams and Pickup 1999). Patients with T1DM most commonly present with excessive urination and thirst, constant hunger, weight loss, vision changes and fatigue (WHO 2016, Williams and Pickup 1999). Type 2 (T2DM) or non-insulin dependent diabetes is the more common type of diabetes and occurs in over 90% of those diagnosed with the condition. In this form the body is able to produce insulin but is unable to use it effectively owing to insulin resistance in insulin's target organs, especially skeletal muscle, liver and adipose tissue. T2D associates with obesity. In the cardiovascular system the disease progresses to vision loss, heart attack or limb gangrene (WHO 2016).

When plasma glucose (more rigorously D-glucose) levels during fasting are above normal but still below those diagnostic of diabetes this is considered as pre-diabetes or impaired fasting glycaemia (IFG) (6.1 to 6.9 mmol/L) or impaired glucose tolerance (IGT) (>7.0 mmol/L). Both are intermediate conditions with no significant risk for microvascular complications but considered as risk factors for T2DM usually in adults >20 years of age and they can exist for a long time before developing in T2DM. Diabetes is diagnosed when plasma glucose concentrations are  $\geq 11.1$  mmol/L (Grundy 2012, Mainous et al. 2016).

### **1.1.1 Type 1 diabetes (T1DM)**

Type 1 diabetes occurs in 5-10% of all cases of diabetes usually presenting in childhood and early adulthood, with long term and short-term complications. Recent data suggested about 50-60% of T1DM cases present at younger than 16-18 years, with huge geographical and ethnicity variations (Atkinson et al. 2014). With strong genetic components, T1DM develops by immune destruction of pancreatic  $\beta$  cells leading to insulin deficiency (Atkinson et al. 2014, Daneman 2006).

T1DM is associated with the formation of islet autoantibodies as an autoimmune response in individuals genetically predisposed, in the presence of environmental agents that alter the immune system. (Atkinson et al. 2014).

The susceptibility to inherit T1DM is through genes involved in the regulation of immune response leading to the abnormal activation of both T cells, producing an inflammatory response within the islets (insulinitis), and  $\beta$  cells, leading to production of antibodies to  $\beta$  cells antigens. The continuing destruction of  $\beta$  cells causes a progressive loss of insulin secretion leading to clinical diabetes and finally the onset of T1DM with absolute insulin deficiency (Atkinson et al. 2014, Daneman 2006).

### 1.1.2 Type 2 diabetes (T2DM)

T2DM develops from an interaction between environmental, genetic and metabolic factors such as ethnicity, family history of diabetes, gestational diabetes earlier in life, obesity, unhealthy diet, physical inactivity and smoking (Figure 1.1). The excess body fat together with an unhealthy diet and physical inactivity are the strongest risk factors (Association 2014, Williams and Pickup 1999). Dietary practices are the principal causes of unhealthy body weight such as high intake of saturated fatty acids and high total fat intake. An inadequate consumption of dietary fibre or the high intake of sugar sweetened beverages increase the risk of diabetes (WHO 2016). Elevated free fatty acids (FFAs) together with hyperglycaemia occur when high glucose inhibits fat oxidation and lipid detoxification. The use of fibre in diets of patients with T2DM is beneficial in reducing blood glucose (El-Assaad et al. 2003).

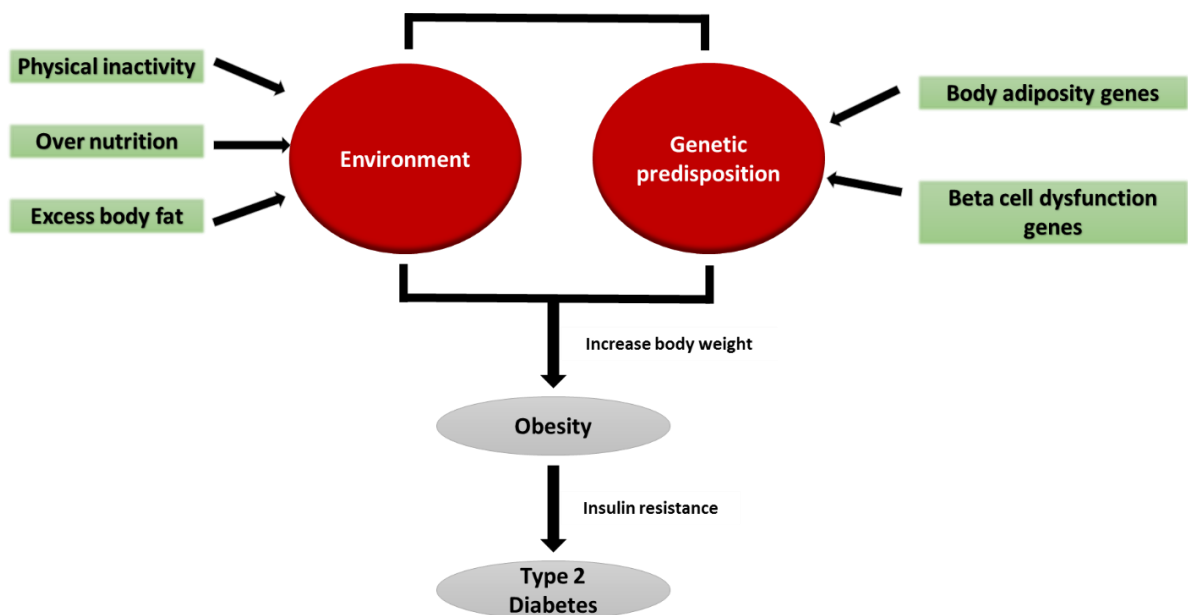


**Figure 1.1. The role of environment and genetics in the development of T2DM**

Figure adapted from American Diabetes Association, 2014 (Association 2014). A combination of environmental factors such as physical inactivity, over nutrition or excess of body fat and genetic predisposition affecting metabolism and  $\beta$  cell activity leads to obesity. When insulin resistance develops, the diagnosis of T2DM is made.

Globally, obesity is the principal cause of T2DM and the prevalence is rising in almost all countries. In 2014, one in three adults over 18 years old were overweight and one in ten

were obese. The number of people overweight or obese is more than double in high- and middle-income countries compared with low-income countries, and this prevalence was highest in America and lowest in the south-east Asian region (WHO 2016).

More than 50 genes are closely associated with T2DM (Li et al. 2013). Recently, genome-wide association studies (GWAS) identified genetic variants related with the causal mutations for the monogenic forms of T2D (Imamura & Maeda, 2011). Other studies showed mutations in genes responsible for childhood obesity including genes encoding for the appetite control proteins: LEP (encoding for leptin acting as an adipocyte-derived hormone), LEPR (encoding for the leptin receptor), and POMC (encodes for Pro-opiomelanocortin, a hypothalamic neuropeptide) (McCarthy 2010, O'Rahilly 2009).

Potential clinical application in the control of T2DM includes establishing susceptibility profiles to predict the disease, early identification and prevention. Examples are: the inherited variation in PPAR $\gamma$ , peroxisome proliferator-activated receptor gamma, a nuclear hormone receptor that regulates adipogenesis (Altshuler et al. 2000); and KCNJ11 (Potassium Voltage-Gated Channel Subfamily J Member 11), a gene encoding a protein acting in the  $\beta$  cell ATP sensitive potassium channel K(ATP) controlling insulin secretion (Gloyn et al. 2003).

Moreover, MCR4 a gene encoding melanocortin-4 receptor involved in modulating fat consumption is related with cases of severe obesity, due to its association with leptin signalling in the central nervous system which reduces the desire for food (Samama et al. 2003). Additionally, TCF7L2 (Transcription Factor 7 Like 2) is a protein-coding gene that modulates pancreatic islet function. TCF7L2 polymorphism is significantly correlated with an enhanced risk of T2DM (Guan et al. 2016), and is also a therapeutic target in T2DM as polymorphism in this gene has a direct correlation with the effectiveness of antidiabetic drugs improving the treatment outcomes in diabetics (Dhawan and Padh 2016).

There is also evidence that polymorphisms in CDKAL1, CDKN2A and CDKN2B, which are genes encoding cyclin-dependent kinase regulatory subunit proteins, are associated with T2DM susceptibility (Li et al. 2013). Finally HHEX (Hematopoietically-expressed

homeobox protein) encodes a member of the homeobox family of transcription factors implicated in developmental processes. HHEX transcription factor acts as a promoter in  $\beta$  cell development (McCarthy 2010).

### **1.1.3 Clinical complications arising from diabetes**

Diabetes is diagnosed when fasting plasma glucose is  $\geq 7.0$  mmol/L. This can be sufficient to cause complications affecting many parts of the body and increasing the risk of dying prematurely. Short-term complications consist of hypoglycaemia diabetic ketoacidosis (DKA), (when blood glucose levels are lower than normal and accompanied by ketoacidosis) and a hyperosmolar hyperglycaemic state (when high levels of glucose cause severe dehydration and increased osmolarity) (Gaw 2008).

Long-term complications of T2DM (Figure 1.2) include microangiopathy consisting of abnormalities in the walls of the small blood vessels, usually thickening of the capillary wall. Retinopathy leads to blindness due to the damage of small blood vessels and neurones of the retina, narrowing of the retina arteries, and reduction of the retinal blood flow (Schlienger 2013). Nephropathy is a progressive kidney disease caused by damage to the capillaries in the kidney, increasing the glomerular size, and reducing the selectivity of the glomerular filter, leading to albuminuria. In a later stage, there is an increase in the proteinuria and marked decline in the renal function resulting in uraemia. Neuropathy is another long-term complication of T2DM and affects mainly peripheral nerves causing nerve damage. Macroangiopathy mainly arising from accelerated atherosclerosis leads to coronary artery disease possibly due to hyperlipidaemia and increased protein glycation (Gaw 2008).

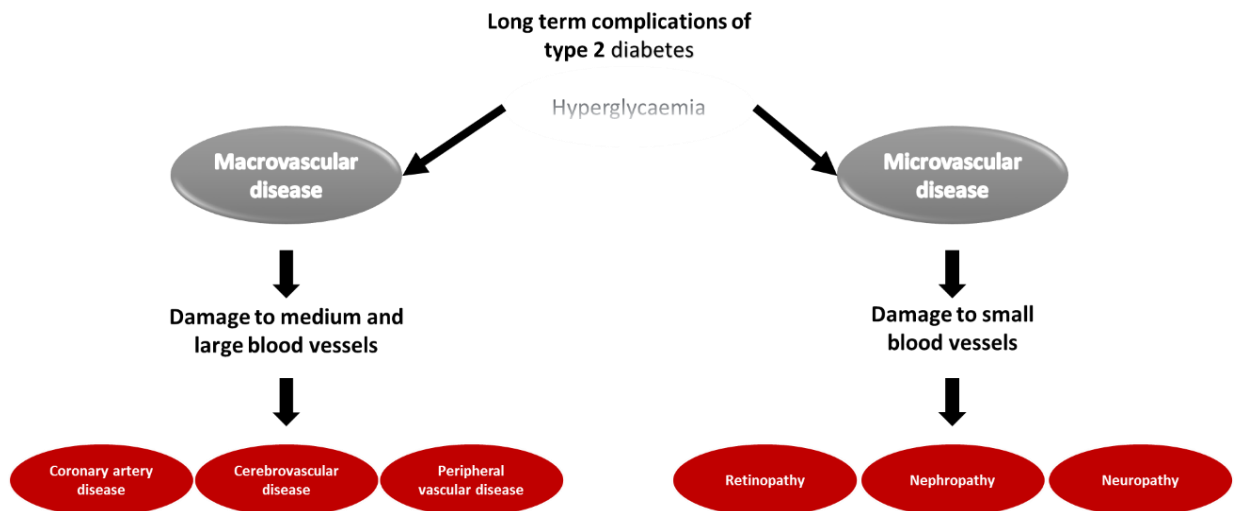


**Figure 1.2. Long-term complications of T2DM**

Figure adapted from Schlienger, 2013 (Schlienger 2013). Long-term complications in T2DM include microvascular disease causing damage to small blood vessels and affecting the eyes (retinopathy), kidneys (nephropathy) or cause nerve damage (neuropathy). The macrovascular complications in T2D can cause damage to the medium and large blood vessels, leading to coronary artery disease, cardiovascular disease or peripheral vascular disease.

#### 1.1.4 $\beta$ cell failure in T2DM and glucotoxicity

Obesity caused by an imbalance between energy intake and expenditure, increases the risk of developing insulin resistance and T2DM (Yao et al. 2016). Over time, islet  $\beta$  cell compensation for the insulin resistance in target organs fails, resulting in a progressive decline in  $\beta$  cell function. As a consequence, subjects progress from normal glucose tolerance (NGT) to impaired glucose tolerance (IGT) and finally to established T2DM (Prentki and Nolan 2006). In the onset of T2DM, chronic high blood glucose concentrations are caused by relative insufficiency of insulin production and secretion (Figure 1.3) (Brownie 1999, Cawston 2010, Joslin and Kahn 2005). Normally in case of changes in insulin resistance, the  $\beta$  cells can adapt to increase the insulin supply. Hence, if  $\beta$  cell dysfunction occurs, it is a critical component in the pathogenesis of impaired glucose tolerance and T2DM, where the  $\beta$  cell function adaptation ultimately fails, and insulin secretion is impaired (Blandino-Rosano et al. 2012, Stumvoll et al. 2005).

The irreversible damage to the  $\beta$  cells and the intensified insulin resistance cause hyperglycaemia leading to the development of T2DM (Marlon 2013). Excessive oxidative

glucose metabolism in  $\beta$  cells leads to the production of reactive oxygen species (ROS) responsible for inducing  $\beta$  cell apoptosis. Chronic hyperglycaemia directly leads to the production of large amounts of ROS generating damage to the cellular components (Stumvoll et al. 2005). This and other toxic effects of high glucose concentration on  $\beta$  cells are referred to as “glucotoxicity” and this, accompanied by toxic effects of elevated circulating concentrations of free fatty acids (lipotoxicity), are thought to play a significant role in long-term  $\beta$  cell failure in T2DM (Del Prato 2009).

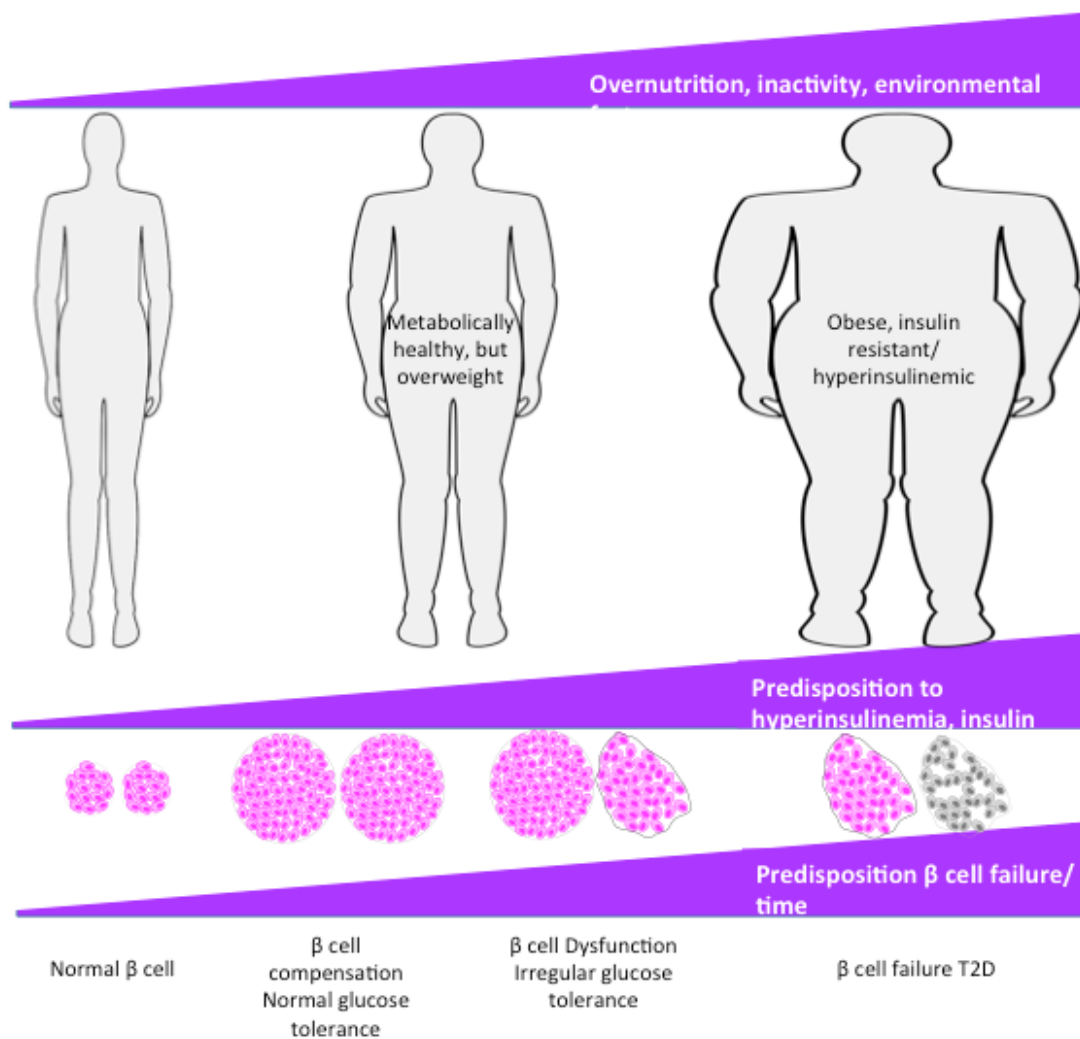


**Figure 1.3. Islet  $\beta$  cell failure and the natural history of T2DM.**

Figure adapted from Prentki and Nolan, 2006. (Prentki and Nolan 2006)

T2D develops in response to overnutrition and physical inactivity in subjects with genetic predisposed to both insulin resistance and  $\beta$  cell dysfunction. Over time, islet  $\beta$  cell compensation fails, resulting in a progressive decline in  $\beta$  cell function. As a consequence, subjects progress from normal glucose tolerance (NGT) to irregular glucose tolerance (IGT) and finally to established T2D.

## **1.2. Pancreatic $\beta$ cells synthesize insulin to control blood glucose concentrations**

The pancreas is an elongated gland located in the abdominal cavity behind the stomach, and is divided in three main sections, the head, the body and the tail. The head of the pancreas is near to the duodenum, the body is the largest part of the pancreas lying behind and is covered by the wall of the stomach, and the tail region ends near the splenic hilus (Figure 1.4.a) (Bardeesy and DePinho 2002, Islam 2010).

The human endocrine pancreas is responsible for the glucose control and metabolism in the body. The pancreatic islets of Langerhans secrete different types of hormones to maintain blood glucose levels, secreting glucagon to increase it and insulin to decrease it. Moreover, the exocrine pancreas has digestive functions through secretion of digestive enzymes to break down carbohydrates, proteins and lipids. In T1DM the immunological response against  $\beta$  cells reduces the main function of the pancreas in controlling the blood glucose levels (Atkinson et al. 2014), while in T2DM the  $\beta$  cell dysfunction causes an insufficient insulin production resulting in the inability to reduce the blood glucose concentrations (Prentki and Nolan 2006). The exocrine pancreas

Microscopically, the pancreas has ducts connecting lobules and epithelial cell clusters performing the two main functions of the pancreas: digestion and glucose homeostasis (Bardeesy and DePinho 2002). The exocrine pancreas, as part of the alimentary tract, releases a mix of digestive enzymes and bicarbonate into the duodenum.

The main function of the exocrine cells in the pancreas is to aid digestion of food producing pancreatic juice rich in  $\text{HCO}_3^-$  and digestive enzymes. The  $\text{HCO}_3^-$  serves to neutralize acidic gastric contents, and the enzymes complete the digestion of ingested carbohydrates, proteins and fat. The exocrine pancreas is divided into lobules containing acinar cells responsible for the synthesis, secretion, and storage of the enzymes, which are released into ducts that join together forming the pancreatic duct that connects the gland to the lumen of the duodenum (Figure 1.4.b) (Boron and Boulpaep 2016).

The ductal cells of the pancreas produce the bicarbonate, stimulated by the hormone secretin, to neutralize gastric acid and allow the correct pH to be obtained to allow efficient enzymatic action. The duodenal cells called “S cells” produce secretin to stimulate bicarbonate juice. Secretin inhibits production of gastrin by “G cells” and stimulates acinar cells. The acinar cells produce pancreatic enzymes or zymogens that are required for digestion. The secretory granules of pancreatic acinar cells contain  $\alpha$ -amylase (an enzyme that hydrolyses polysaccharides, such as starch and glycogen, producing glucose and maltose) or mucins (heavily glycosylated proteins that are components of mucus, produced by epithelial tissue for lubrication and protection).

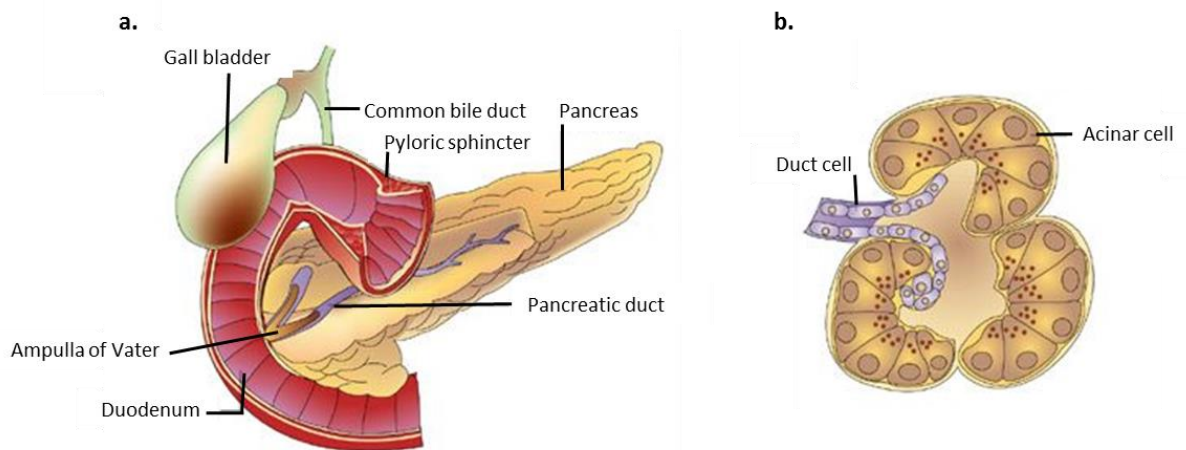


### Figure 1.4. Anatomy of the pancreas

Figure adapted from Bardeesy and DePinho, 2002 (Bardeesy and DePinho 2002). The acinar cells of the exocrine pancreas produce digestive enzymes and are organized into grape-like clusters. The duct cells bring mucous and bicarbonate to the enzyme mixture that empty into the duodenum. Islets (Figure 1.5) are embedded in exocrine tissue. **a)** Gross anatomy of the pancreas and **b)** A single acinus.

#### 1.2.1. The endocrine pancreas

The endocrine pancreas produces functionally important hormones that are secreted in response to nutrients. Such hormones are insulin, glucagon, somatostatin and pancreatic polypeptide which ultimately circulate in the blood (Boron and Boulpaep 2016, Metzgar et al. 1993).

### 1.2.1.1. The islets of Langerhans

The pancreatic endocrine cells form the islets of Langerhans (Figure 1.5), which are micro-organs spread throughout the pancreatic parenchyma in between the exocrine acini and ductal structures (Islam 2010). The islets of Langerhans contain at least 5 types of secretory cells (Table 1.1); including  $\alpha$  cells (producing glucagon),  $\delta$  cells (producing somatostatin), PP or  $\gamma$  cells (producing pancreatic polypeptide),  $\epsilon$  cells (producing ghrelin) and the most numerous cells, the  $\beta$  cells, with the important function of synthesizing and secreting insulin and amylin (islet amyloid polypeptide) (Ackermann and Gannon 2007, Bouwens and Rooman 2005, Joslin and Kahn 2005, Wierup et al. 2014).

**Table 1.1. Cell types in the endocrine pancreas**

Cell type	$\alpha$	$\beta$	$\delta$	PP	$\epsilon$
Peptide hormone	Glucagon	Insulin	Somatostatin	Pancreatic polypeptide	Ghrelin
Number of amino acids	29	51	14	36	28
Total volume % of the gland (adult)	15-20	70-80	05-10	15-25	1

Table adapted from Islam, 2010. (Islam 2010)

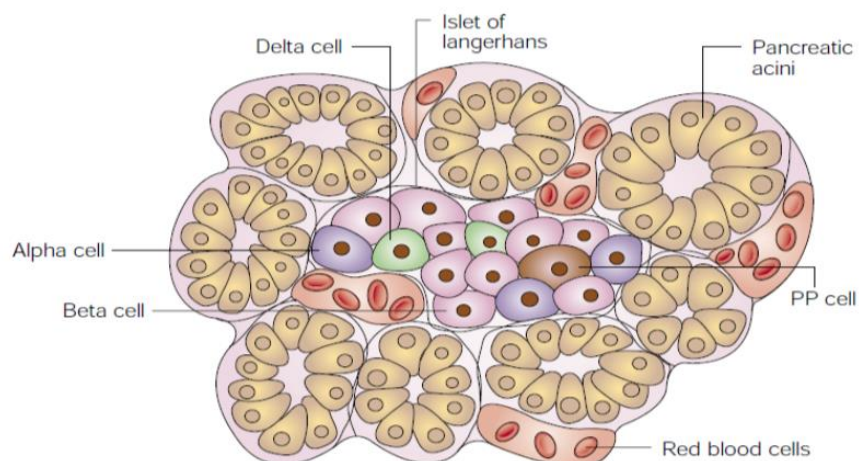


**Figure 1.5. Pancreatic islet endocrine tissue surrounded by exocrine acini**

Figure adapted from Bardeesy and DePinho, 2002 (Bardeesy and DePinho 2002). The endocrine pancreas consists of islets that include four cell types embedded within acinar tissue and secretes hormones into the bloodstream. The  $\alpha$  and  $\beta$  cells produce glucagon and insulin, respectively to regulate blood glucose. PP and  $\delta$  cells produce pancreatic polypeptide and somatostatin to modulate other secretory properties of the pancreas.

The islets are composed of hormones secreting cells. The  $\alpha$  cells secrete glucagon, a peptide derived from proglucagon that promotes gluconeogenesis and glycogenolysis and is stored in secretory granules. Glucagon is released in response to low concentrations of glucose, causing the liver to convert its stored glycogen into glucose. Glucagon and insulin are part of a feedback system that keeps the blood glucose levels in normal conditions at about 5.5 mmol/L (100 mg/dL) (Islam 2010, Wierup et al. 2014).

Somatostatin (or somatotropin release inhibiting factor) is secreted at several locations in the digestive system, in the pyloric antrum, the duodenum and the pancreatic islets by the  $\delta$  cells (or D cells). Somatostatin is a peptide hormone that inhibits multiple secretory processes including:

- Glucagon and insulin release from the pancreas.
- Gastrin, secretin, cholecystokinin (CCK), vasoactive intestinal peptide, glucagon-like peptide 1, gastric inhibitory peptide, ghrelin, pepsin, and gastric acid secretion from the digestive tract.
- T3, T4, and calcitonin secretion from the thyroid gland.
- Aldosterone release from the adrenal gland

Pancreatic polypeptide is a hormone secreted by PP cells in the Islets of Langerhans mainly in the head of the pancreas and is also expressed in endocrine cells of both small and large intestine. PP is an important regulator of pancreatic secretion activities. PP also has an effect depleting the liver glycogen levels and the secretion of PP itself is decreased by somatostatin and intravenous glucose (Islam 2010, Kim et al. 2014, Wierup et al. 2014).

The  $\epsilon$  cells produce ghrelin, an insulinostatic hormone that also stimulates growth hormone release. The function of ghrelin hormone as an appetite-stimulatory signal affects directly the body weight and its plasma levels are decreased by glucose and insulin levels (Klok et al. 2007, Thorens 2015). In addition, ghrelin acts in the regulation of insulin release and glycaemia, increasing blood glucose and decreasing insulin levels. Ghrelin was found to act as a paracrine regulator of  $\beta$  cells in the islets of Langerhans.

Ghrelin also acts regulating the energy homeostasis, modulating hunger signals and controlling the production of ATP, fat storage, glycogen storage and short-term heat loss (Islam 2010, Wierup et al. 2014, Yada et al. 2014).

The  $\beta$  cells in the islets of Langerhans are the most numerous, located mainly in the core of the islets and having the important function of synthesizing insulin essential in the maintenance of glucose levels. Moreover,  $\beta$  cells also secrete islet amyloid polypeptide (IAPP or amylin), which is part of the calcitonin gene peptide superfamily together with calcitonin (CT), and calcitonin gene-related peptide (CGRP). During  $\beta$  cell failure in T2DM, IAPP polymerizes to form pancreatic islet amyloid deposits (Ackermann and Gannon 2007, Bouwens and Rooman 2005, Islam 2010, Joslin and Kahn 2005).

The hormones of the islets of Langerhans also interact with each other, e.g. glucagon raises the blood glucose levels, opposite to the effect of the insulin, and somatostatin inhibits insulin and glucagon secretion from pancreatic islets (Strowski et al. 2000). Moreover, the parasympathetic innervation from the vagus stimulates the insulin release, and conversely the adrenergic sympathetic nerves inhibit insulin secretion and stimulate glucagon release (Williams and Pickup 1999).

### **1.2.2. Insulin**

Insulin is the hormone responsible for reducing blood glucose concentrations in response to hyperglycaemia. Insulin contains two polypeptide chains with 21 and 30 amino acids linked through disulphide bridges (Figure 1.6). Insulin is first synthesized in  $\beta$  cells as proinsulin in a single polypeptide chain and packaged into secretory vesicles in the Golgi apparatus. It is cleaved into insulin and connecting C peptide in the maturing secretory granules (Joslin and Kahn 2005).  $\beta$  cells in the islets of Langerhans release insulin rapidly in response to increased blood glucose levels by a mechanism whereby the D-glucose enters into the cell via glucose transporter 2 (GLUT2) and undergoes glycolysis, being phosphorylated to glucose-6-phosphate by glucokinase, and ultimately producing ATP (Thorens 2015).

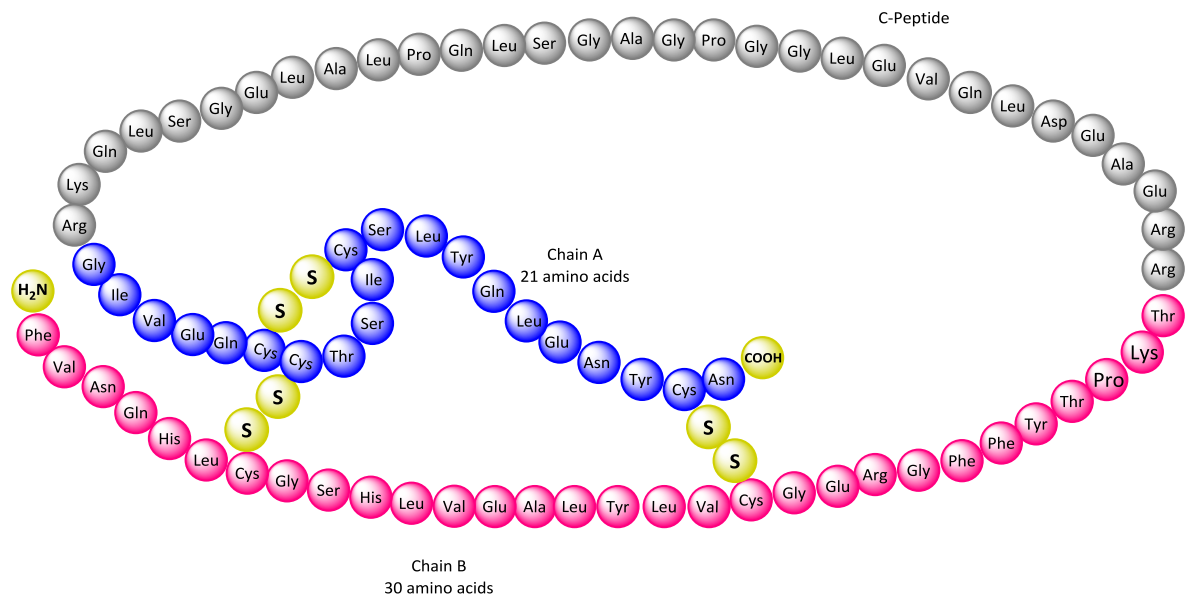


**Figure 1.6. Insulin structure**

Figure redrawn from Correia et al., 2012 (Correia et al. 2012). The insulin amino acid sequence is composed of an A-chain (21 amino acids), a C-peptide (31 amino acids), a B-chain (30 amino acids), and a signal sequence. The signal sequence is cleaved from the N-terminus of the peptide by a signal peptidase, leaving proinsulin. After proinsulin is packaged into vesicles in the Golgi apparatus (beta-granules), the C-peptide is removed, leaving the A-chain B-chain, bound together by disulfide bonds, which constitute the processed insulin molecule. Insulin multimerises in the granules.

When the intracellular ATP:ADP ratio consequently increases, ATP-sensitive potassium channels close, thus preventing potassium ions from leaving the cell (see KCNJ11 in Section 1.1.3). Consequently, the cell becomes electrically more positive inside versus outside i.e. there is depolarization of the plasma membrane. Such depolarization opens the voltage sensitive calcium ion channels in the plasma membrane and allows calcium ions to enter the cells by facilitated diffusion down their electrochemical gradient. The resulting increased calcium ion concentration in the cytosol triggers exocytotic release of the insulin previously synthesized and stored in the secretory vesicles (Brownie 1999, Cawston 2010 ).

### 1.3. The role of leucine as essential amino acid in $\beta$ cell biology

Branched chain amino acids (BCAA) (L-leucine, L-isoleucine and L-valine) are important nutrients associated with the regulation of body weight, muscle protein synthesis and *in vitro* glucose metabolism (Lynch and Adams 2014). L-leucine stimulates insulin

secretion in pancreatic  $\beta$  cells and it also regulates gene transcription and protein synthesis (Yang et al. 2010). In rat pancreatic islets, L-leucine increases insulin secretion (Yang et al. 2006). BCAA, especially L-leucine, are important in the stimulation of protein synthesis via activation of the mechanistic target of rapamycin complex 1 (mTORC1) (Moberg et al. 2016), activating the translocation of mTORC1 to the surface of the lysosome where its action as a protein kinase takes place (Puertollano 2014). This translocation and activation occurs by mechanisms involving formation of complexes with proteins including RAG (Ras-related GTPases) and Ragulator, v-ATPase, GATOR (GAP activity towards Rags), and folliculin (FLCN) complexes (Bar-Peled and Sabatini 2014) (see Section 1.8).

Changes in the intra-lysosomal free amino acid concentration (including L-leucine) play an important role in the activation of mTORC1 (see Section 1.8). In mice, mTORC1 hyperactivation stimulates  $\beta$  cell function and promotes mass (Xie and Herbert 2012). In  $\beta$  cells, deletion of the negative regulator of mTORC1, tuberous sclerosis complex-2 (Tsc2), induces stimulation of  $\beta$  cell mass, increasing both proliferation and cell size (Rachdi et al. 2008). In pancreatic  $\beta$  cells, the upstream kinase Akt also increases mTORC1 activity again stimulating protein synthesis, cell growth, differentiation and survival (Balcazar M and Aguilar de P 2012).

L-leucine has been demonstrated to have an important effect in countering the insulin resistance characteristic of obesity-induced metabolic dysfunction (Yao et al. 2016). It has been reported that L-leucine-rich high-protein diets promote weight loss, improve glucose homeostasis, and increase energy expenditure and fat oxidation (Freudenberg et al. 2012). In part this occurs because in pancreatic  $\beta$  cells, L-leucine stimulates insulin secretion and in human diabetic islets it improves insulin secretory dysfunction. L-leucine does this (at least partly) by acting as a metabolic fuel and allosteric activator of glutamate dehydrogenase to enhance glutaminolysis (Yang et al. 2010).

L-leucine or its metabolic intermediate  $\alpha$ -ketoisocaproate (KIC), control insulin secretion by regulating ATP-sensitive potassium K(ATP) channels activity in pancreatic  $\beta$  cells (Ashcroft 2005), a mechanism related to that seen with other insulin secretagogues including D-glucose (Ashcroft and Rorsman 2004). However, in INS1E insulinoma cells

and rat islets, L-leucine seems to be a more potent insulin secretagogue than its non-metabolisable analogue BCH, suggesting that L-leucine metabolism contributes to the stimulation of the secretion of insulin (MacDonald et al. 2008). Interestingly, KIC seems to have a bigger effect on insulin secretion than L-leucine as, in pancreatic  $\beta$  cells, the effect of L-leucine is totally blocked by D-glucose whereas the effect of KIC is not blocked (Yang et al. 2010).

Glutamate dehydrogenase (GDH) plays an important role in L-leucine-induced insulin secretion. This mechanism is via the allosteric regulation of GDH activity by L-leucine, catalysing the oxidative deamination of endogenous glutamate to  $\alpha$ -ketoglutarate and increasing the ratio of NADH/NAD<sup>+</sup> and NADPH/NADP<sup>+</sup> in pancreatic  $\beta$  cells. The production of  $\alpha$ -ketoglutarate then exerts effects on the Krebs Cycle where it inhibits isocitrate dehydrogenase and stimulates synthesis of acetyl CoA, which are thought to be important facilitators of insulin secretion (Fahien and MacDonald 2011).

In addition to its effects on insulin secretion, L-leucine regulates gene transcription and protein synthesis in pancreatic  $\beta$  cells, via the mTORC1 pathway (see Figure 1.8) and has been found to improve insulin dysfunction in T2DM diabetic islets (Yang et al. 2010). The use of L-leucine as a supplement in the diet inhibits food consumption, possibly via increased release of leptin, and of ghrelin in gastrointestinal tract (Chungchunlam et al. 2015). In turn, leptin activates AMPK (Section 1.6) in muscle which induces oxidation of fatty acids and increased glucose uptake (Yao et al. 2016).

At the onset of T2DM,  $\beta$  cells respond to insulin resistance by  $\beta$  cell compensation, thus increasing insulin secretion. This compensation consists of increasing  $\beta$  cell mass, insulin biosynthesis, and enhanced insulin secretion without a change in K(ATP) channel activity (nutrient secretion coupling) (Rutter 2001). Over time, the  $\beta$  cell compensation for the insulin resistance eventually fails, resulting in a progressive decline in  $\beta$  cell function and mass due to apoptosis, finally leading to the development and progression of T2DM (Abe et al. 2013, Chan 2013, Talchai 2012). Therefore, T2DM progresses partly due to a  $\beta$  cell failure in terms of mass and function, resulting in inadequate compensation for insulin resistance. Growth factors, insulin and nutrients, such as glucose and amino acids are thought to be the principal factors responsible for functional  $\beta$  cell mass expansion

(Blandino-Rosano et al. 2012). At this point, exogenous insulin may be therapeutically needed to control blood glucose levels.

#### **1.4. The role of mTOR in the regulation of pancreatic $\beta$ cell mass and function**

mTOR is a highly conserved and ubiquitously expressed Ser/Thr protein kinase that regulates cell growth, proliferation, motility, survival, protein synthesis and transcription (Xie and Herbert 2012, Zhou 2011 ). mTOR is part of two intracellular signalling complexes, mTOR complex 1 (mTORC1) and mTOR complex 2 (mTORC2) (Figure 1.7) (Guertin 2007 , Zhou 2011 ). The activation of mTORC1 stimulates cell growth and proliferation, promoted by growth factors and amino acids, and is acutely inhibited by the immunosuppressant drug rapamycin (Figure 1.7); whereas the activation of mTORC2 regulates a number of targets including cell polarity and the cytoskeleton (Bhaskar and Hay. 2007).

Both complexes have in common mLST8 (mammalian orthologue of lethal with SEC13 protein 8) and DEPTOR (DEP domain-containing mTOR-interacting protein), which are positive and negative regulators, respectively. Both complexes also contain GRP58 (58kDa glucose-regulated protein), Tti1 (Tel2 interacting protein 1), Tel2 (telomere maintenance 2) and Rac1 (Ras-related C3 botulinum toxin substrate 1) (Guertin 2007 ).

However, mTORC 1 and 2 comprise two different scaffolding proteins that link mTOR to particular signalling pathways. mTORC1 has RAPTOR (regulatory-associated protein of mTOR) that recruits downstream targets to mTOR, interacting with the TOS (TOR signalling) motif, and the negative regulator, PRAS40 (Pro-rich Akt substrate of 40 kDa, also known as AKT1S1) (Figure1.7).

The specific components of mTORC2 are RICTOR (rapamycin-insensitive companion of mTOR) which acts as a scaffold to maintain the integrity of mTORC2, and PROTOR (protein observed with RICTOR) which works in the assembly of other subunits to the complex, and mSIN1 (mammalian stress-activated MAP kinase-interacting protein 1, also known as MAPKAP1) which may target the complex to the lysosome (Figure 1.7) (Zoncu et al. 2011).

The main biological function of mTORC1 is to stimulate cell growth and proliferation through the phosphorylation of its downstream targets 4EBP translation initiation factor (4E-binding protein) and the p70S6K (70kD ribosomal S6 Kinase (see Figure 1.7) (Wang and Proud 2009).

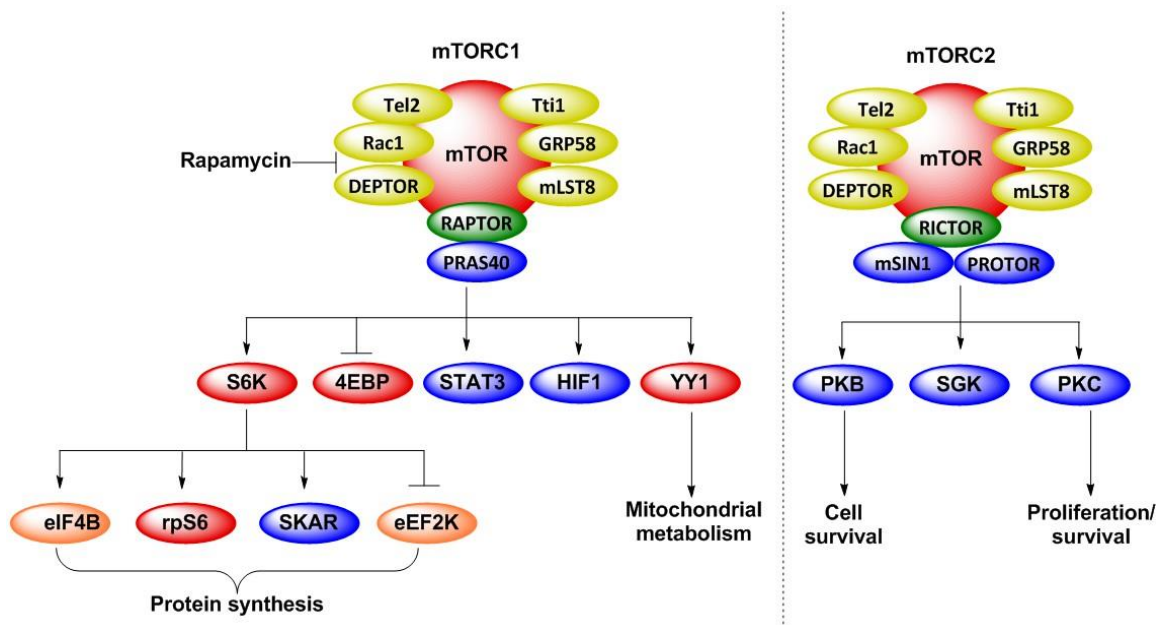


**Figure 1.7. Composition of mTORC1 and mTORC2**

Figure adapted from Limon and Fruman, 2012 and Zoncu et al., 2001 (Limon and Fruman 2007, Zoncu et al. 2011). mTORC1 and mTORC2 complexes have in common mLST8 (mammalian orthologue of lethal with SEC13 protein 8) and DEPTOR (DEP domain-containing mTOR-interacting protein), also contain GRP58 (58kDa glucose-regulated protein), Tti1 (Tel2 interacting protein 1), Tel2 (telomere maintenance 2) and Rac1 (Ras-related C3 botulinum toxin substrate 1). mTORC 1 and 2 have two different scaffolding proteins. mTORC1 has RAPTOR (regulatory-associated protein of mTOR) and PRAS40 (Pro-rich Akt substrate of 40 kDa, also known as AKT1S1). mTORC2 has RICTOR (rapamycin-insensitive companion of mTOR) and PROTOM (protein observed with RICTOR). Distinctly related functions are indicated.

### 1.5. Upstream regulators of mTORC1

mTORC1 activation initiates after the stimulation of the class I phosphoinositide 3-kinase (PI3K) (Dibble and Cantley 2015) by growth factors via activation of receptor tyrosine kinases (RTKs) and possibly after stimulation of class III PI3K by amino acids (Xie and Herbert 2012, Zhou 2011 ). PI3Ks then phosphorylate PIP<sub>2</sub> to PIP<sub>3</sub> (Figure 1.8). In  $\beta$  cells class I PI3K is an important intermediary of autocrine insulin signalling (Bartolome

and Guillen 2014). PI3K action is negatively regulated by PTEN (phosphatase and tensin homolog on chromosome 10), which dephosphorylates PIP<sub>3</sub> back to PIP<sub>2</sub> (Lieberthal 2009). PIP<sub>3</sub> acts as a second messenger activating PDK1 (phosphoinositide-dependent protein kinase-1), which in turn activates the protein kinase Akt by phosphorylating amino acid residue Thr<sup>308</sup>. Even though the contribution of Akt-Thr<sup>308</sup> phosphorylation to  $\beta$  cell preservation is greater than that mediated by an alternative Akt phosphorylation on Ser<sup>473</sup> mediated by mTORC2, Ser<sup>473</sup> phosphorylation is necessary for complete activation of Akt (Figure 1.8) (Bartolome and Guillen 2014).

Akt, TSC complex, and Rheb are the primary intermediates through which PI3K signalling activates mTORC1 (Dibble and Cantley 2015).

The first direct target of Akt is GSK3 $\beta$  (glycogen synthase kinase 3 $\beta$ ), a serine/threonine protein kinase that acts as a negative regulator of mTORC1 signalling (Manning and Cantley 2007). Akt also interacts with the Forkhead box O (FoxO) transcription factor, important in the regulation of cell survival, growth and proliferation (Zhang et al. 2011). Phosphorylation of GSK3 $\beta$  and FoxO by Akt inhibits transcriptional functions for example suppressing transcription of E3 ligases in the ubiquitin-proteasome pathway of protein degradation, thus supplementing the growth-promoting effects arising from the activation of the mTORC1 signalling. Recent studies demonstrated the role of GSK3 in the regulation of mTORC1 activity by phosphorylation of the mTOR-associated scaffold protein RAPTOR on Ser 859 (Stretton et al. 2015).

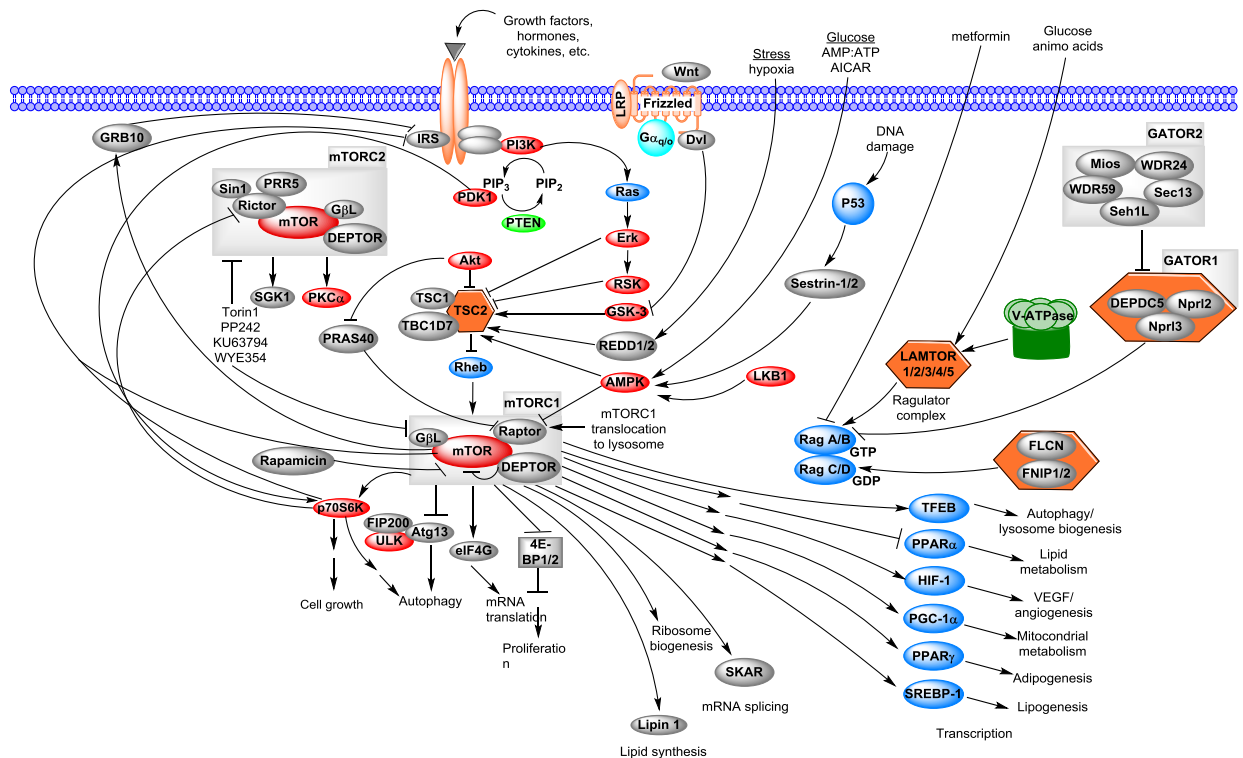


**Figure 1.8. mTORC1 is activated by growth factors and amino acids.**

Figure redrawn from Zoncu et al., 2011 (Zoncu et al. 2011)

TSC (tuberous sclerosis complex) is composed of TSC1 (hamartin) and TSC2 (tuberin): the binding of TSC1 to TSC2 is necessary for TSC2 activity. TSC2 inhibits Rheb, a Ras family GTPase necessary for mTORC1 activation. Akt phosphorylates and inhibits TSC2, releasing Rheb from the inhibitory effects of TSC and hence activating mTORC1 (Bartolome and Guillen 2014, Lieberthal 2009). Rheb acts downstream of TSC1/TSC2 and upstream of mTOR to regulate cell growth (Inoki et al. 2003).

Growth factor receptor tyrosine kinase activates PI3K. PI3K phosphorylates PIP2 to PIP3, activating Akt through PDK1. PI3K action can be counterbalanced by PTEN, a phosphatase that dephosphorylates PIP3 back to PIP2. Activated Akt, phosphorylates and inhibits TSC, a negative regulator of Rheb which is an activator of mTORC1. AMPK is activated by any cell stress that decreases ATP, increasing AMP:ATP ratio and inhibiting mTORC1 through phosphorylation and activation of TSC. Activated mTORC1, phosphorylates p70S6K and 4EBP, inducing translation of mRNAs and protein synthesis, necessary for cell growth and cell-cycle progression.

### 1.6. Energy status, AMPK and mTORC1

AMP activated protein kinase (AMPK) (Figure 1.9) is a multimeric serine/threonine protein kinase with  $\alpha$  (catalytic),  $\beta$  (scaffold) and  $\gamma$  (regulatory) subunits (Hardie 2011,

Leclerc and Rutter 2004). AMPK activates D-glucose transport, inhibits lipid and protein synthesis, and activates fuel metabolism and physiological events such as cellular growth and proliferation (Ruderman et al. 2013). It is activated by phosphorylation on threonine 172 of its  $\alpha$  subunit in response to depletion in the ATP/AMP ratio under low cellular energy conditions (Figure 1.9). The activation of AMPK occurs when AMP binds to AMPK  $\alpha$  subunit and this increases its susceptibility to phosphorylation by the upstream kinase LKB1 (Park et al. 2013).

When activated, AMPK limits the depletion of ATP by promoting compensatory changes to maintain the cellular energy homeostasis. AMPK is also negatively regulated by protein phosphatases (PP2A) mediated by intracellular calcium: under chronic exposure to calcium the activity of AMPK is reduced (Park et al. 2013).

An important aspect of AMPK action is that it conserves energy by shutting down global protein synthesis via inhibiting translation through a key phosphorylation event on TSC2 which inhibits mTORC1 (Mihaylova and Shaw 2011).

AMPK also restores the energy state of the cell by activating D-glucose uptake into cells through the insulin-regulated glucose transporter 4 (GLUT4) by promoting translocation of GLUT4 to the plasma membrane (Figure 1.9). Recent studies in muscle suggest that AMPK stimulates GLUT4 translocation, but also increases the intramuscular levels of GLUT4 protein by stimulating the transcription of the GLUT4 gene (Park et al. 2009).

It has been suggested that there is a potential use of AMPK stimulation as a treatment for T2DM since changes in AMPK activity may be involved in the activation of insulin secretion (Leclerc and Rutter 2004). The activation of AMPK by the use of the AMP analogue AICAR in T2DM is associated with reduced gluconeogenesis and enhanced D-glucose uptake (Leclerc and Rutter 2004), and the widely used drug Metformin may exert part of its therapeutic effect in T2DM by activating AMPK in liver resulting in inhibition of gluconeogenesis (Gong et al. 2012).

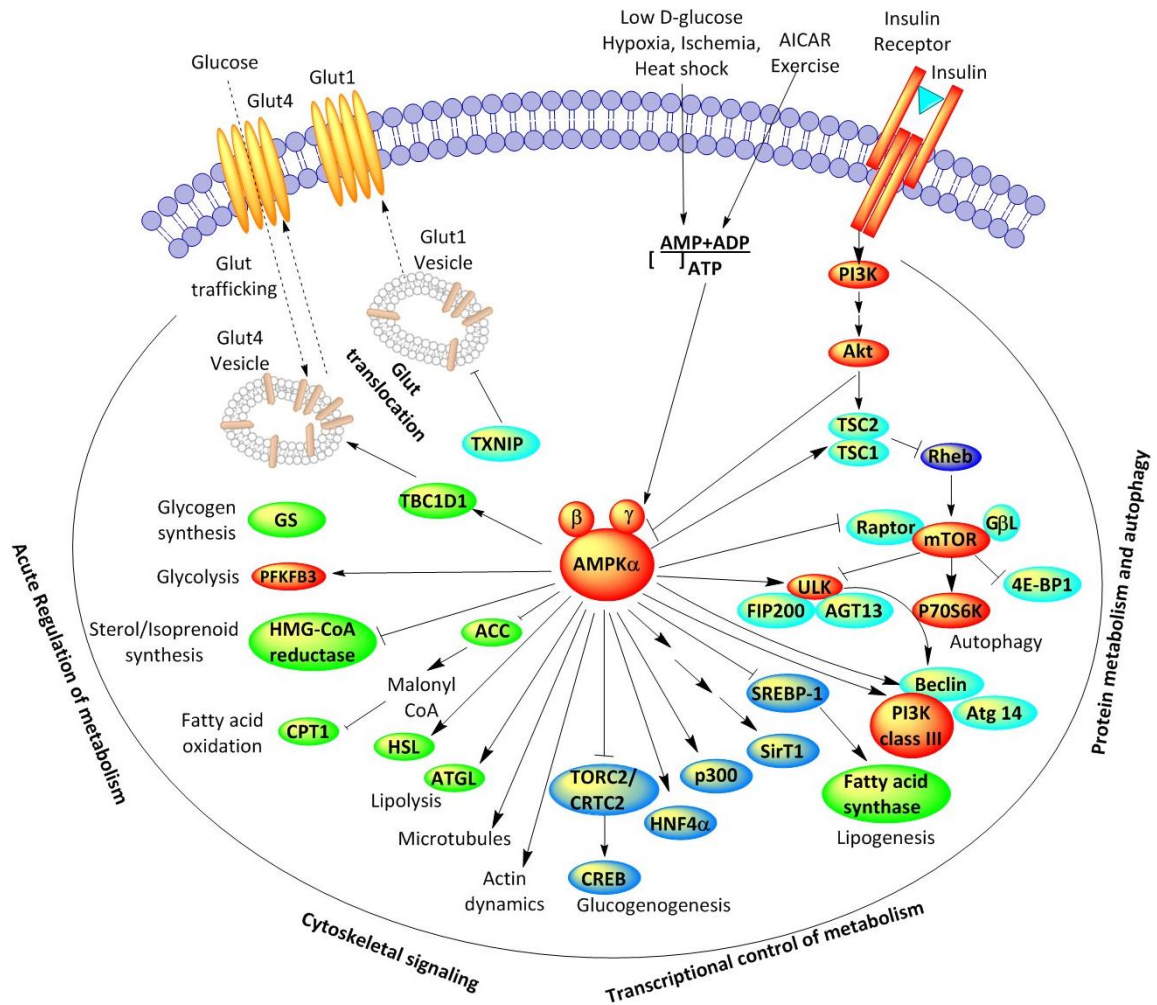


**Figure 1.9. AMPK pathway**

Schematic diagram summarising AMPK activation by energy status (increased AMP/ATP ratio) and the actions of activated AMPK in mammalian cells (redrawn from Jewell et al. 2013, Kurth-Kraczek et al. 1999, Leclerc and Rutter 2004, Luiken et al. 2015, Ruderman et al. 2013, Zheng et al. 2001)

### 1.7. Downstream targets of mTORC1

In the presence of nutrients, mTORC1 stimulates biosynthetic pathways, especially protein synthesis, and represses autophagy to promote cell growth (Jewell et al. 2013). This occurs through the downstream targets of mTORC1, which are the 4EBP (eukaryotic initiation factor 4E-binding protein) and p70S6K (70-kDa ribosomal S6 Kinase) (Figure 1.8). The 4EBP is a translation repressor protein. Unphosphorylated, it binds and inhibits the activity of the translation initiation factor eIF4E. When activated, mTORC1 promotes multiple phosphorylation of 4EBP and releases eIF4E allowing mRNA translation.

mTORC1 also phosphorylates p70S6K, which in turn, phosphorylates rpS6 (ribosomal protein S6), increasing translation of ribosomal and translation factor mRNA and subsequent protein translation initiation (Walker et al. 2014). However, P70S6K also facilitates a negative feedback loop in response to mTORC1 signalling, by phosphorylation of insulin receptor substrate protein 1 (IRS1) (Ginion et al. 2011), thus blocking mTORC1 activation through the RTK/IRS/PI3K/PDK1 pathway (Figure 1.8) (Shah 2004 ).

mTORC1 inhibits autophagy and is activated by amino acids which can be released by lysosomal digestion of proteins (Altman et al. 2014). Under D-glucose starvation, autophagy is stimulated by AMPK by inhibition of mTORC1 both of them acting through phosphorylation of the protein kinase Ulk1 (Kim et al. 2011).

### **1.8. Amino acid regulation of mTORC1**

Amino acids are essential nutrient signals for the activation of mTORC1. The important links in the amino acid signalling to mTORC1 are RAG GTPases, composed of four RAG proteins: RAGA, RAGB, RAGC and RAGD (Figure 1.8). RAGA or RAGB forms a heterodimer with RAGC or RAGD, forming four different possible complexes. This dimerization is important for mTORC1 activation and RAG protein stability (Jewell et al. 2013) . In the presence of amino acids, RAG GTPases form an active complex in which RAGA and RAGB are GTP-bound, and RAGC and RAGD are GDP-bound. These active complexes bind to the RAPTOR component of mTORC1 (Figure 1.7) to relocate it to the lysosome, where amino acids and growth factor signals converge and activate mTORC1. Ragulator is a protein complex consisting of p18, p14 and MP1, and acts as a scaffold for the active RAG heterodimeric complex at the lysosome where Rheb-GTP is localized (Figure 1.8). In the presence of amino acids, Ragulator binds RAG GTPases to the lysosome, and relocalizes and activates mTORC1 (Sengupta 2010 , Zoncu et al. 2011). Another biochemical mediator on the lysosomal membrane which is thought to regulate mTORC1 activation is the Vacuolar H<sup>+</sup>-ATPase (v-ATPase), which interacts with RAG GTPases and Ragulator (Jewell et al. 2013).

Other proteins are also associated with the amino acid sensing by mTORC1 including MAP4k3 (mitogen-activated protein kinase kinase kinase) (Sengupta 2010 , Zoncu et al. 2011) and IPMK (inositol polyphosphate monokinase). However, is not clear how these molecules connect to the RAG-Ragulator System (Laplante 2012 ).

Recent evidence suggests that free amino acids that are sensed by mTORC1 are inside the lysosome (Figure 1.10). Evidence for this comes from the fact that some of the solute carrier (SLC) group of membrane transport proteins work in the lysosomal amino acid sensing and regulate mTORC1 activity (Rebsamen et al. 2015) and the particular SLC (see Section 1.10) proteins involved are amino acid transporters. For example, the human member 9 of the solute carrier family 38 (SLC38A9) is a lysosomal amino acid transporter and forms part of the ragulator-RAG GTPases machinery important in the control of the activation of mTORC1 (Wang et al. 2015). It has been shown SLC38A9, vacuolar adenosine triphosphatase (v-ATPase) and another amino acid transporter (SLC36A1) interact with RAG GTPases, necessary for mTORC1 activation by amino acids (Wang and Holst 2015) (Figure 1.10).

As L-leucine is known to be the most potent amino acid involved in mTORC1 stimulation, a mechanism is needed for the uptake of L-leucine into lysosomes. The lysosomal protein LPTM4b recruits the heterodimeric protein LAT1-4F2hc, leading to the activation of mTORC1 via V-ATPase (Figure 1.10) following L-leucine stimulation (Milkereit et al. 2015). In xenopus oocytes, the co-expression of the components of this heterodimer i.e. LAT1 and 4F2hc (also known as CD98) increased the transport of large neutral amino acids with branched or aromatic side chains, especially L-leucine (Thompson 2001); and LAT1-4F2hc is regarded as one of the most functionally important L-leucine transporters in mammalian cells (see Section 1.10.1). in addition to the mechanism shown in Figure 1.10, the enzyme Leucyl-tRNA sythetase (LRS), has also been suggested to act as an L-leucine sensor that activates vacuolar protein sorting 34 (Vps34) - Phospholipase D1 (PLD1) upstream of mTORC1, thus inducing its translocation to the lysosome (Yoon et al. 2016).

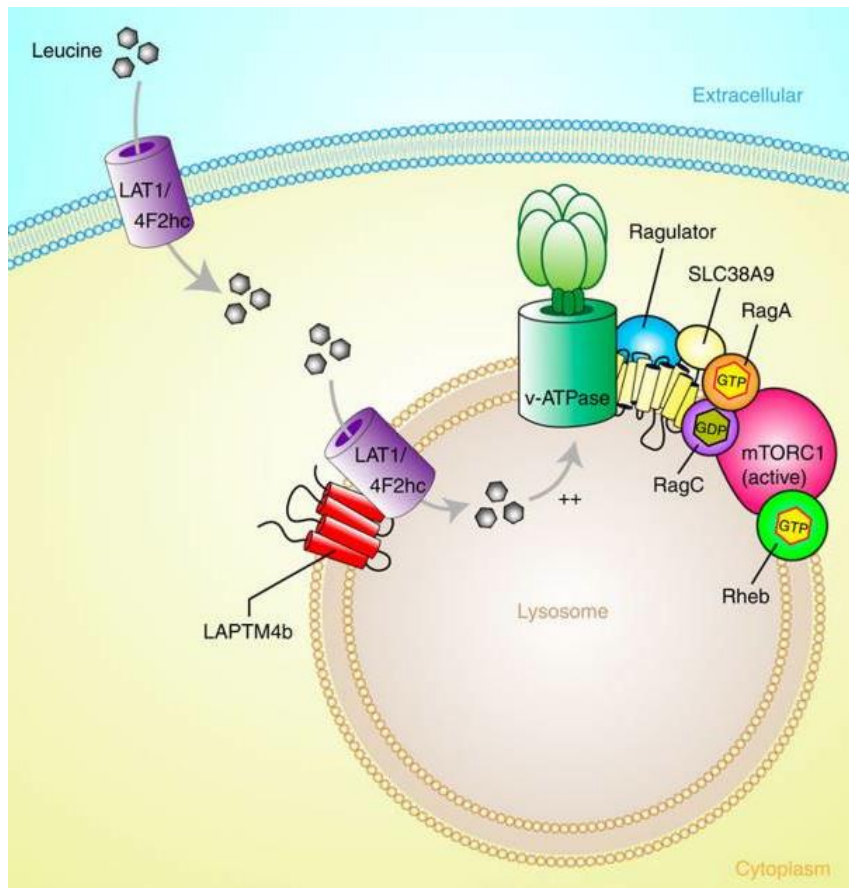


**Figure 1.10. Activation of mTORC1 via recruitment of L-leucine transporter to lysosomes**

Figure taken from Milkereit et al., 2015 (Milkereit et al. 2015). LAPT4b promotes extracellular L-leucine uptake into lysosomes to activate mTORC1 via v-ATPase by recruiting LAT1-4F2hc to the lysosomal membrane.

Of the three branched-chain amino acids L-leucine, L-isoleucine and L-valine, L-leucine is thought to have the biggest effect on mTORC1 signalling (Gran and Cameron-Smith 2011, Proud 2007). In the case of 4E-BP1 phosphorylation, L-leucine has been reported to play an important role; however, the presence of other amino acids is necessary to achieve the full effect (Fox 1998). The use of a potent lysosomal inhibitor (chloroquine) to disrupt lysosomal function, blocked the L-leucine activation of mTORC1 signalling in skeletal muscle cells (Borack Michael and Rasmussen. 2014), confirming the functional importance of the L-leucine action in lysosomes shown in Figure 1.10.

### 1.9. Amino acid transporters

Amino acid transporters are integral membrane proteins which have an important role

in tissue nutrient supply, mediating amino acid exchange or uni-directional flux between extracellular and intracellular fluid compartments, and delivering substrates to intracellular amino acid sensors (Taylor 2014). Intracellular amino acid homeostasis is maintained partly through external amino acid supply and some of the amino acid transporters that do this are active transporters, which can perform accumulation of free amino acids against an electrochemical gradient. For some of these e.g. SLC38 transporters, the rate of amino acid uptake is coupled with co-transport of Na<sup>+</sup> in an energy dependent manner, using the plasma membrane Na<sup>+</sup> ion gradient across the membrane to drive transport. This is called “secondary active transport” (Dodd and Tee 2012). Amino acid transporters have been classified into distinct so-called “systems” based upon their substrate specificity, transport mechanism and regulatory properties (Hyde and Hundal 2003 ). For example Na<sup>+</sup>-dependent transporters which were inhibited at low pH and transported L-alanine efficiently were classed as “System A”, whereas Na<sup>+</sup>-independent, pH insensitive L-leucine transporters were classed as “System L”.

Furthermore, since the cloning of the genes that encode these transporters that has taken place during the past 30 years, they have also been classified into a series of solute carrier (SLC) gene families (see Section 1.10).

The expression and activity of some amino acid transporters have positive correlation with the activation of mTORC1, such as the System A transporter (SNAT2), the System N transporter (SNAT3), some of the System L transporters (LAT1 and LAT2), and the proton-assisted amino acid transporters (PAT1 and PAT2) (Hyde and Hundal 2003 ). However, mTORC1 signalling is particularly influenced by LAT1 exchanging BCAAs for other intracellular amino acids, and it couples with the glycoprotein CD98 (also known as 4F2hc) (Figure 1.11) (Dodd and Tee 2012). Some transporters need to be attached to other proteins forming heterodimers to localize the transporter, modulate activity, or increase the substrate supply. Some of these partner proteins are cell surface antigens (CD98), endoplasmic reticulum proteins (GTRAP3-18 or 41), or enzymes (ACE2 and aminopeptidase N) (Makrides et al. 2014).

The System L transporters which are the main carriers for L-leucine are inhibited by BCH

(2-Aminobicyclo-(2,2,1)-heptane-2-carboxylic acid), a non-metabolizable substrate analogue of L-leucine that binds to the L-type amino acid transport system with high affinity, performing a competitive inhibition. This has been demonstrated by experiments using BCH that showed a decrease in the L-leucine uptake rate (Chand and Legge 2011).

### **1.10. SLC gene families**

The solute carrier superfamily (SLC) is made up of 52 human gene families which encode about 400 transporter proteins, including the amino acid transporters that facilitate movement of these across the membrane (Lin et al. 2015). These transporters and their properties are tabulated in an online database at (<http://slc.bioparadigms.org/>).

The SLC proteins use a variety of mechanisms to perform this transport, including secondary active transport, and interaction with other SLC superfamily members such as the SLC3 family that do not have transport capability on their own but form functional heterodimers (see Figure 1.11) (Colas et al. 2016) with proteins that directly carry the amino acids. The members of each gene family are designated A1, A2, etc. where the number indicates the approximate order in which the transporter was discovered.

#### **1.10.1. System L transporters**

L-type amino acid transporters (LATs) capable of transporting L-leucine and the other BCAAs are encoded by the *SLC7* and *SLC43* gene families and recently one member of the *SLC6* gene family has also been shown to be involved (Table 1.2). The SLC7 proteins are the light or catalytic subunits of the heteromeric amino acid transporters (HATs), which are heterodimers which are held together by a disulphide bridge between the light subunits and the heavy subunits 4F2hc (SLC3A2 (CD98)) or rBAT (SLC3A1), which are members of the *SLC3* family (Figure 1.11) (Fotiadis et al. 2013).

##### **1.10.1.1. LAT1**

4F2hc/LAT1 (SLC7A5) (Figure 1.11) mediates the sodium-independent obligatory exchange of amino acids with bulky side-chains i.e. large neutral and aromatic amino acids or the non-metabolizable analogue 2-aminobicyclo-(2,2,1)-heptane-2-carboxylic

acid (BCH) (Mastroberardino et al. 1998, Meier et al. 2002). The affinity for L-leucine measured on the extracellular side of the transporter is high ( $K_m$  = approximately 30  $\mu\text{M}$ ) (<http://www.uniprot.org/uniprot/Q01650>), but a lower substrate affinity is found on the cytosolic side, suggesting that it may play a role in amino acid efflux when cytosolic amino acid concentration is high. LAT1 is expressed in many tissues including pancreatic  $\beta$  cells (Cheng et al. 2016), brain, ovary, testis, placenta, spleen, colon, blood-brain barrier, foetal liver, activated lymphocytes, and tumour cells. In addition to facilitating the transport of large neutral L-amino acids, it also transports thyroid hormones T3 and T4 and the neurotransmitter precursor L-DOPA (see Table 1.2) (102).

#### 1.10.1.2. LAT2

4F2hc/LAT2 (SLC7A8) has similar properties to LAT1. It is a sodium-independent, high-affinity obligatory exchanger, whose substrates include bulky neutral amino acids, but also some smaller neutral L-amino acids, T3, T4 and BCH (Meier et al. 2002). Similar to LAT1, LAT2 has lower intracellular than extracellular apparent substrate affinities and is expressed in many tissues e.g. small intestine, kidney, lung, heart, spleen, liver, brain, placenta, prostate, ovary, foetal liver, testis and skeletal muscle (Pineda et al. 1999).

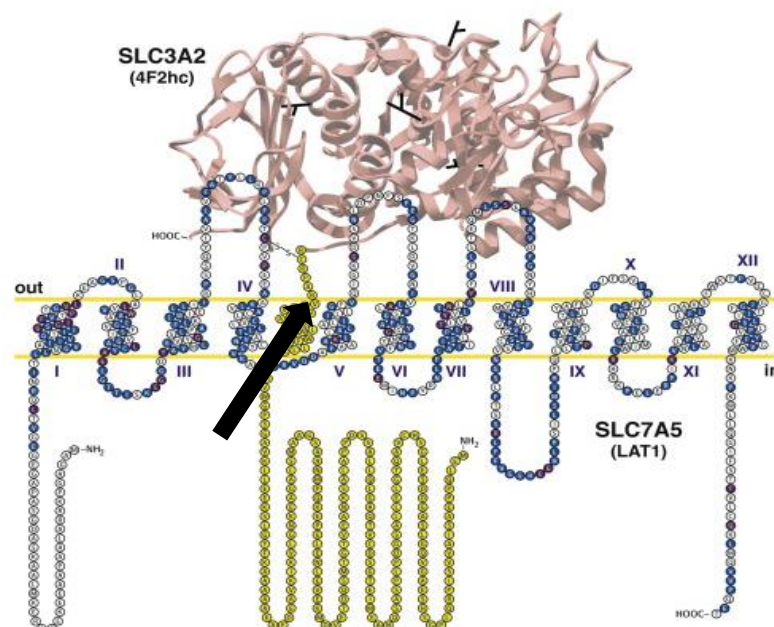


**Figure 1.11. Model of the human 4F2hc/LAT1 heterodimer**

Figure taken from Fotiadis et al., 2013 (Fotiadis et al. 2013). The light subunit consists of 12 predicted transmembrane domains (TMDs shown as roman numerals) associated with the heavy subunit 4F2hc through a disulphide bridge. The heavy subunit (1 TMD,

shown by an arrow) has 4 glycosylation sites and an intracellular N-terminus and an extracellular C-terminus. In contrast, the light subunit has intracellular termini and is not glycosylated.

#### 1.10.1.3. LAT3 and LAT4

Members of the SLC43 family of transporters LAT3 (SLC43A1) and LAT4 (SLC43A2) share around 57% amino acid sequence identity, transport neutral amino acids in a Na<sup>+</sup> and Cl<sup>-</sup> independent manner and unlike the other LATs, LAT3 and LAT4 do not need co-expression of other proteins to associate with them in the plasma membrane; and they work as amino acid facilitated diffusers rather than exchangers (Bodoy et al. 2013). LAT3 and LAT4 transport activity has preferential substrate specificity for L-BCAAs and L-Phe and amino alcohols, and they are localized mainly in liver, skeletal muscle and pancreas (Babu et al. 2003). However the physiological role of these transporters is poorly understood, and their low substrate affinity (e.g. Km > 180 μM for L-Phe) may mean that their contribution to amino acid transport is low in some of the cells in which they are expressed (Bodoy et al. 2013).

#### 1.10.2. System γ<sup>+</sup> L transporters

System γ<sup>+</sup> transporters (Table 1.2) are responsible mainly for the uptake of cationic amino acids in non-epithelial cells, with important functions in cell metabolism such as the formation of nitric oxide, urea, creatine, and agmatine from arginine, and polyamines, proline and glutamine from ornithine (Closs et al. 2006). Like LAT1 and LAT2 their light sub-units are SLC7 proteins which form heterodimers with 4F2hc and their SLC7 sub-units are sufficiently similar to those in LAT1 and LAT2 to allow them to transport large neutral L-amino acids e.g. L-leucine.

However, their strong tendency to transport cationic amino acids means that, in the presence of physiological amino acid mixtures *in vivo*, they are unlikely to be significant contributors to L-leucine transport.

##### 1.10.2.1. γ<sup>+</sup>LAT1

4F2hc/γ<sup>+</sup>LAT1 (SLC7A7) is a sodium-independent obligatory exchanger of cationic amino acids in exchange for extracellular neutral amino acid with an extracellular Na<sup>+</sup> ion

(Deves and Boyd 1998). System  $\gamma^+L$  are mainly expressed in small intestine, kidney, spleen, leucocytes, placenta and epithelial cells including lung (Kanai et al. 2000).

#### 1.10.2.2. $\gamma^+LAT2$

4F2hc/ $\gamma^+LAT2$  (SLC7A6) functions in a similar way to  $\gamma^+LAT1$  in that it mediates the efflux of L-arginine in exchange for L-glutamine and  $Na^+$ .  $\gamma^+LAT2$  is expressed in many organs like brain, small intestine, testis, parotids, heart, kidney, lung and thymus (Bröer et al. 2000).

### 1.10.3. System $b^{0,+}$ transporters

System B and  $b^{0,+}$  transporters were originally described as a transport activity largely expressed in epithelia, which carried a number of amino acids including neutral amino acids such as L-alanine (Pan and Stevens 1995) and L-leucine.

#### 1.10.3.1. $b^{0,+}AT$

The rBAT/ $b^{0,+}AT$  (SLC7A9) transporter is involved in the sodium independent exchange of extracellular cationic amino acids and cystine for intracellular neutral amino acids (Bertran et al. 1992). rBAT/ $b^{0,+}AT$  has an extracellular high affinity for cationic amino acids and cystine and an intracellular affinity for neutral amino acids (Reig et al. 2002). Like the  $\gamma^+LAT$  transporters,  $b^{0,+}AT$  is a heterodimer containing an SLC7 protein, but unlike  $\gamma^+LAT$  transporters its binding partner is the glycoprotein rBAT not 4F2hc. As for  $\gamma^+LAT$  they can transport large neutral amino acids including L-leucine (Table 1.2) but, in the presence of physiological amino acid mixtures their contribution to L-leucine transport is again probably small.

#### 1.10.3.2. $B^0AT1$

$B^0AT1$  (SLC6A19) is a  $Na^+$  dependent amino acid transporter that binds to all large neutral non-aromatic system L amino acids, but L-leucine seems to be the preferred substrate.  $B^0AT1$  activity requires the co-expression of collectrin (transmembrane protein 27 (TMEM27)) or angiotensin-converting enzyme 2 (ACE-2) (rather than rBAT) for surface expression in the kidney and intestine, respectively (Bröer 2009). A recent

study has described novel inhibitors for B<sup>0</sup>AT1 which may be useful to restrict intestinal absorption of gluconeogenic amino acids as a possible therapy in T2DM (Cheng et al. 2017, Jiang et al. 2015).

Even though B<sup>0</sup>AT1 is an efficient L-leucine transporter, its expression is largely confined to epithelia (Table 1.2) and there is no evidence at present that it is expressed in pancreatic  $\beta$  cells.

In view of the above, in the remainder of this thesis, attention will focus on L-leucine transporters LAT1 (Section 1.10.1.1), LAT2 (Section 1.10.1.2) and LAT3/4 (Section 1.10.1.3).

**Table 1.2. SLC gene families encoding proteins that transport L-leucine in humans.**

(Summarised from SLC tables at <http://slc.bioparadigms.org/>)

System	Gene name	Protein name	Aliases*	Transport type**	Substrates	Tissue and cellular expression
L	SLC7A5	LAT1	[4F2hc], 4F2Ic, system L	E (similar intra- and extracellular selectivities, lower intracellular apparent affinity)	large neutral L-amino acids, T3, T4, L-DOPA, BCH	pancreatic $\beta$ cells, brain, ovary, testis, placenta, spleen, colon, blood-brain barrier, fetal liver, activated lymphocytes, tumour cells
L	SLC7A8	LAT2	[4F2hc], system L	E (similar intra- and extracellular selectivities, lower intracellular apparent affinity)	Neutral L-amino acids, T3, T4, BCH	small intestine, kidney, lung, heart, spleen, liver, brain, placenta, prostate, ovary, fetal liver, testis, skeletal muscle
L	SLC43A1	LAT3	POV1	F	L-BCAAs, amino alcohols	liver, skeletal muscle, placenta, kidney podocytes
L	SLC43A2	LAT4		F	L-BCAAs, amino alcohols	placenta, kidney, peripheral blood leukocytes, small intestine
$\gamma^+$ L	SLC7A7	$\gamma^+$ LAT1	[4F2hc], system $\gamma^+$ L	E (preferentially intracellular cationic amino acid against extracellular neutral amino acid / Na <sup>+</sup> )	Cationic amino acids (Na <sup>+</sup> indep.), large neutral L-amino acids (Na <sup>+</sup> dep.)	small intestine, kidney, spleen, leucocytes, placenta, lung/ basolateral in epithelial cells
$\gamma^+$ L	SLC7A6	$\gamma^+$ LAT2	[4F2hc], system $\gamma^+$ L	E (preferentially intracellular cationic amino acid against extracellular neutral amino acid / Na <sup>+</sup> )	Cationic amino acids (Na <sup>+</sup> indep.), large neutral L-amino acids (Na <sup>+</sup> dep.)	brain, small intestine, testis, parotids, heart, kidney, lung, thymus
$b^{0,+}$	SLC7A9	$b^{0,+}$ AT	[rBAT], system $b^{0,+}$	E (preferentially extracellular cationic amino acid and cystine against intracellular neutral amino acid)	Cationic amino acids, large neutral amino acids	kidney, small intestine, liver, placenta
None assigned	SLC6A19	$B^0$ AT1	[TMEM 2T, ACE-2] $B^0$ AT1, HND	Na <sup>+</sup> -dependent	Large neutral non-aromatic amino acids	intestine (duodenum, jejunum, ileum), stomach, kidney, liver, prostate

\*Alternative names shown in square brackets e.g. [4F2hc] indicate proteins which form heterodimers with the L-leucine transporter shown in this row of the table.

\*\*Abbreviations for transport type: E: Exchanger; F: Facilitated transporter.

#### 1.10.4. Coupling between System L and active transporters

Even though LAT1 and LAT2 amino acid transporters are regarded as passive exchangers of amino acids across biological membranes (Table 1.2), it is possible for such transporters to perform overall active transport (“pumping”) of amino acids across membranes by coupling to amino acid concentration gradients generated by a primary (ATP-utilising) active  $\text{Na}^+$  transporter (Na, K-ATPase) and a secondary active  $\text{Na}^+$  - dependent amino acid transporter (e.g. SNAT2, SLC38A2) as shown in Figure 1.12 (Baird et al. 2009). In this way some cells (e.g. L6 skeletal muscle cells) can effectively “pump” L-leucine from extracellular fluid to accumulate a higher concentration in the cytosol (Evans et al. 2007). Overall therefore, SNAT2 mediates the uptake of small neutral amino acids (principally L-glutamine) and couples with LAT1 since LAT1 exports L-glutamine in exchange for L-leucine import (Figure 1.12) (Dodd and Tee 2012).

In many cancer cell lines a similar coupling between amino acid transporters to drive active L-leucine uptake occurs, but in this case the System A transporter SNAT2 is replaced by the System ASC transporter ASCT2 (SLC1A5) (Nicklin et al. 2009).

In epithelia, active transport of L-leucine into cells can be performed more directly (without  $\text{Na}^+$ -dependent SNAT2 or ASCT2 as intermediate) by direct  $\text{Na}^+$ -dependent transport of L-leucine on  $\text{B}^0\text{AT1}$  (Section 1.10.3.2).

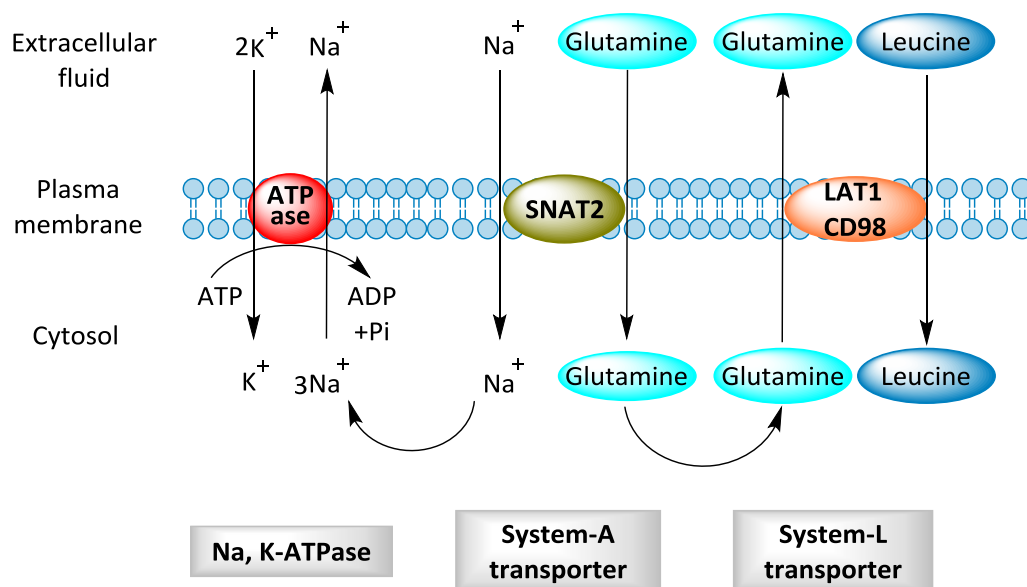


### **Figure 1.12. Coupled SNAT2/LAT1 system**

Figure redrawn from (Hundal and Taylor 2009). Coupling between a primary active transporter (Na, K-ATPase), a secondary active System A amino acid transporter (SNAT2, SLC38A2), and a tertiary active System L amino acid transporter (the LAT1/CD98, SLC7A5/SLC3A2 heterodimer) (Baird et al. 2009).

#### **1.11. Physiological responses of System L amino acid transporters**

Of the four LAT transporters (Sections 1.10.1.1 to 1.10.1.3) that may regulate L-leucine transport in mammalian cells, attention has focused mostly on LAT1 as the System L amino acid transporter that probably plays the most important role in the mTORC1 activation, and may regulate both  $\beta$  cell signalling and function (Cheng et al. 2016). LAT1 is highly expressed in pancreatic  $\beta$  cells (Cheng et al. 2016) and it responds to physiological stresses or growth factors. For example, not only does LAT1 play a fundamental role in promoting cell growth and survival by providing cells with the necessary levels of essential amino acids including L-leucine; studies have also demonstrated that conversely growth factors stimulate L-leucine uptake by inducing the expression of LAT1 via mTOR, for example in the action of platelet-derived growth factor on vascular smooth muscle cells (Liu et al. 2004). This observation that not only does L-leucine activate mTORC1 but that mTORC1 also activates L-leucine transport through LAT1 has also been made in human primary trophoblast cells, using the BCH-inhibitable uptake of L-[ $^3$ H]-leucine. These studies revealed an effect of mTOR inhibition on amino acid uptake (Rosario et al. 2013), suggesting that expression of the transporter on the cell surface was being altered.

As the LAT1 System L transporter is a Na<sup>+</sup>-independent obligatory exchanger of aromatic amino acids and BCAAs composed of two protein subunits, the amino acid permease (SLC7A5 (LAT1) and the 4F2hc or CD98 (SLC3A2) glycoprotein (Baird et al. 2009), this leads to the question of whether physiological stimuli that increase the activity and expression of the transporter are acting mainly on SLC7A5 or SLC3A2. There is evidence that SLC7A5 isoform expression has a higher correlation with System L transport function than SLC3A2 in many tissues including skeletal muscle, adipose, placenta and brain (Poncet et al. 2014).

Chand and Legge (Chand and Legge 2011), investigated the uptake of L-leucine by ovarian follicles, measuring L-[<sup>3</sup>H]-leucine uptake to demonstrate specificity of influx via LATs, and test whether uptake rates were dependent on intracellular amino acid availability (Chand and Legge 2011). Studying dependence of transport on intracellular amino acid availability, or rates of efflux of L-leucine from inside to outside across the plasma membrane, is difficult because of the problem of incorporation of L-[<sup>3</sup>H]-leucine into intracellular metabolites, especially protein. Such problems in studying the cellular mechanism of transporters can be partially overcome by performing a radioactive assay to measure transport across transporter-containing liposomes isolated from cell membranes. This is potentially useful to determine transport with elimination of routing into metabolites or removal of amino acids from the cytosolic side of the membrane. In human placental microvillous plasma membrane vesicles, with no amino acid added inside the vesicles, amino acid uptake was measured in this way to demonstrate that, in addition to operating as amino acid exchangers, LAT1 and LAT2 transporters may also be able *in vitro* to perform non-exchange facilitated transport, suggesting that exchange transporters do not function exclusively as obligate exchangers. (Widdows et al. 2015)

In view of the suspected functional importance of changes in LAT1 activity or expression in mammalian cells, a number of important molecular methods have been developed to knock out LAT1 experimentally. For example in KB human oral cancer cells *in vitro* an investigation of the effects of silencing LAT1 expression with small interfering RNA (siRNA) on cell growth, showed that the expression of LAT1 mRNA and protein were successfully inhibited. Also, the uptake of L-leucine was inhibited by the siRNA silencing of LAT1, and growth inhibition was induced by the LAT1-mediated blocking of neutral amino acid transport (Kim et al. 2006). Similarly siRNA silencing of LAT1 expression in rat pancreatic islets has been used to show inhibition of mTORC1 signalling (Cheng et al. 2016).

In order to find the relevance of SLC7A5 in the amino acid uptake for activation of mTOR signalling *in vivo*, Cre-Lox technology has been used to generate transgenic mice with tissue-specific knockout of SLC7A5 expression (for example in skeletal muscle) by means of SLC7A5-Flox and Cre transgenes (Poncet et al. 2014). This shows that Cre-Lox

knockout of LAT1 may also be possible in islets *in vivo*.

### **1.12. Regulation of LAT1 expression in response to D-glucose**

In the pancreatic  $\beta$ -cells, LAT1 is responsible for the supply of essential amino acids including L-leucine (Cheng et al. 2016). In view of the importance of L-leucine in regulation of mTORC1 signalling and  $\beta$  cell mass (Section 1.8) and the role of D-glucose and L-leucine in stimulating insulin secretion from  $\beta$  cells (Sections 1.2.3 and 1.9), it is important to understand the mechanisms that regulate LAT1 in response to D-glucose supply in these cells, and whether such effects might play a role in the toxic effects of high D-glucose concentration on  $\beta$  cells (glucotoxicity) as discussed in Section 1.1.5.

In cell types other than  $\beta$ -cells there have been several studies of the effect of D-glucose on LAT1 expression, either by D-glucose starvation *in vitro* or by investigation of factors such as hypoxia or ischaemia, which promote anaerobic glycolysis and hence severe D-glucose depletion *in vivo*. In cultured rat retinal capillary endothelial cells, 8 – 24h of D-glucose deprivation led to increased expression of mRNA for both LAT1 (SLC7A5) and 4F2hc/CD98 (SLC3A2) (Matsuyama et al. 2012). Similarly, 30h of D-glucose deprivation in the leukaemia cell line HL60 increased LAT1 (SLC7A5) protein expression detected by immunoblotting (Polet et al. 2016). *In vivo* a study of tumours from 160 non-small cell lung cancer patients showed by immunohistochemistry that LAT1 (SLC7A5) protein expression correlated strongly (as expected) with expression of 4F2hc/CD98 (SLC3A2), but also showed a strong positive correlation with expression of a number of hypoxia markers including HIF-1 $\alpha$  and the glucose transporter GLUT1 (Kaira et al. 2011).

A clinically important situation in which hypoxia and ischaemia lead to high mortality and morbidity is neonatal hypoxic-ischaemic brain damage (Hristova et al. 2016). LAT1 is regarded as a functionally important transporter at the blood-brain barrier (i.e. in brain capillary endothelial cells) where it plays a major role in controlling entry of large neutral amino acids into brain interstitial fluid (Killian and Chikhale 2001), including the neurotransmitter precursor L-glutamine (Dolgodilina et al. 2016). Interestingly, in contrast to the D-glucose-deprived retinal capillary endothelial cells described above (Matsuyama et al. 2012), cultured bovine brain capillary endothelial cells exposed to

hypoxia (1% O<sub>2</sub>) for 24-48h showed a decline in LAT1 (SLC7A5) mRNA expression, arising from destabilisation of the mRNA (Boado et al. 2003), but GLUT1 mRNA increased.

Effects of this type on LAT transporters have not been reported in  $\beta$  cells. However, as a major biological role of the  $\beta$  cell is to sense changes in intracellular energy status (i.e. ATP/ADP ratio and AMP concentration) in response to changes in supply of metabolic fuels, and to respond by secreting insulin (Sections 1.2.3 and 1.9), it is possible that changes in D-glucose supply may act on LATs through the energy status sensor AMPK (Section 1.6).

AMPK as an energy regulator plays a key role in energy homeostasis. Moreover, in response to increase in the AMP:ATP ratio, AMPK is activated by phosphorylation of threonine 172 (Thr172) in the  $\alpha$  subunit (Park et al. 2013) (Section 1.6) (Figure 1.9). Interestingly, in skeletal muscle increased intracellular concentration of AMP as a result of utilization of ATP activates AMPK during exercise, and this activation is an important signal leading to exercise induced D-glucose uptake. In skeletal muscle, the increment of D-glucose uptake during exercise is regulated by AMPK stimulating translocation of the GLUT4 D-glucose transporter protein from an intracellular location to plasma membrane (Kurth-Kraczek et al. 1999) (Figure 1.9). Additionally, the AMP analogue 5-Aminoimidazole-4-carboxamide-1-beta-D-ribofuranoside (AICAR), which selectively increases AMPK activity, up-regulates GLUT4 protein levels in the muscle cells. This increased GLUT4 protein synthesis arises because AICAR-activated AMPK increases GLUT4 gene transcription in muscle (Zheng et al. 2001). Recent studies in diabetic heart also showed increase in D-glucose uptake arising from a similar contraction and AMPK-induced GLUT4 translocation (Luiken et al. 2015).

### **1.13. Hypothesis and aims of this study**

In view of the effects described in the previous section, it is of interest to investigate whether AMPK regulates LAT transporters in  $\beta$  cells.

**The hypothesis to be tested in this thesis is therefore that D-glucose supply, modulates AMPK, regulating LAT transporters and therefore controls the rate of L-leucine**

**transport in the rat  $\beta$  cell line INS1E.** This D-glucose-responsive insulinoma cell line has been widely used previously as a cultured  $\beta$  cell model (Hohmeier et al. 2000) and has recently been shown in this laboratory to exhibit LAT-dependent mTORC1 activation (Cheng et al. 2016).

In cultured  $\beta$  cells it has also been shown that *increasing* the extracellular concentration of D-glucose or of amino acids strongly inhibits AMPK (Leclerc and Rutter 2004). Therefore this thesis will also test the related hypothesis that an elevated extracellular D-glucose concentration (as in T2DM), down regulates LAT transporters, which might be a possible contributor to glucotoxicity, for example through acute inhibition of mTORC1.

The specific aims of this project were:

- 1) To characterise L-leucine transport & signalling in INS1E cells and confirm the conclusion from the earlier study that these cells show LAT-dependent mTORC1 activation (Cheng et al. 2016).
- 2) To investigate the effect of extracellular D-glucose concentration on L-leucine transport and LAT transporter expression in INS1E cells, and the possible involvement of AMPK in these effects
- 3) To test a possible AMPK-mediated activation mechanism for LAT1 transporters arising from the work in (2) above by over-expressing a human LAT1 (SLC7A5) cDNA construct in a readily transfected human cell line (HEK293A), thus attempting to reconstitute the effects observed in (2).

The experiments arising from these 3 aims are presented in Chapters 3, 4 and 5 of this thesis respectively.

## Chapter 2. Methods

---

### 2.1. Culture

INS1E cells (rat insulinoma cell line 1E) (Hohmeier et al. 2000) were routinely propagated in a humidified atmosphere (95% air, 5% CO<sub>2</sub>) in Growth Medium (GM) comprising RPMI 1640 medium (Sigma) containing 11 mM D-glucose supplemented with 5% (v/v) heat inactivated batch-tested foetal bovine serum (FBS), 1 mM sodium pyruvate, 10mM HEPES, 55 µM β-mercaptoethanol, and 1% P/S/N (100 µg/ml streptomycin, 100 units/ml penicillin sulphate and 100 units/ml Neomycin). Fresh GM was added every 2 to 3 days. Stock cultures (80% confluent) were passaged at 7 day intervals by aspirating the GM and rinsing the monolayer with phosphate-buffered saline (PBS), followed by incubation in the culture incubator for 3-5 min in 1ml of 0.5% trypsin/EDTA per 9cm diameter Petri dish to allow cell detachment. Cells were then suspended in GM and seeded onto fresh 9cm Petris at a density of 75 x 10<sup>4</sup> per Petri.

The cells were used at passage number 70 to 80 and were seeded for amino acid transport experiments at a density of 20 x 10<sup>4</sup> on 15mm diameter culture wells in 0.5ml of GM per well, and used for experimental incubations 3 days after seeding. By this stage the cells had reached 80% confluence.

MIN6 cells (mouse insulinoma cell line 6) (Ishihara et al. 1993) at passage number 25 to 45 were cultured as above, but the GM was made from DMEM (Dulbecco's modified Eagle's Medium, Sigma D6429) with 25mM D-glucose, supplemented with 15% (v/v) heat-inactivated FBS, 1% P/S/N, 75 µM β-mercaptoethanol and 40mM sodium bicarbonate.

HEK293A cells - a sub-clone of the Human Embryonic Kidney (ATCC® CRL-1573™) cell line which shows flattened morphology and improved adherence on culture vessels, was obtained from Dr David Lodwick, Department of Cardiovascular Sciences, University of Leicester. The cells were cultured as for the MIN6 cells above, but the GM was supplemented with 10% (v/v) heat-inactivated FBS, and 1% P/S/N.

L6 rat skeletal muscle cells (sub-clone G8C5 (Evans et al. 2007)) were propagated under

humidified 95% air, 5% CO<sub>2</sub> in GM comprising DMEM (Life Technologies 11880-028) with 5 mM D-glucose and 1 mM sodium pyruvate, supplemented with 10mg Phenol Red/L, 1% v/v Penicillin and Streptomycin (as above but without Neomycin), 2mM L-glutamine and 10% v/v heat inactivated batch-tested FBS). The cells were used at passage number 5 to 25 and were seeded for transport experiments at a density of  $7.5 \times 10^4$  on 15mm diameter culture wells in 0.5ml of GM per well, and used for experimental incubations 2 days after seeding. By this stage the cells had reached 80% confluence and had not fused to myotubes.

Low (0 D-glucose), normal (5mM D-glucose) or high (25mM Glucose) were used in INS1E cells to study the effect on L-leucine transport and were chosen based on previous studies in retinal capillary endothelial cells where the D-glucose deprivation increased L-[<sup>3</sup>H]-leucine uptake and LAT transport activity (Matsuyama 2012).

### **Collagen coated plates**

To improve cell adhesion in HEK293A transfections, culture plates were coated with collagen. Under sterile conditions, 5.75ml of Glacial Acetic Acid (BDH AnalaR) was mixed with 50ml of ultra-pure water and filtered through a 0.2u Acrodisc. The Collagen Solution (Bovine Calf Skin Collagen, Type I Sigma C8919) was diluted in sterile 0.1M Acetic Acid (1mg/ml or 0.1% in 0.1M Acetic Acid). Collagen Solution was added to the plates at a density of 5µg/cm<sup>2</sup>. The plates were left with the Collagen with the lid off, incubating overnight with the fan running in the culture hood at room temperature (about 20°C). The following morning, plates were rinsed (each vessel 3x) with a volume of HBSS slightly greater than the original volume of Collagen Solution to remove the Acetic Acid, and then stored wrapped in their original plastic bags at 4°C.

### **2.2. Isolation of rat islets of Langerhans**

Islets were isolated from male Wistar Albino rats (200g-250g) obtained from Charles River, UK and held in specific pathogen-free conditions at the University of Leicester's Preclinical Research Facility, receiving standard chow, and when reached the appropriate weight, rats were killed by cervical dislocation by trained animal

technicians. 2-3ml of cold collagenase solution (from *Clostridium histolyticum*, Type Xi, Sigma-Aldrich, Poole, UK; 1mg/ml in Modified Eagle's Medium (MEM), Sigma-Aldrich) was injected into the pancreas via the common bile duct following clamping at the Ampulla of Vater. The distended pancreas was then removed and incubated in a stationary water bath at 37°C for 17 min for enzymatic digestion. The pancreatic islets were washed twice (340 x g, 4°C, acceleration speed 9, brake speed 9, for 3 minutes on an Eppendorf, 5810R centrifuge, in MEM supplemented with 10% Newborn Calf Serum (NCS) and 100U/ml penicillin + 0.1mg/ml streptomycin to stop the digestion and remove any remaining collagenase solution. After the second wash the pancreatic tissue was vortexed and passed through a sieve in order to discard as much of the exocrine and other contaminating tissue as possible. In order to obtain a pure preparation of islets, a purification gradient was set up by adding Histopaque (a polysucrose solution with a density of 1.077g/ml) to the pancreatic tissue and centrifuging 1500 x g, 4°C, for 20 minutes. Islets were removed from the interphase of the histopaque and MEM and washed three times by centrifuging as above and handpicked (using a pipette with a wide orifice) under a stereomicroscope in 5ml of RPMI supplemented with 10% Foetal Bovine Serum (FBS) and 100U/ml penicillin + 0.1mg/ml streptomycin.

### **2.3. Culture of rat islets of Langerhans**

Islets were cultured as groups of approximately 150 islets in 60mm sterile bacterial grade Petri dishes, using RPMI 1640 medium (as in Section 2.1) supplemented with 10% FBS, 100U/ml penicillin + 0.1mg/ml streptomycin, with a D-glucose concentration of 11 mM and maintained in a humidified incubator (37°C, 95% air/5% CO<sub>2</sub>). The medium was changed every second day.

### **2.4. LAT1 and CD98 cDNA construct design**

For functional expression of human LAT1 (SLC7A5) cDNA in HEK293A cells, a human LAT1 ORF Shuttle Clone (Source Bioscience, reference OCAo5051G0753D; GenBank DQ893338.2) had previously been cloned into the pLEICS29 expression vector (Figure 2.1 and Table 2.1) by the University of Leicester Protein Expression Laboratory PROTEX in collaboration with Dr TP Herbert, Department of Cell Physiology & Pharmacology. The

LAT1 construct in pLEICS-29 had been designed to express a LAT1 protein with an enhanced Green Fluorescent Protein (eGFP) tag and linker sequence at its C-terminus, giving the following C-terminal sequence: EFMQSTVPRARDPPVAT-**EGFP** EFMQSTVPRARDPPVAT-**EGFP**.

The 8260 bp plasmid arising from this (made up of 6696 bp from the pLEICS-29 vector plus 1564bp from the LAT1 ORF clone) and the eGFP-tagged LAT1 fusion protein expressed from it are referred to in the rest of this thesis as LAT1-eGFP.

Similarly a human CD98/4F2hc (SLC3A2) ORF Shuttle Clone (ACRO biosystems Ref HC00322 NM\_001013251.2) had previously been cloned into the pLEICS49 expression vector (Figure 2.1 and Table 2.1) by PROTEX. This CD98 construct had been designed to express a CD98 protein with a His4 3xFLAG (i.e. DYKDDDDK) tag and linker sequence at its C-terminus, giving the following C-terminal sequence:

TEV-2-His4- DYKDDDDKDYKDDDDKDYKDDDDK-GSEN.

The 9182 bp plasmid arising from this (made up of 7592 bp from the pLEICS-49 vector plus 1590 bp from the CD98 ORF clone) and the HisFLAG-tagged CD98 fusion protein expressed from it are referred to in the rest of this thesis as CD98-FLAG.

For control experiments, the empty ligated vectors pLEICS-29 and pLEICS-49 (without the LAT1 and CD98 amino acid transporter inserts) were also obtained from PROTEX and were used in the HEK293A transfection experiments in Chapter 5 to assess non-specific effects on L-leucine transport that may have arisen from plasmid transfection.

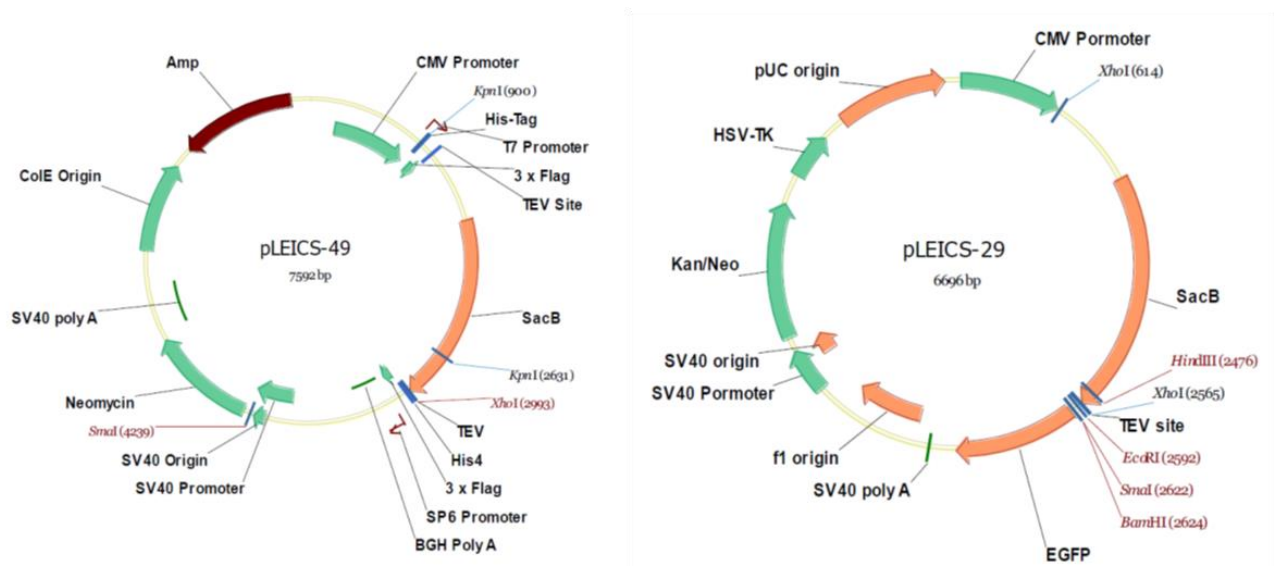


**Figure 2.1. Plasmids with 3xFlag His4 (pLEICS-49) and EGFP (pLEICS-29)**

The plasmid diagrams are taken from:

<https://www2.le.ac.uk/colleges/medbiopsych/facilities-and-services/cbs/protein-and-dna-facility/protex/available-vector/maps/view> (PROTEX 2017).

**Table 2.1.** Details of the pLEICS-29 and pLEICS-49 vectors shown in Figure 2.1

Vector Name	AR	Tag/Flag	Secretion Signal	Protease cleavage	Tag and linker	Sequence primers
pLEICS-29	Kan	C-EGFP	TEV, Extra ENLYFQ	L-TEV site-2- EFMQSTVPRARD PPVAT -EGFP	EFMQSTVPRA RDPPVAT - EGFP	pLEICS-29-Seq-F pLEICS-29-Seq-R
pLEICS-49	Amp	C-His4/3 x Flag	TEV, Extra ENLYFQ	TEV-2-His4- DYKDDDDKDYKD DDDKDYKDDDDK -GSEN	T7 Promoter pLEICS-12- Seq-R	

AR denotes antibiotic resistance, Kan is kanamycin, Amp is ampicillin.

## 2.5. Bacterial (competent cell) transformation

Transformation of bacteria with the plasmids was carried out to replicate the plasmids by adding 2µl of plasmid DNA (50-100 ng/µl) into a vial of One Shot® TOP10 chemically competent *E-coli* cells (Invitrogen Cat. No. C4040-10) and incubating for 30 minutes on ice

The vial was then heat shocked at 42°C in water bath for 30-60 secs and then placed

back on ice for 2 minutes. After that 500 µl of Lysogeny broth or S.O.C. Medium (supplied with the kit) was added to the bacteria and incubated at 37°C in a shaker for 45 minutes. This outgrowth step was performed to allow the bacteria time to generate the antibiotic resistance proteins encoded on the plasmid backbone so that they would be able to grow once plated on the antibiotic-containing agar plate. The mix contained in the vial was then spread on a pre-warmed antibiotic selective plate (Kanamycin for pLEICS-29 and Ampicillin for pLEICS-49) and incubated overnight at 37°C. On the following day the colonies were selected to culture on a shaker at 37°C for 6 hours in Lysogeny broth buffer containing 100 mg/L of the relevant antibiotic. The colony culture was then inoculated into a 1L conical flask containing 250ml of Lysogeny broth mixed with antibiotic as above and shaken overnight.

To isolate the plasmid DNA from the recombinant *E-coli* culture, a GeneJET™ plasmid maxiprep kit (Thermo Scientific 11551645) was used after centrifuging the content of the culture and the pelleted bacterial cells were suspended and subjected to SDS/alkaline lysis to liberate plasmid DNA. The resulting lysate was neutralized with SDS following the manufacturer's instructions to re-anneal plasmid DNA. Cell debris and the SDS precipitate (including precipitated proteins and chromosomal DNA) were pelleted by centrifugation. The supernatant containing plasmid DNA was loaded onto the purification column. The high salt concentration of the lysate created appropriate conditions for plasmid DNA binding to the silica membrane in the spin column. The adsorbed DNA was washed to remove contaminants and eluted with the manufacturer's Elution Buffer.

The integrity and size of the isolated plasmids was confirmed by running out an aliquot of the plasmid preparation (1 µg DNA per lane) on a 2% agarose gel for 60 min at 100 volts using a 1 – 10 kilobase ladder (NEB Ref #N3232) as a size marker. The size of the plasmids was checked and shown to be consistent with the sizes stated in Section 2.4 above. The LAT1 insert sequence was confirmed by amplification by PCR using the PROTEX pLEICS-29 sequencing primers listed in Table 2.1 and the purified plasmid as template, followed by sequencing of the amplicons (Level 2 sequencing performed by the Protein and Nucleic Acid Chemistry Laboratory, University of Leicester). The

reported sequence is shown in Appendix 1.

## **2.6. Transfection of HEK293A cells by calcium phosphate precipitation**

Transfections were performed on HEK293A cells which had been plated at  $10 \times 10^4$  cells per 15mm well on collagen-coated 24-well culture plates 6 h before transfection. A mixture of 0.6  $\mu\text{g}$  of plasmid DNA was made with 5.5 $\mu\text{l}$  of 2M  $\text{CaCl}_2$  and made up to a total volume of 45 $\mu\text{l}$  with sterile water for each transfection. This solution was then mixed with 45 $\mu\text{l}$  of double strength HBS at pH 7.0 (i.e. 50mM HEPES, 280mM NaCl, 1.5mM  $\text{Na}_2\text{HPO}_4$  pH 7.0). After 20 minutes to allow calcium phosphate precipitation and binding of the DNA to the precipitate, 90 $\mu\text{l}$  of the DNA- $\text{CaCl}_2$ -HBS mix was added drop-wise over the plated cells in each culture well containing 500 $\mu\text{l}$  of DMEM-based growth medium and the dishes were returned to the incubator and cultured with the minimum of disturbance. Medium was changed 24 h later by aspirating the transfection mixture and adding the same volume of DMEM-based growth medium, and transport experiments were performed 48h post-transfection.

For cultures transfected with eGFP plasmids, efficiency of transfection was confirmed from the intensity of fluorescence detected on an inverted Olympus IX81 motorized microscope with a Scan<sup>R</sup> screening platform and a Cell<sup>R</sup> imaging station (Advanced Imaging Facility, University of Leicester).

## **2.7. Transport Assays**

For estimation of L-leucine transport activity, cells in 15mm multi-wells were pre-incubated for 3-6 hours in the culture incubator in DMEM (modified to contain 0.8 mM L-leucine, 2mM L-glutamine and 0, 5 or 25mM D-glucose). This was made by adding the required amounts of L-leucine, L-glutamine or D-glucose to a home-made stock which lacked these components (shown in Appendix) 2. AICAR was also added to some cultures with a final concentration of 750  $\mu\text{M}$ . Transport experiments were carried out with Krebs Ringer Buffer (KRB) containing 115mM NaCl, 5mM KCl, 10mM  $\text{NaHCO}_3$ , 2.5mM  $\text{MgCl}_2$ , 2.5mM  $\text{CaCl}_2$ , 20 mM HEPES pH 7.4, 16.7mM D-glucose and 2 mM L-glutamine. L-[4,5- $^3\text{H}$ ]-Leucine (Perkin Elmer) plus unlabelled L-Leucine was then added

to the KRB to give a final radio-isotope concentration of 5 $\mu$ Ci/ml and a final total L-Leucine concentration of 0.05mM. BCH was also added to some cultures to give a final concentration of 2.5 mM to abolish System L amino acid transport activity. Cultures with  $^3\text{H}$  were then incubated at room temperature (20°C) for exactly 1 minute to allow transport of the L-[4,5- $^3\text{H}$ ]-leucine into the cells. ( $^3\text{H}$  uptake in each well was corrected by subtraction of the  $^3\text{H}$  uptake in another well on the same multi-well plate measured in the presence of 10mM L-leucine as a measure of the non-specific binding of the L-[4,5- $^3\text{H}$ ]-leucine to the well). The cells were then immediately placed on ice, the medium aspirated off, and the cells rapidly washed 3 times in ice-cold KRB to remove extracellular  $^3\text{H}$ . NaOH (200  $\mu$ l of 0.05M) was then added to each well, the cells were scraped with a 1ml rubber-tipped syringe plunger and the lysates transferred to microcentrifuge tubes. The lysates were then incubated at 70°C for 30 min to dissolve the cell proteins. A fraction of the lysate was then transferred to a scintillation vial containing Ecoscint A scintillant and allowed to stand for at least an hour to allow chemiluminescence to decay before quench-corrected scintillation counting using a Beckman LS6500 multi-purpose scintillation counter. An aliquot of lysate was also taken for measurement of total cell monolayer protein by the Folin protein assay (Section 2.8). The L-[4,5- $^3\text{H}$ ]-leucine influx transport rate is expressed as pmoles / mg protein / min.

For estimation of System A transport activity, the same method was used, but instead of Krebs Ringer Buffer, the transport incubation was performed in Heps-buffered Saline (HBS) comprising 140 mM NaCl, 20 mM Heps, 2.5 mM MgSO<sub>4</sub>.7H<sub>2</sub>O, 5 mM KCl, 1 mM CaCl<sub>2</sub>.2H<sub>2</sub>O and 10 mg / L Phenol Red, pH 7.4. The radio-labelled amino acid that was added to the cultures was the selective System A substrate  $\alpha$ -[1- $^{14}\text{C}$ ]-methylaminoisobutyrate (MeAIB) (NEN-Du Pont NEC 671, 1.85MBq or 50 $\mu$ Ci in 500 $\mu$ l of 0.01M HCl; about 58.7 pCi/pmol). This was added to the HBS in each well and was incubated with the cells for exactly 5 min. Unlabelled MeAIB was also added to some cultures to give a final concentration of 10mM to abolish System A amino acid transport activity. ( $^{14}\text{C}$  uptake in each well was corrected by subtraction of the  $^{14}\text{C}$  uptake per well measured in the presence of 10 mM MeAIB as a measure of the non-specific binding of the  $\alpha$ -[1- $^{14}\text{C}$ ]-methylaminoisobutyrate to the well). Again the influx transport rate is expressed as pmoles / mg protein / min.

## **2.8. Folin protein assay**

To determine the total level of protein per cell sample for transport assays, a Folin protein assay was performed by mixing the protein standards (0 to 500 µg / ml of bovine serum albumin (BSA)) or the protein assay samples with Folin Ciocalteu Reagent and alkaline copper tartrate solution and incubating for 40 minutes at room temperature to allow to allow the blue colour of the reduced Folin reagent to develop (Lowry et al. 1951). Finally the concentration of the protein was estimated by reading absorbance at 650 nm on a 96-well plate reader.

## **2.9. Cell viability test (MTT)**

Change in the mass of viable cells was measured by using (3-(4,5-Dimethylthiazol-2-yl)-2,5-diphenyltetrazolium bromide, a yellow tetrazole) (MTT) (Sigma, Ref M5655). This assay is based on the enzymatic cleavage and conversion of the soluble yellow dye MTT to the insoluble purple formazan in the mitochondria of living cells. Therefore, the amount of formazan produced is proportional to the number of living cells and the rate of metabolic activity of those cells. After the cells achieved the required state of confluence, they were treated with experimental test media on a 24 well plate (0.5ml/well). 1 hour before the end of the test media incubation, 30µl of the MTT solution (2mg/ml in DMEM) was added to each well and incubated for 1 hr at 37°C under 5% CO<sub>2</sub>. Care was taken to minimise the exposure of MTT to light. Then the MTT medium was aspirated, each well was rinsed with 3 x 1ml 0.9% w/vol NaCl at room temperature, and the insoluble purple formazan was solubilized by adding 280µl DMSO to each well and shaking on a mechanical shaker for 15 min at room temperature. Aliquots (50µl) of the resulting purple solution were transferred to wells of a 96-well plate. The absorbance of the converted dye was measured at 520nm using a 96-well plate reader. Results are expressed as the optical density (OD) value.

## **2.10. SDS-Polyacrylamide Gel Electrophoresis and Western Blot Analysis**

After experimental treatments, INS1E cells, rat islets or transfected HEK293A cells were scraped off the culture dishes and lysed with Lysis Buffer (200 µl per 35 mm diameter

culture well; Appendix 3). Protein lysates were centrifuged at 14000 rpm on a microcentrifuge at 4°C for 10 minutes to remove insoluble material, and total protein content was determined in the supernatant using the Biorad DC™ Protein Assay.

### **2.11. Protein Assay (BioRad DC™ Protein Assay)**

As the Lysis Buffer (Appendix 3) contains detergent, which interferes with the Lowry protein assay, a separate detergent-compatible (DC) protein assay (BioRad ref #500-0122EDU) had to be used to determine the protein content of lysates prepared with this buffer. Standard solutions were prepared using different concentrations (0, 0.4, 0.8, 1.2, 1.6, 2.0 mg/ml) of BSA to construct a standard curve. 5 µl of each standard/sample was added into a 96 well plate plus 25 µl of Reagent A, an alkaline copper tartrate solution (with 20 µl of supplementary reagent S added to each ml of reagent) and 200 µl of reagent B (a diluted Folin-like reagent) per sample. After 15 minutes, absorbances were read at 750 nm.

### **2.12. SDS-Polyacrylamide Gel Electrophoresis and Western Blot Analysis**

The cell lysates (25-50µg of protein per sample) were mixed with (4X) Laemmli SDS sample buffer (62.5 mM Tris-HCl, pH 6.8, 4% SDS, 40% glycerol, 10% β-mercaptoethanol) to give a 1X final concentration. Then, samples were boiled for 3 minutes at 100°C and separated by 10% or 12.5% of ATTO mini SDS-PAGE (polyacrylamide gel electrophoresis) with a prestained protein marker (5-175 kDa).

The gels were transferred onto polyvinylidene fluoride (PVDF) microporous membranes (Millipore) (100 volts for 60 minutes) using a wet transfer System (Bio-Rad) and a transfer buffer containing 25 mM Tris, 192 mM glycine, 20% methanol, 0.2% SDS. After transfer, the membrane was blocked in 5% skimmed milk in 1xTTBS (phosphate-buffered saline (PBS) containing 0.1% Tween 20) for one hour at room temperature on an orbital shaker to block non-specific binding sites. Afterwards, the blot was washed three times for 10 minutes with 1xTTBS and incubated with a specific primary antibody (see Table 2.2) in TTBS containing 5% bovine serum albumin overnight at 4°C.

Membranes were then washed with 1xTTBS and incubated with appropriate horse-

radish peroxidase (HRP) conjugated secondary antibody (anti-rabbit IgG or anti-mouse IgG) (see Table 2.2) in 5% milk/1xTTBS for 1 hour at room temperature. The membrane was then washed three times for 10-min each in 1xTTBS, followed by 5 minutes enhanced chemiluminescence reaction (Fisher SuperSignal™ West Pico Chemiluminescent Substrate). Images were then taken using a Biorad GelDoc™ and ChemiDoc phosphorimager system and quantified and analysed by Image Lab™ Software.

**Table 2.2.** List of antibodies

Primary Antibody	Source	Catalog number	Dilution	Secondary antibody
Phospho-Akt (Ser473)	New England Biolabs	4060	1/1000	Rabbit
Phospho S6 Ribosomal Protein (Ser 240/244)	New England Biolabs	5364	1/1000	Rabbit
Phospho-p70 S6 Kinase (Thr389)	New England Biolabs	9205	1/1000	Rabbit
Ribosomal Protein S6	Santa Cruz Biotechnology	sc-74459	1/1000	Mouse
GFP (D5.1) XP Rabbit mAb	Cell Signaling Technology	2956	1/1000	Rabbit
Phospho-AMPK $\alpha$ (Thr172) (40H9) Rabbit mAb	Cell Signaling Technology	2535	1/1000	Rabbit
AMPK $\alpha$ antibody	Cell Signaling Technology	2532	1/1000	Rabbit

### 2.13. Lipofectamine transfection for siRNA

INS1E cells were plated on 35mm 6-well plates at  $50 \times 10^4$  cells per well and cultured for 24 hours in INS1E Growth Medium (Section 2.1) prior to transfection using Lipofectamine® RNAiMAX Reagent (Invitrogen) according to the manufacturer's instructions. For LAT1 knock-down, the cells were transfected for 48 hours with two alternative silencing siRNA preparations at a final concentration of 100 nM in the medium (Table 2.3). The two preparations designated **SLC7A5 (1)** and **SLC7A5 (2)** were:

**SLC7A5 (1)** ON-TARGET plus SMART pool, Rat SLC7A5 (Dharmacon, L-092749-01-0005)

OR

**SLC7A5 (2)** Silencer® Select Pre-Designed siRNA (Invitrogen/Ambion ref s132356) against SLC7A5.

As a control for non-specific effects of double-stranded RNA on amino acid transporters (Liong and Lappas 2017) a 100nM irrelevant scrambled siRNA was used as a control

(non-silencing) preparation. Powdered pre-annealed siRNA was dissolved in DEPC (diethylpyrocarbonate)-treated water (Invitrogen) to make a stock concentration of 20 $\mu$ M or 100 $\mu$ M before use.

**Table 2.3.** Silencing siRNA used for transfections

siRNA	Targets	Target Sequence
ON-TARGET plus SMART pool, Rat SLC7A5 (Dharmacon, L-092749-01-0005)	ON-TARGET plus SMART pool siRNA (J-092749-09, TA1)	UGGUCUAUGUGCUGACGAA
	ON-TARGET plus SMART pool siRNA (J-092749-10, TA1)	ACUGACAAACGGACGAUGA
	ON-TARGET plus SMART pool siRNA (J-092749-11, TA1)	AAGAAACCUGGUACGAAUU
	ON-TARGET plus SMART pool siRNA (J-092749-12, TA1)	CGACUAUGCCUACAUGCUA
Silencer Select Pre-designed (Non-inventoried) siRNA, rat SLC7A5 (Ambion s132356)	SLC7A5 (NM_017353AB015432.1, U00995.1)	AGAGACAUCUUCUCAUCatt UGAUGGAGAAGAUGUCUCUgg
Scrambled Control sequence of siRNA - Eurogentec (Non-inventoried)		CGCUCUACUCUACUUGUCC
		GGACAAGUAGAGUAGAGCG

Before transfection, Growth Medium was first replaced by 1.7 ml of Opti-MEM® I + Glutamax™-I medium (Invitrogen) per well (optimized Eagle's Minimum Essential Medium, abbreviated as Opti-MEM from here on), and then the following mixtures were prepared in 2 tubes (Table 2.4):

**Table 2.4.** Reagents used for Silencing siRNA transfections

Tube 1		Tube 2	
<b>Opti-MEM</b>	<b>Lipofectamine RNAiMAX</b>	<b>Opti-MEM</b>	<b>20<math>\mu</math>M siRNA</b>
150 $\mu$ l	10 $\mu$ l	150 $\mu$ l	10 $\mu$ l

Tubes were incubated at room temperature for 5min, and then the content of tube 2 was transferred to tube 1. The mixture was further incubated for 20 min, before adding to their respective wells. Opti-MEM medium was replaced by INS1E Growth Medium 24 hours post-transfection. Cells were then incubated for a further 24h before performing measurements.

#### **2.14. RNA isolation for qRT-PCR**

After each experiment, medium was removed and 600  $\mu$ l of Trizol reagent (Invitrogen Ref 15596) was added per 35mm well on 6 well plates. Plates were allowed to stand at room temperature for 10 minutes before scraping the wells and transferring to a microcentrifuge tube. 120  $\mu$ l of molecular biology grade chloroform (200  $\mu$ l per ml of Trizol) was added to each tube and vortexed for 15 seconds. Samples were centrifuged at 11,800 rpm for 15 minutes at 4°C on a Sarstedt Desaspeed refrigerated microcentrifuge and the upper clear (aqueous) phase containing RNA was transferred into a second autoclaved 2ml screw-cap tube. RNA was precipitated by adding 300  $\mu$ l of molecular biology grade isopropyl alcohol (propan-2-ol) (500  $\mu$ l per 1ml of Trizol) and gently vortexing. Samples were allowed to stand for 10 min for the precipitation to complete and centrifuged at 11,800 rpm for 15 minutes at 4°C. At the end of this spin, RNA was visible as a faint smear on the bottom of the tube. Isopropyl alcohol was decanted by gently inverting the tube. The RNA pellet was washed by adding 1ml of RNAase-free 75% ethanol (freshly diluted and chilled to minus 20°C before used), vortexing, and centrifuging the pellet fragments at 11,800 rpm for 10 min at 4°C on the Sarstedt Desaspeed refrigerated microcentrifuge. 75% ethanol was decanted by gently inverting the tube over a wad of tissue paper and the pelleted RNA was allowed to air dry for 15 min. Finally 20  $\mu$ l of DEPC water was added to each tube to dissolve the pellet by vortexing and heating on water bath at 65°C for 10 minutes. The ODs of the RNA samples were measured on a NanoDrop 1000 Spectrophotometer V3.7 and used to calculate the RNA content of the sample.

#### **2.15. cDNA synthesis**

For the reverse transcription reaction 1  $\mu$ g of total RNA from each extraction was used as template with Reverse Transcription System A3500 (Promega). A 20  $\mu$ l total reaction mixture was prepared using the following reagents:

**Table 2.5.** Reagents used for cDNA synthesis

Component	Amount
MgCl <sub>2</sub> , 25mM	4 µl
Reverse Transcription 10x Buffer	2 µl
dNTP Mixture, 10mM	2 µl
Recombinant RNasin Ribonuclease Inhibitor	0.5 µl
AMV Reverse Transcriptase	0.75 µl (15U)
Oligo(dT) <sub>15</sub> Primer or Random Primers	1 µl (0.5 µg)
DEPC Water	7.75 µl
1 µg RNA	2 µl

The samples were heated on a Techne TC-3000X PCR thermal cycler at 42°C for 1 hour followed by 95°C for 5 minutes to inactivate the enzyme, then incubated at 0–5°C for 5 minutes.

### 2.16. Quantitative real-time polymerase chain reaction (qRT-PCR)

Using the cDNAs that were synthesized in Section 2.15 as templates, qRT-PCR reactions were performed on an Applied Biosystems 7500 Fast Real-Time PCR System using reaction mixtures prepared from the following gene-specific PCR primers:

**Table 2.6.** PCR primers Sequences

Primer	Forward	Reverse
SLC7A5 (Rat LAT1)	5'-TTGTTTCGTTTCAGTAGCACATTG-3'	5'-ATTCATCGTCCGTTTGTTCAGT-3'
SLC7A8 (Rat LAT2)	5'-CCAGTTCCTCTCCCCTCCT-3'	5'-CAAAGTGAGTGCCATCCTGTC-3'
SLC7A6 (Rat LAT3)	5'-ACACTGAAGTTTTGTCTCCGTTG-3'	5'-TTGGGCAGAGTAAGTGAGGTAAA-3'
SLC43A2 (Rat LAT4)	5'-CAGAAGCGAGACAGGCAGAT-3'	5'-TGTAGAGGCAGATTAGGAATGAGG-3'
Rat 18S rRNA (housekeeping)	5'-GTTGGTTTTCGGAACTGAGG-3'	5'-GCATCGTTTATGGTCGGAAC-3'

The following reagents and cDNA (or DEPC water for negative control) were mixed in each well of a 96-well PCR Plate:

**Table 2.7.** PCR primers Sequences

Component	Amount
Power SYBR®Green PCR Master Mix (Applied Biosystems)	12.5 µl
Primer Forward	0.5 µl
Primer Reverse	0.5 µl
DEPC water	10.5 µl
cDNA or DEPC water (for negative control)	1 µl (1µg cDNA)

The mixtures were then subjected to the following thermal cycling:

**Table 2.8.** Thermal cycling for PCR reaction

	<b>Holding Stage</b>	<b>Holding Stage</b>	<b>Cycling stage (40 cycles)</b>		<b>Melt curve stage</b>			
<b>Temperature (°C)</b>	50	95	95	60	95	60	95	60
<b>Time min:sec</b>	02:00	10:00	00:15	01:00	00:15	01:00	00:15	00:15

The number of cycles required to reach the amplification threshold (CT value) for the LAT genes and the corresponding housekeeping genes was obtained using 7500 Fast SDS Software (Applied Biosystems V.2.0.6). From the difference between the CT values for the gene of interest and the housekeeping gene (the Delta CT value), the mean normalised expression ( $MNE = 2^{-(\Delta CT)}$ ) was calculated (Simon 2003).

### **2.17. High-performance liquid chromatography (HPLC Analysis)**

To separate, identify, and quantify free amino acids from the INS1E cell samples, HPLC was performed. After the experiment incubating at the specified D-glucose concentration, INS1E cells were rapidly chilled on ice and rinsed three times with ice-cold 0.9% w/v NaCl to remove extracellular amino acids and other metabolites. Then immediately 150 µl of 0.3 M perchloric acid was added to each 35 mm well and scraped. The resulting lysate was transferred to microcentrifuge tubes, followed by incubation for at least 30 minutes on ice to allow as much protein as possible to precipitate. Precipitated protein was sedimented (10min, 4°C, 14000 rpm on a microcentrifuge) and retained for total protein assay. Acid in the supernatant was neutralized with Freon-Tri-octylamine (Evans et al. 2007) then the neutralised extract was filtered through a 0.45 µm microfilter and was used for determination of amino acids on an Agilent 1100 high-performance liquid chromatograph with a Zorbax Eclipse AAA column (4.6 x 75mm, 3.5µm) at 40°C with o-phthalaldehyde/3-mercaptopropionate/9-fluorenylmethylchloroformate pre-column derivatization and ultraviolet post-column detection (Evans et al. 2007).

### **2.18. Statistical Analysis**

Unless stated, pooled data are presented from at least 3 independent replicates of each

experiment. Data were analysed using GraphPad Prism 7.0. Data normality was checked with the D'Agostino-Pearson normality test. Normally distributed data are presented as the mean  $\pm$  SEM, and were analysed by Student's t-test or by repeated measures ANOVA, followed by Tukey's multiple comparisons test. Non-normally distributed data are presented as linked data curves for the individual experiments, and were analysed by Friedman's nonparametric repeated measures ANOVA, followed by Dunn's multiple comparison test. Blinded scoring of fluorescence images of cells was analysed by the Mann Whitney U test or by Fisher's exact test for 2 independent samples. P values < 0.05 were considered statistically significant.

### 3.1. Introduction

Branched chain amino acids (BCAA) play a critical role in cellular signalling and metabolism (Shihai Zhang et al. 2017). mTORC1 is highly activated by nutrients, growth factors and hormones and its activation leads to the control of cell growth and proliferation of mammalian cells (Sections 1.3 – 1.8). The presence of BCAAs in  $\beta$  cells, especially L-leucine is critical for the activation of mTORC1, as L-leucine stimulates the dimerization of the RAG proteins, which activate mTORC1 by the translocation to the lysosome (Section 1.8). In T2DM, L-leucine stimulates insulin secretion and activates mTORC1, promoting increased  $\beta$  cell mass and function (Yuan et al. 2016). The concentration of this amino acid in cells is controlled by the amino acid exchange through the plasma membrane performed by System L amino acid transporters (Section 1.10.1). Defining the mechanisms by which system L transporters may act in the mTORC1 signalling in  $\beta$  cells is crucial in the understanding of the type-2 diabetes. The potential of  $\beta$  cells to expand in response to insulin resistance is a critical factor in the development of type 2 diabetes and mTORC1 signalling plays a key role in the regulation of pancreatic  $\beta$ -cell mass.

Therefore an important early aim in this project was to characterise L-leucine transport and signalling in the rat INS1E  $\beta$  cell culture model, to compare this with primary cultures of rat islets of Langerhans, and to confirm the conclusion from our recent study (Cheng et al. 2016) that these cells show LAT-dependent mTORC1 activation.

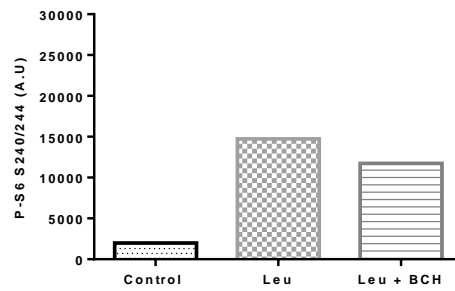
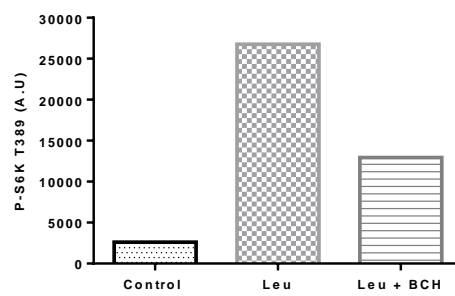
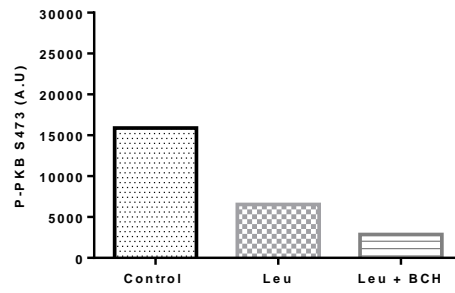
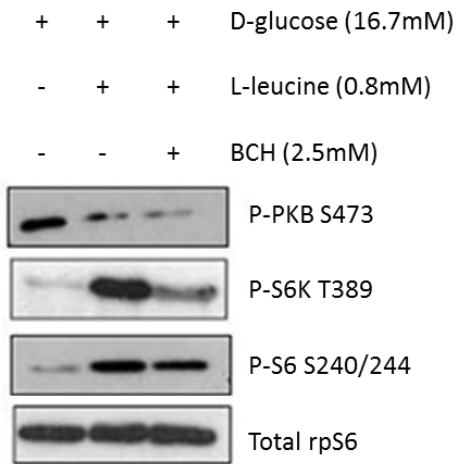
## **3.2. Results**

### **3.1.1 BCH inhibits leucine-stimulated mTORC1 activation in rat islets of Langerhans and INS1E cells.**

To investigate the effect of L-leucine-stimulated mTORC1 activation, rat islets of Langerhans (Figure 3.1.a) were pre-incubated in DMEM without L-leucine in the presence of 16.7 mM D-glucose and 2 mM L-glutamine for 1 hour prior to the addition of 0.8 mM L-leucine in the absence or presence of system L transport inhibitor (2.5 mM BCH) for 30 minutes. The re-addition of L-leucine significantly stimulated the activation of mTORC1, as shown by the phosphorylation of S6K at Thr389 and S6K's downstream target rpS6 at Ser240/244, and this effect was inhibited by BCH. Interestingly, L-leucine also caused a slight decrease in the phosphorylation of PKB at Ser473, and BCH caused a further decrease.

Previous work in the group has shown that these effects also occur in INS1E cells (Cheng et al. 2016). This was confirmed in the present project by running a single confirmation experiment on INS1E cells, which gave similar results to those observed on rat islets of Langerhans (Figure 3.1.b) and in previous experiments on INS1E where L-leucine-stimulated mTORC1 activation was found with the increased phosphorylation of S6K at Thr389 and rpS6 at Ser240/244.

### a. Rat islets of Langerhans



## b. INS1E cells

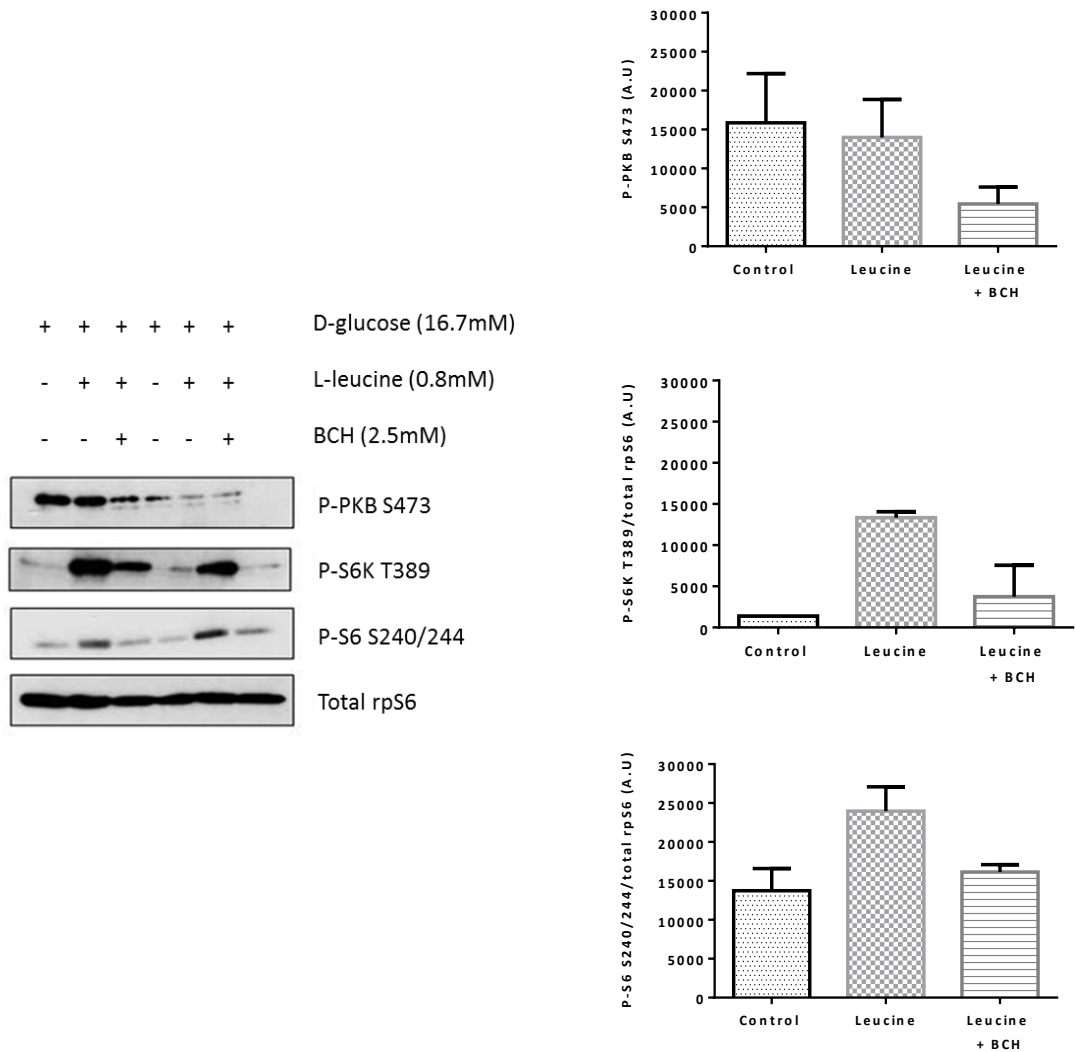


**Figure 3.1. BCH inhibits leucine-stimulated mTORC1 activation in rat islets of Langerhans and INS1E cells.**

Rat islets of Langerhans (a) and INS1E cells (b) were incubated in DMEM (16.7 mM glucose and 2 mM glutamine) minus L-leucine for 1 hour before the re-addition of 0.8 mM leucine for 30 minutes in the presence or absence of 2.5 mM BCH. Proteins were resolved by SDS-PAGE, and Western blotted using antisera against the proteins indicated. Graphical representations of the results show the mean  $\pm$  S.E.M for three independent experiments for islets  $^*$ ( $p < 0.05$ )  $^{***}$ ( $p < 0.001$ ) compared with the control. Data for INS1E are from a single confirmation experiment presented as mean  $\pm$  range for duplicate determinations (Blots represent 2 separate experiments).

### 3.1.2 Blocking Ca<sup>2+</sup> channels, which are relevant for insulin secretion, has no impact on the effect of L-leucine on mTORC1 activation in INS1E cells

To determine whether the L-leucine effect on mTORC1 signalling is just a consequence of L-leucine stimulating insulin secretion, which then exerts an autocrine effect, activating mTORC1 via the IRS1/PI3K/Akt pathway, the Ca<sup>2+</sup> channel inhibitor nifedipine was used to inhibit the Ca<sup>2+</sup> dependent mechanism of insulin secretion that was described in Section 1.2.3. INS1E cells were pre-incubated in DMEM minus L-leucine for 1 hour before the addition of 0.8 mM leucine in the absence or presence of 10 μM nifedipine for a further 30 minutes. Compared with the control, nifedipine had no effect in the phosphorylation of PS6 S240/244. However, the re-addition of L-leucine significantly increased the phosphorylation of PS6 S240/244 and this increase was similar in the presence of L-leucine and nifedipine (\*\*p<0.01).

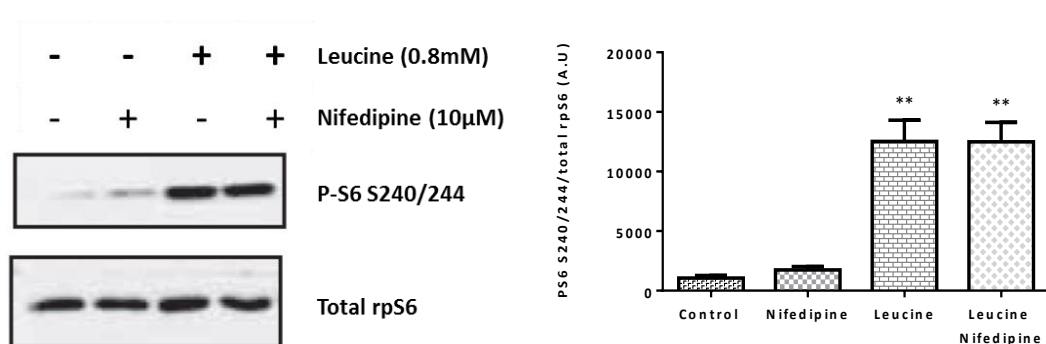


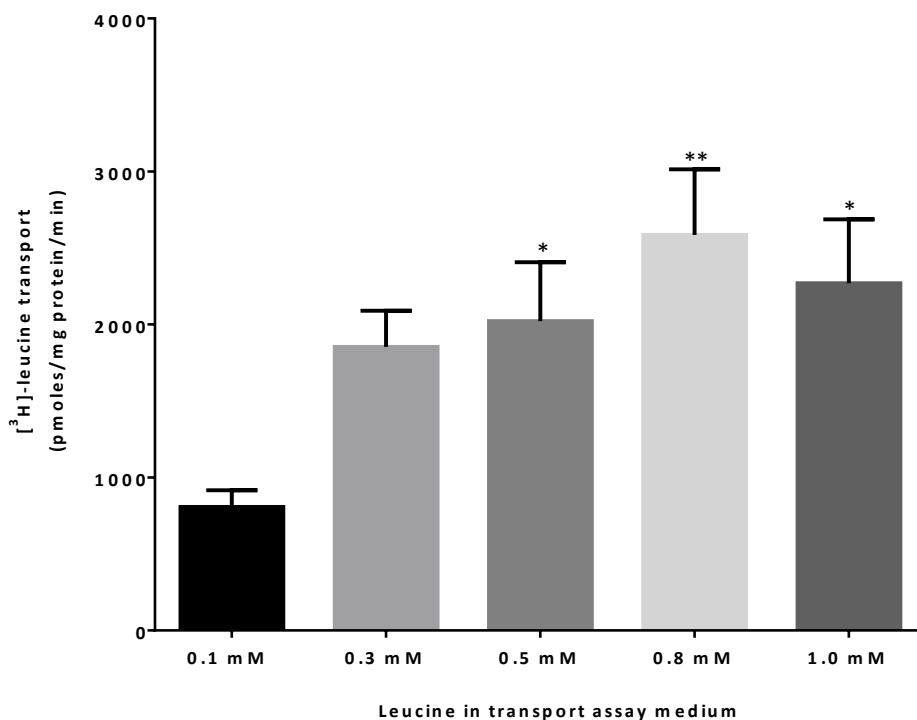
**Figure 3.2. Effect of Ca<sup>2+</sup> channel blocker (nifedipine) on mTORC1 signalling in INS1E cells.**

INS1E cells were pre-incubated in DMEM minus L-leucine for 1 h. The cells were then incubated for a further 30 min supplemented with 0.8 mM leucine in the absence or presence of 10 μM nifedipine. In all cases, proteins were resolved by SDS-PAGE, and Western-blotted using antisera against the proteins indicated. Graphical representations of the results show the mean ± S.E.M for three independent experiments. (\*\*p<0.01 compared with the corresponding cultures without L-leucine).

### 3.1.3 L-[<sup>3</sup>H]-leucine uptake increases in a concentration-dependent and saturable manner in INS1E cells

To determine whether the L-[<sup>3</sup>H]-leucine transport flux into INS1E cells shows saturable kinetics consistent with LAT transporters, INS1E cells were pre-incubated for 10 minutes with L-leucine-free medium to deplete intracellular concentrations and then treated with different concentrations of L-[<sup>3</sup>H]-leucine (from 0.1 to 1.0mM) for 1 minute. L-leucine uptake was found to increase in a concentration-dependent manner (Figure 3.4.a) and 0.8 mM was found to be the approximate concentration where the L-[<sup>3</sup>H]-leucine transport reached saturation. Kinetics of L-leucine influx into INS1E cells were determined by fitting a Michaelis-Menten curve (Figure 3.4.b), with an apparent V<sub>max</sub> of 3211 ± 375 pmoles/mg protein/min and a K<sub>m</sub> of 0.2031 ± 0.082 mM (mean ± S.E.M).

a. L-[<sup>3</sup>H]-Leucine uptake



### b. Michaelis-Menten kinetics

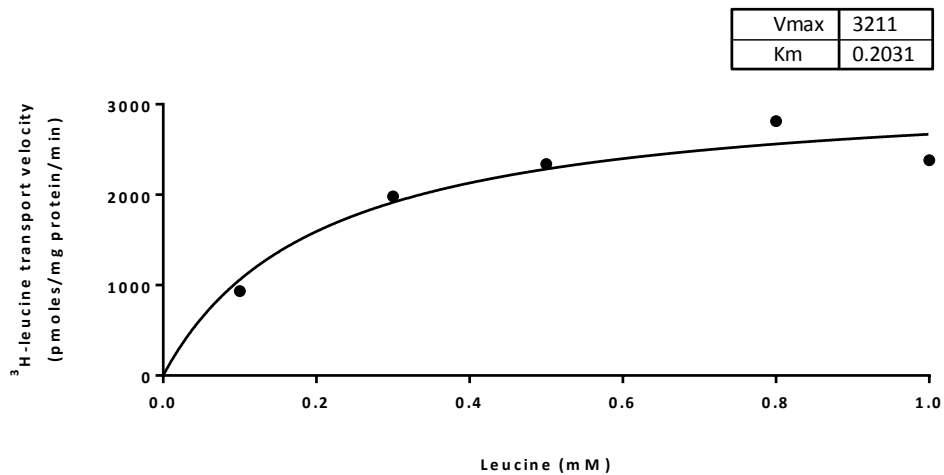


**Figure 3.3. L-leucine transport dose-response experiment on INS1E cells.**

L- $^3\text{H}$ -leucine uptake was measured in INS1E cells by incubating in DMEM (with 16.7 mM D-glucose and 2 mM L-glutamine) minus L-leucine for 10 minutes before the re-addition of L-leucine (0.1, 0.3, 0.5, 0.8 and 1.0 mM L- $^3\text{H}$ -leucine for 1 minute (a). All transport values are expressed as picomoles per mg of protein per minute. The results presented are the mean  $\pm$  S.E.M of three independent experiments. \*\*( $p < 0.01$ ) \*( $p < 0.05$ ) compared with 0.1mM. Curve-fitting was performed using the Michaelis-Menten equation velocity,  $v = V_{\text{max}}/(1+K_m/S)$  (b).

### 3.1.4 L-[<sup>3</sup>H]-leucine transport assay in INS1E cells and rat islets of Langerhans

To confirm that L-[<sup>3</sup>H]-leucine transport into  $\beta$  cells is mediated by System L transporters (LATs), INS1E cells (Figure 3.3.a) and rat islets of Langerhans (Figure 3.3.b), were pre-incubated for 1 hour without L-leucine in KRB Buffer prior to the re-addition of 0.8 mM L-leucine in absence or presence of a LAT inhibitor (2.5 mM BCH) and 0.8 mM L-[<sup>3</sup>H]-leucine. The uptake of L-[<sup>3</sup>H]-leucine into cells was significantly inhibited in the presence of BCH in INS1E and rat islets of Langerhans, confirming that LATs are the dominant contributor to L-leucine transport in these cells.

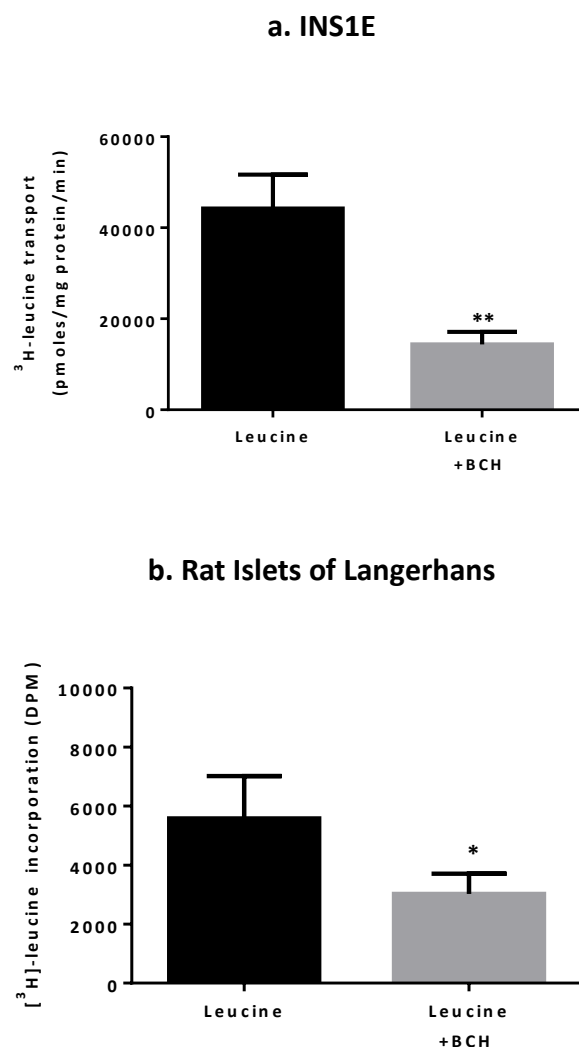


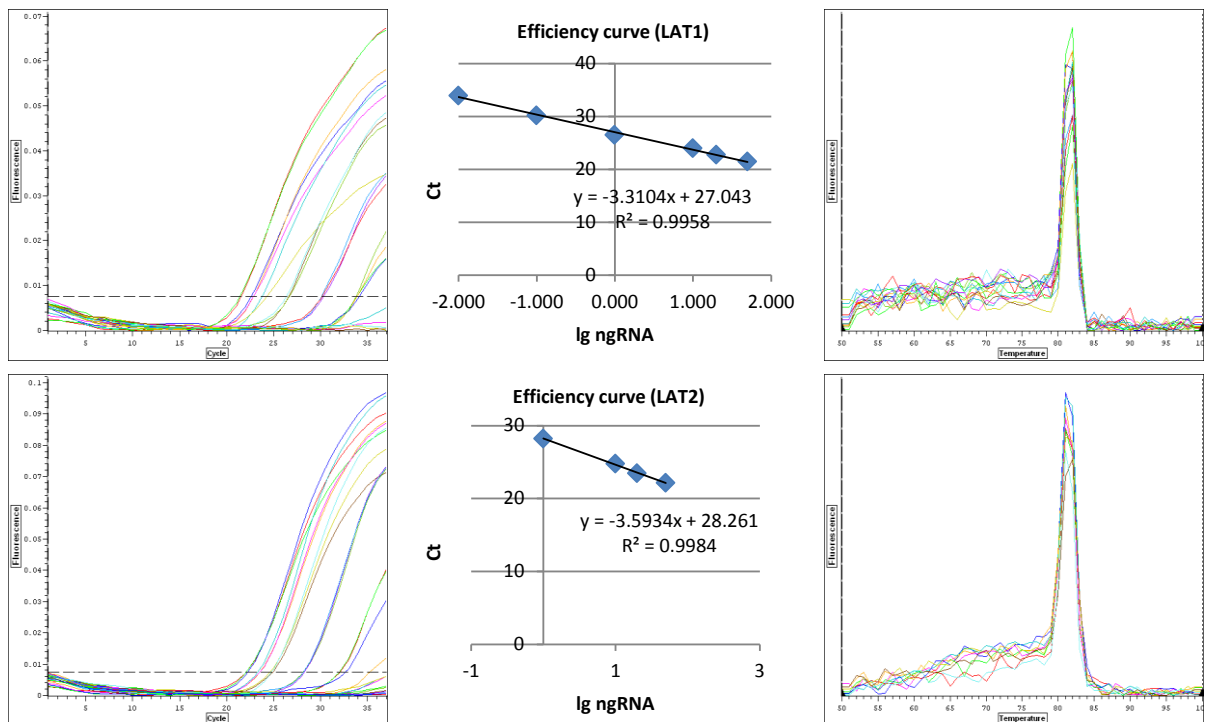
**Figure 3.4. L-leucine transport analysis in INS1E cells and rat islets of Langerhans.**

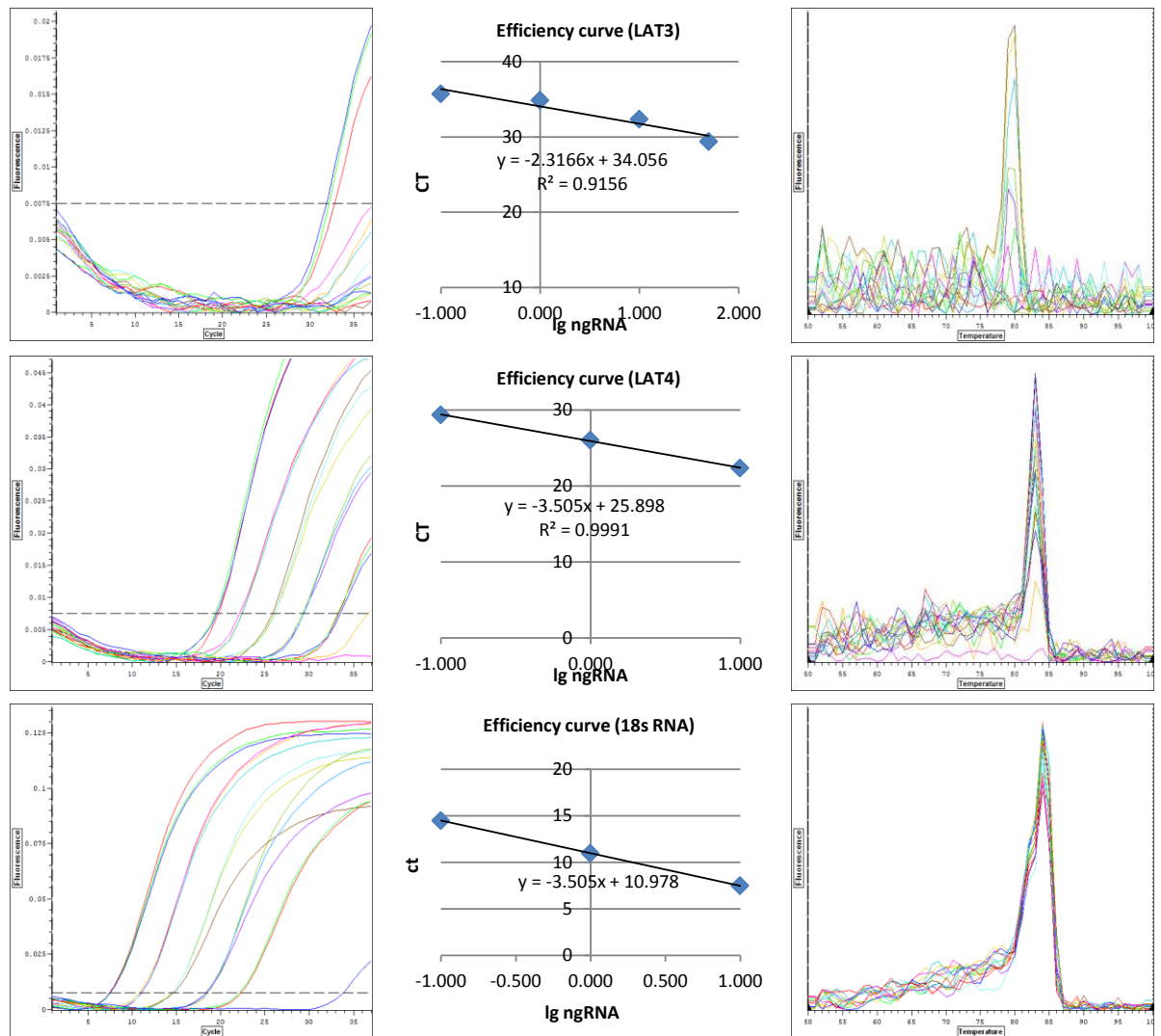
L-[<sup>3</sup>H]-leucine uptake was measured in INS1E cells (a) and rat islets of Langerhans (b) by incubating in DMEM (with 16.7 mM D-glucose and 2 mM L-glutamine) minus L-leucine

for 1 hour before the re-addition of 0.8 mM L-[<sup>3</sup>H]-leucine for 30 minutes in the absence or presence of 2.5 mM BCH. INS1E transport values are expressed as picomoles per mg of protein per minute. In islets the protein content of the  $\beta$  cells within the islets was unknown so the transport data are presented as DPM per culture well. The results presented are the mean  $\pm$  S.E.M of three independent experiments. \*( $p < 0.05$ ), \*\*\*( $p < 0.01$ ) compared with control without BCH.

### 3.1.5 Expression of system L amino acid transporter (LAT) mRNAs in INS1E cells

The kinetics of the L-leucine uptake in INS1E shown in the transport saturation curve above (Figure 3.4.b) indicate a (high influx)  $K_m$  of 0.2 mM, suggesting that the L- $[^3H]$ -leucine transport may not be mediated only by LAT1 (see Discussion). The technique of qRT-PCR (quantitative reverse transcription/real time polymerase chain reaction) was therefore used to assess the expression of LAT transporter genes in INS1E cells. In order to assess the efficiency of each primer set of the four system-L amino acid transporters LAT1 (SLC7A5), LAT2 (SLC7A8), LAT3 (SLC43A1) and LAT4 (SLC43A2) and the 18s rRNA (control) in INS1E cells, plots of CT versus amount of serially diluted cDNA (efficiency curves) were constructed for each primer set (Figure 3.5) The efficiency of the LAT1 primer set was found to be 100%, 90% for LAT2 primers, 93% for LAT4 and 93% for 18s rRNA. As very low LAT3 expression was detected, no reliable estimate of efficiency could be made for the LAT3 primers (Figure 3.5).





	LAT1 (SLC7A5)	LAT2 (SLC7A8)	LAT3 (SLC43A1)	LAT4 (SLC43A2)	18S RNA
<b>Efficiency</b>	2	1.9	Not determined	1.93	1.93
<b>Efficiency %</b>	100.50%	89.80%	Not determined	92.90%	92.90%

**Figure 3.5. Expression of system L amino acid transporters (LATs) in INS1E cells.**

The efficiency of amplification of the target gene templates (LAT1, LAT2, LAT3, and LAT4) and the reference gene (18S RNA) was obtained by qRT-PCR. Serial dilutions of INS1E cDNA were amplified by qRT-PCR using gene-specific rat primers (LAT1, LAT2, LAT3 and LAT4) and reference gene primers (18s RNA). Data were fitted using least-squares linear regression analysis (n=3). Reaction curves and melting curves are indicated in the figure. The efficiency of each primer set is shown in the table.

### 3.3. Discussion

#### 3.3.1. The role of L-leucine availability in the activation of mTORC1 in pancreatic $\beta$ cells

Nutrient signals generated by amino acids, especially L-leucine, are essential for the activation of mTORC1 (Section 1.8). Therefore, these experiments first investigated the effect of L-leucine-stimulated mTORC1 activation in clonal rat pancreatic  $\beta$  cells (INS1E cells) and pancreatic islets (Figure 3.1) in the presence or absence of the competitive inhibitor of system L, BCH (2-aminobicyclo-(2,2,1)-heptane-2-carboxylic acid). The addition of L-leucine, stimulated the activation of mTORC1 by phosphorylation of S6 kinase 1 (S6K1) on Thr389 and the substrate of S6K1, the ribosomal protein S6 (rpS6) on Ser240/244. The addition of BCH reduced L-leucine-stimulated mTORC1 activation. These results were as expected from the previously reported effects of L-leucine on mTORC1 and the effect of activated mTORC1 on its downstream targets S6K1 and rpS6 (Sections 1.3 – 1.8). However, an unexpected finding was the apparent inhibition of PKB (also known as Akt) phosphorylation on S473 in islets treated with BCH (Figure 3.1.a). This did not reach statistical significance and, unlike mTORC1, PKB is not usually regarded as an amino acid-sensitive kinase, although an apparent activation of PKB by the SNAT2 (SLC38A2) amino acid transporter has previously been reported in L6 rat skeletal muscle cells (Evans et al. 2008). For this reason, in future it may be of interest to examine the effects of L-leucine and BCH on PKB/Akt in  $\beta$  cells in more detail.

These results correlate with previous studies in rat cortical neurons where L-leucine induced phosphorylation and activation of S6K1 and rpS6 protein and increased L-leucine uptake, and this effect was also inhibited by BCH (Ishizuka et al. 2008). In other experiments using human myotubes treated with leucine and/or insulin, the phosphorylation of S6K1 was again increased under L-leucine exposure (Gran and Cameron-Smith 2011). These results confirm that L-leucine plays a critical role in mTORC1 activation and may also promote translation via S6K by stimulating lysosomal translocation of mTORC1 (Averous et al. 2014). The activation of mTORC1 occurs via the Rag guanosine triphosphatases (GTPases), regulated by the pentameric regulator

complex, the vacuolar H<sup>+</sup> adenosine triphosphatase (v-ATPase) and the Gator complex (Zoncu et al. 2011), (Jewell et al. 2015).

To assess whether the L-leucine effect on mTORC1 activation was indirectly caused by L-leucine-stimulated insulin secretion, leading to autocrine activation of mTORC1 via PI3K/Akt activation, nifedipine (an L-type voltage-gated calcium channel inhibitor), was used in INS1E cells to block insulin secretion. L-leucine again significantly increased the phosphorylation of PS6 S240/244; the combination with nifedipine failed to block the effect of L-leucine (Figure 3.2), demonstrating that L-leucine activation of mTORC1 is not likely due to the action of insulin.

### **3.3.2. The uptake of L-leucine by LATs**

System L amino acid transporters mediate Na<sup>+</sup>-independent transport of large neutral amino acids including branched-chain and aromatic amino acids. Among system L transporters, LAT1 is thought to play the main role in the uptake of L-leucine in many cell types, especially in cancer cells (Wang and Holst 2015). The role of system L transporters in L-leucine transport into INS1E cells and rat islets of Langerhans was confirmed here by showing that BCH caused a significant decrease in the uptake of L-[<sup>3</sup>H]-leucine transport (Figure 3.3), demonstrating the competitive inhibition by BCH by the binding to the L-type amino acid transport system. These findings agree with studies in cholangiocarcinoma cells where a treatment with BCH reduced the uptake of L-leucine, and it was associated with an inhibition of cell motility and, to a smaller extent, cell proliferation (Janpipatkul et al. 2014). Also inhibitory studies in canine mammary gland tumours of amino acid uptake were performed using L-[<sup>3</sup>H]-leucine, with or without BCH, and BCH inhibited L-[<sup>3</sup>H]-leucine uptake in a concentration-dependent manner (Fukumoto et al. 2013).

To determine whether the L-[<sup>3</sup>H]-leucine transport increases in a concentration-dependent and saturable manner, INS1E cells were incubated with increasing concentrations of L-leucine and it was found that 0.8 mM is the approximate

concentration where L-[<sup>3</sup>H]-leucine transport reached saturation (Figure 3.4).

Analysing the kinetics of the L-leucine influx with the Michaelis-Menten curve, it was found here that there was an apparent V<sub>max</sub> of about 3200 pmoles/mg protein/min and a K<sub>m</sub> of about 0.2 mM. The measured affinity for L-leucine on the extracellular side of the LAT1 transporter is usually found to be high (K<sub>m</sub> = approximately 30 μM) (Section 1.10.1.1), suggesting that a lower affinity LAT transporter such as LAT4 (Section 1.10.1.3) might be a significant contributor to L-leucine transport in INS1E cells, and this might be consistent with the apparent strong expression of LAT4 mRNA that was detected here (Section 3.3.3.). However, it cannot be concluded at this stage that LAT1 plays no significant role in INSE L-leucine transport for two reasons. Firstly, even in cells in which LAT4 is strongly expressed, it is uncertain whether LAT4 plays a major role in L-leucine transport, indeed the precise biological role of the SLC43 transporters LAT3 and LAT4 is still uncertain (Bodoy et al. 2013). Secondly, studies in brain endothelial cells expressing LAT1, suggested that there it had a V<sub>max</sub> = 7039 pmoles/million cells/min and a high K<sub>m</sub> of 530 μM (Dickens et al. 2013). This K<sub>m</sub> is even higher than the one found here in INS1E cells, and may mean that LAT1's K<sub>m</sub> for L-leucine varies depending on the cell in which it is expressed.

### **3.3.3. LAT1 expression in primary β cells**

The LAT family includes four Na<sup>+</sup>-independent neutral amino acid transporters grouped in two sub-families SLC7 (LAT1 and LAT2) and SLC43 (LAT3 and LAT4) (Section 1.10.1).

LAT1 was previously identified to be expressed in islet cells (Fukushima et al. 2010), and also was shown to have special functions in several kinds of cells such as proximal to proliferative zones in gastrointestinal mucosa, testicular sertoli cells, ovarian follicular cells and endothelial cells that work as a barrier between tissues i.e. blood-brain, blood-retinal and blood follicle barrier (Nakada et al. 2014). Moreover LAT1 is highly up-regulated in multiple cancer cell lines and the use of transporter inhibitors has been proven to be a therapeutic target for cancer (Hayashi and Anzai 2017).

In order to assess the expression of LATs in INS1E cells, qRT-PCR was performed (Figure 3.5). As in rat islets, LAT1 was shown to be expressed in INS1E cells, but there was also clear expression of LAT2 and especially LAT4, whereas the expression of LAT3 was extremely low.

### **3.4. Conclusion**

The experiments presented in this chapter suggest that INS1E is a suitable cell culture model in which to study L-leucine transporters and their biological role in  $\beta$  cell biology. INS1E cells in the present experiments showed an L-leucine-dependent activation of mTORC1, which was LAT-dependent (i.e. inhibited by BCH) and resembled that seen in islets and in earlier experiments with INS1E cells from this laboratory (Cheng et al. 2016). This suggests that, even though D-glucose-dependent insulin secretion from these cells has been reported to show significant decline in magnitude in response to serial passaging (Hohmeier et al. 2000), the L-Leucine biology of INS1E seems sufficiently stable (comparing the earlier study with the present one) to be used in the remaining experiments required in this project.

## Chapter 4. Characterization of L-leucine transport & signalling in $\beta$ cells

---

### 4.1. Introduction

As the transport of L-leucine across the plasma membrane by LAT transporters is an important mechanism to regulate protein synthesis via mTORC1 activation (Wang and Holst 2015) and, in pancreatic  $\beta$  cells, LATs may therefore have an important role in controlling  $\beta$  cell mass and functions (Cheng et al. 2016) such as L-leucine-induced insulin secretion, it is important to understand how LAT transporters are regulated in  $\beta$  cells, and particularly their response to changes in the D-glucose concentration of the sort that would occur in T2DM (Section 1.12). D-glucose supply in  $\beta$  cells can affect the energy status of the cell and the activity of the regulatory protein kinase AMPK, which might then act on LAT transporters as proposed in Section 1.12. Furthermore LAT transporters (and most other plasma membrane amino acid transporters) are thought to be glycosylated and D-glucose deprivation can inhibit the activity of some amino acid transporters (such as ASCT2) by inhibiting glycosylation (Polet et al. 2016). However, the role of D-glucose uptake and glycolysis in the uptake of L-leucine in pancreatic  $\beta$  cells through LAT transporters is not well known. Retinal capillary endothelial cells under D-glucose deprivation, upregulate the expression and transport function of LAT1 (Matsuyama et al. 2012), and in HL60 leukaemia cells, inhibition of ASCT2 glycosylation by D-glucose deprivation led to an upregulation of LAT1 as a compensatory effect (Polet et al. 2016). The aim of the experiments described in this chapter was therefore to investigate:

- 1) the molecular mechanisms involved in the regulation of LAT transporter expression and activity in pancreatic  $\beta$  cells in response to changes in energy status induced by D-glucose starvation, and
- 2) the possible involvement of AMPK in these processes.

The experiments presented in Chapter 3 suggested that INS1E is a suitable cell culture model in which to study L-leucine transporters and their biological role in  $\beta$  cell biology. For that reason, INS1E was used for the experiments on the effect of D-glucose supply on the regulation of L-leucine transport in the present chapter.

## 4.2. Results

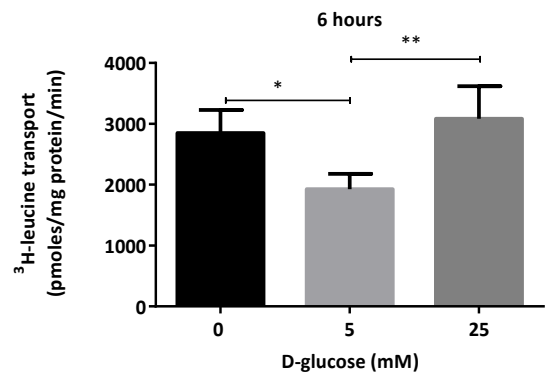
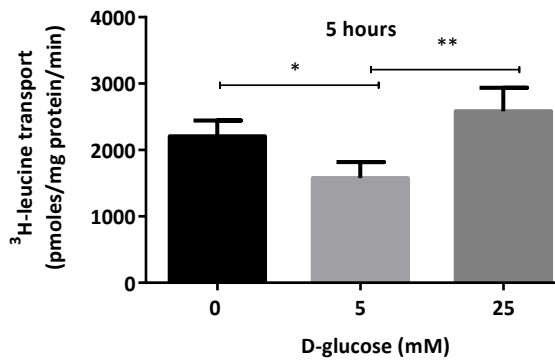
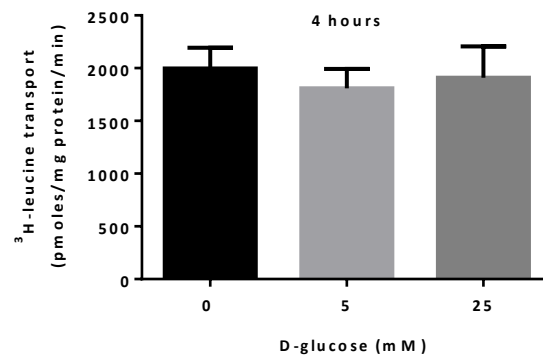
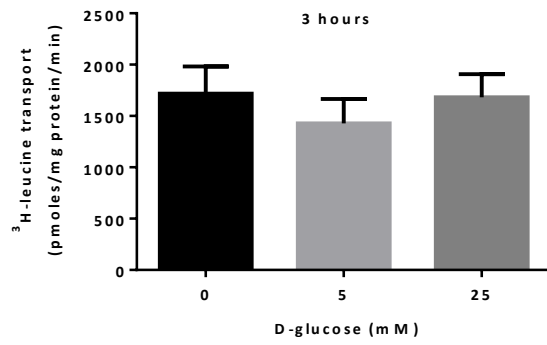
### 4.2.1. The effect of aglycaemia and hyperglycaemia in the L-[<sup>3</sup>H]-leucine transport in INS1E cells

To determine the effect of D-glucose concentration on L-[<sup>3</sup>H]-leucine transport in INS1E cells, cultures were treated (for 3, 4, 5 or 6 hours) with (0), normal (5 mM) and high (25 mM) concentrations of D-glucose (Figure 4.1.a). After 5 and 6 hours there was a reproducible effect whereby L-[<sup>3</sup>H]-leucine uptake was significantly increased by D-glucose starvation compared with 5mM D-glucose (Figure 4.1.a). There was also a smaller apparent effect after 3 and 4 hours on D-glucose deprivation, however this did not reach statistical significance (Figure 4.1.a).

The effect of a high concentration of D-glucose (25 mM) on L-[<sup>3</sup>H]-leucine transport was found to be variable between batches of cells. In the series of experiments shown in Figure 4.1.a, 25 mM D-Glucose gave a statistically significant increase in transport after 5 and 6 hours when compared with 5mM D-glucose. However, this was not reproducibly observed in later experiments (see Figure 4.2 onwards).

To investigate whether this effect of D-glucose supply might be a universal stress effect on mammalian cells, a non- $\beta$  cell line was also tested. In HEK293A epithelial cells, only a small stimulatory effect of D-glucose starvation on L-[<sup>3</sup>H]-leucine transport was observed after 3 hours of incubation, but this was not statistically significant at later time points (Figure 4.1.b).

a. INS1E



## b. HEK293

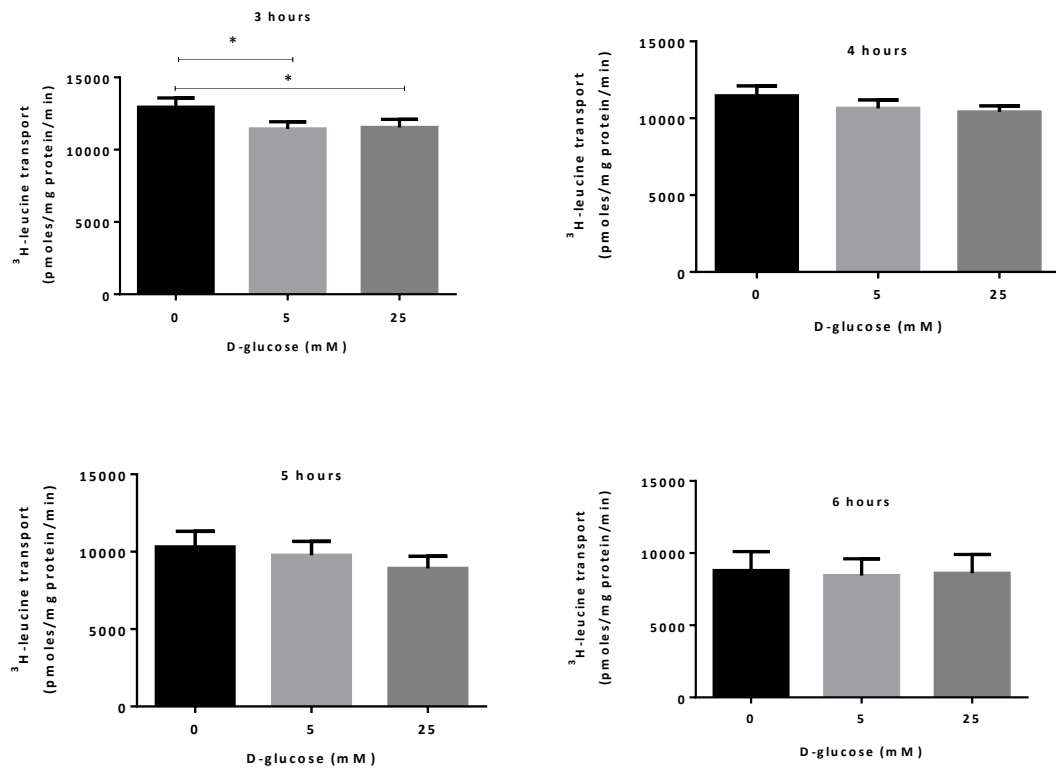


**Figure 4.1. Effect of D-glucose concentration on L-[<sup>3</sup>H]-leucine transport in INS1E and HEK293A cells after 3 to 6 hours incubation**

L-[<sup>3</sup>H]-leucine uptake (after incubation with 50  $\mu$ M L-[<sup>3</sup>H]-leucine for 1 min) in (a) INS1E cells and (b) HEK293A cells after 3, 4, 5 or 6 hours in DMEM containing 2 mM L-glutamine, 0.8 mM L-leucine and D-glucose (0, 5, 25 mM). All transport values are expressed as picomoles per mg of protein per minute. The results presented are the mean  $\pm$  S.E.M of three independent experiments \*\*( $p < 0.01$ ), \*( $p < 0.05$ ).

#### 4.2.2. Blocking Ca<sup>2+</sup> channels with nifedipine does not affect the action of high D-glucose on L-[<sup>3</sup>H]-leucine transport

As a high concentration of D-glucose (25 mM) had a very variable effect on L-[<sup>3</sup>H]-leucine transport in INS1E cells, the possibility that high D-glucose was acting partly through stimulating an indirect autocrine effect of insulin was investigated. A possible explanation of the variable high D-glucose effect on L-[<sup>3</sup>H]-leucine transport is that high D-glucose stimulates insulin secretion (Hohmeier et al. 2000) which then has an autocrine activating effect on mTORC1, which is itself a known activator of LAT1 transporters (Milkereit et al. 2015). To determine the direct effect of D-glucose concentration on L-[<sup>3</sup>H]-leucine transport when the insulin secretion is blocked, INS1E cells were treated with different concentrations of D-glucose (0, 5 and 25 mM) in the absence or presence of insulin secretion blockade with the calcium channel blocker nifedipine (10  $\mu$ M) over 6 hours. In the presence of 25 mM D-glucose, nifedipine had no significant effect on L-[<sup>3</sup>H]-leucine transport, suggesting that the effect of autocrine insulin was negligible. However, in the absence of D-glucose, nifedipine increased L-[<sup>3</sup>H]-leucine transport significantly and this effect was not found at the other D-glucose concentrations. Consequently, the stimulatory effect of D-glucose starvation on L-leucine transport was amplified by nifedipine, suggesting that a calcium-dependent process (but probably not insulin secretion) may be involved.

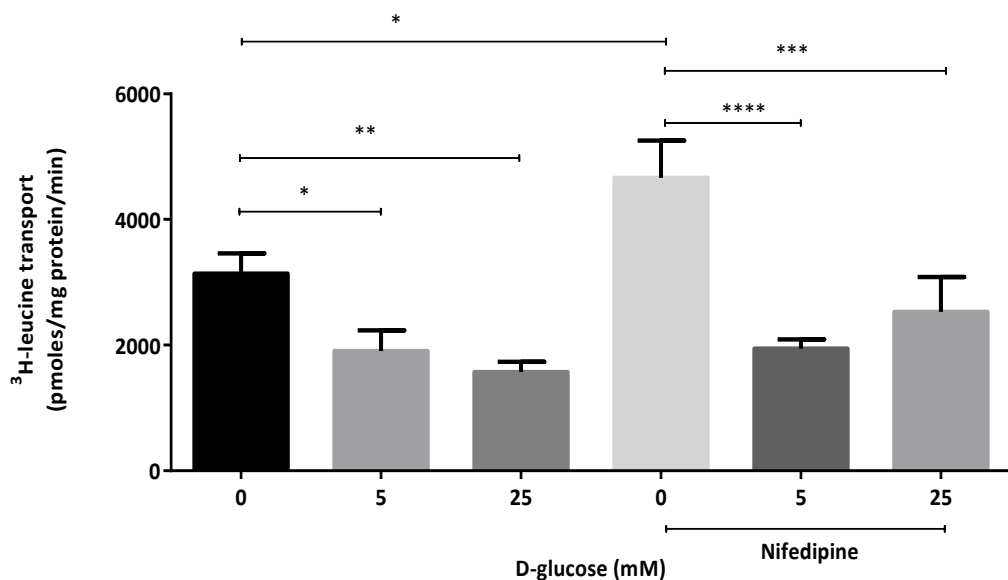


**Figure 4.2. INS1E D-glucose/nifedipine effect on L-[<sup>3</sup>H]-leucine transport after 6 hours of incubation.**

L-[<sup>3</sup>H]-leucine uptake in INS1E cells (after incubation with 50 μM L-[<sup>3</sup>H]-leucine for 1 min) after 6 hours in DMEM containing 2 mM L-glutamine, 0.8 mM L-leucine and D-glucose (0, 5, 25 mM) in the absence or presence of 10 μM nifedipine. All transport values are expressed as picomoles per mg of protein per minute. The results presented are the mean ± S.E.M of three independent experiments \*\*\*\*(p<0.0001), \*\*\*(p<0.001), \*\* (p<0.01), \*(p<0.05) compared with the control conditions shown.

#### **4.2.3. AMPK activation by AICAR and the absence of D-glucose activate L-[<sup>3</sup>H]-leucine transport in INS1E cells**

The experimental absence of D-glucose in INS1E cells may lead to a decline in energy status, which may be sensed by AMP-activated kinase (AMPK). The effect demonstrated above (Figure 4.1.a), leading to significantly increased L-[<sup>3</sup>H]-leucine transport might therefore be mediated by AMPK. To assess the role of AMPK activity, L-[<sup>3</sup>H]-leucine transport was measured in INS1E cells during 6 hours with different concentrations of D-glucose (0, 5 and 25 mM) in the absence or presence of the AMPK agonist AICAR (750  $\mu$ M), an analogue of AMP that stimulates AMPK activity. In INSE cells (Figure 4.3.a), L-[<sup>3</sup>H]-leucine transport significantly increased under D-glucose deprivation compared with 5 mM and 25 mM D-glucose. A significant stimulatory effect was also seen in the presence of AICAR with 5 mM D-glucose. L-[<sup>3</sup>H]-leucine transport significantly increased in INS1E cells with 5 mM D-glucose, when AICAR was added compared with the same concentration of D-glucose without AICAR. The stimulatory effect of AICAR with 5 mM D-glucose was similar in size to the stimulatory effect of D-glucose deprivation. However, when AICAR was added in D-glucose-free medium, no further significant increase was observed, compared with that seen with D-glucose deprivation alone (Figure 4.3.a), consistent with the idea that AICAR and D-glucose deprivation act through the same pathway (i.e. AMPK).

To assess the specificity of this effect for  $\beta$  cells, HEK293 cells (Figure 4.3.b) and L6 myoblasts (Figure 4.3.c) were also analysed. Even though there seemed to be a small stimulation of transport in HEK293 cells under D-glucose deprivation (Figure 4.3.b) as in Figure 4.1.b, this was not statistically significant, and AICAR had no detectable effect. In L6 myoblasts (Figure 4.3.c) D-glucose deprivation had no effect, nor was there any significant difference in the presence of AICAR.

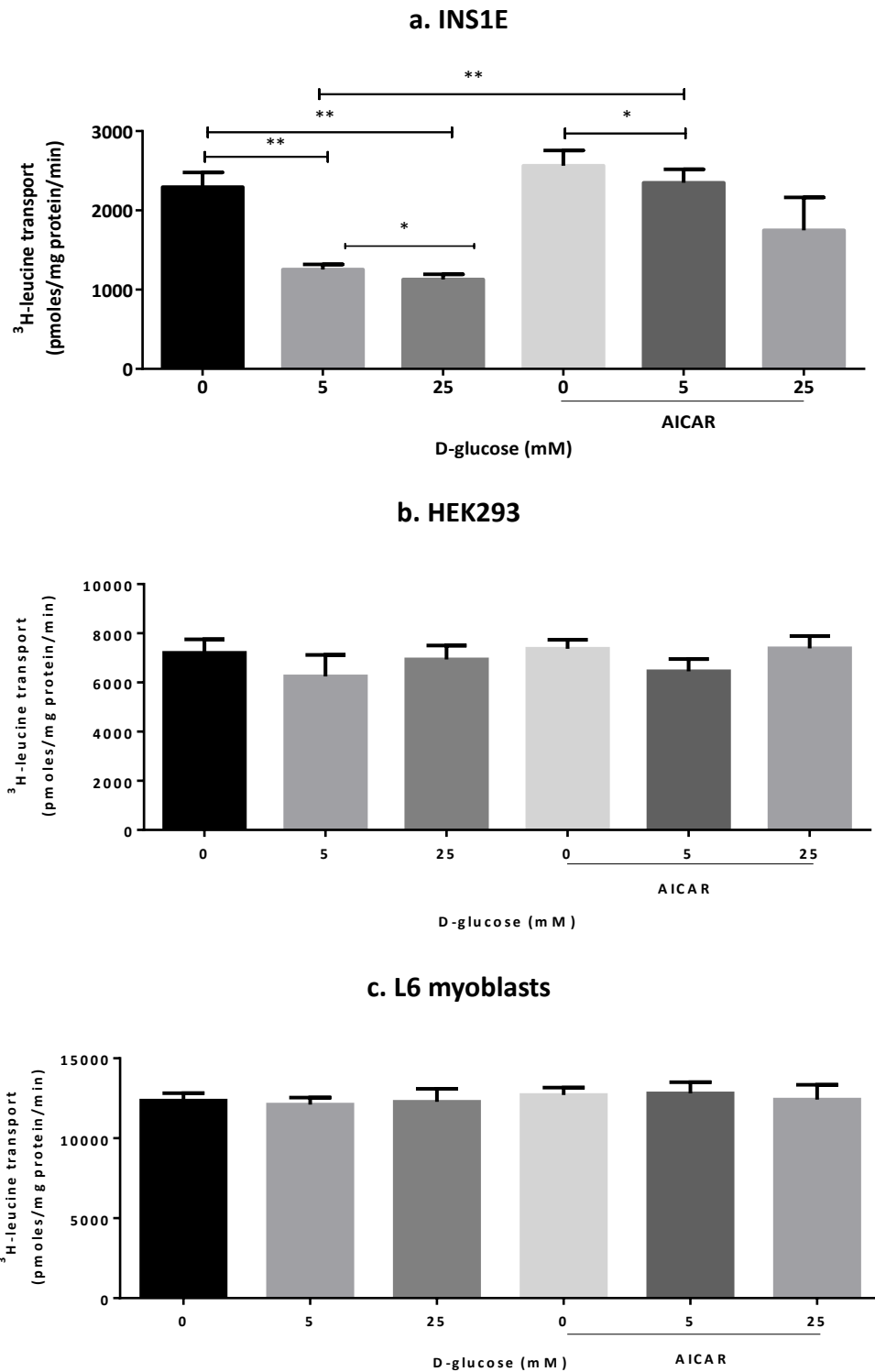


**Figure 4.3. INS1E, HEK293 and L6 cells D-glucose/AICAR effect on L-[<sup>3</sup>H]-leucine transport at 6 hours incubation.**

L-[<sup>3</sup>H]-leucine uptake (after incubation with 50 μM L-[<sup>3</sup>H]-leucine for 1 min) in INS1E (a), HEK293 (b) and L6 myoblasts (c). L-[<sup>3</sup>H]-leucine uptake was assayed by incubation with

50  $\mu\text{M}$  L-[ $^3\text{H}$ ]-leucine for 1 min after 6 hours in DMEM containing 2 mM L-glutamine, 0.8 mM L-leucine and D-glucose (0, 5, 25 mM) in the absence or presence of 750  $\mu\text{M}$  AICAR. All transport values are expressed as picomoles per mg of protein per minute. The results presented are the mean  $\pm$  S.E.M of four independent experiments. \*\*( $p < 0.01$ ), \*( $p < 0.05$ ) compared with the stated control.

#### **4.2.4. D-glucose deprivation and AICAR effects on System A amino acid transport in INS1E cells and L6 myoblasts**

Even though transporters such as LAT1 usually act as passive exchangers of neutral amino acids across the plasma membrane, they can mediate active pumping of amino acids such as L-leucine into cells by coupling to active System A transporters (Section 1.10.4) (Baird et al. 2009). For example, such coupling controls the intracellular L-leucine concentration in L6 cells (Evans et al. 2007). If the biological role of the effects of D-glucose deprivation and AICAR on L-leucine transport observed above is to drive L-leucine into the cell, D-glucose deprivation and AICAR might also be expected to stimulate System A amino acid transport. To test this,  $^{14}\text{C}$ -MeAIB transport (a measure of System A activity) was measured in INS1E cells (Figure 4.4.a), and L6 myoblasts (Figure 4.4.b) during 6 hours with different concentrations of D-glucose (0, 5 and 25 mM) in the absence or presence of 750  $\mu\text{M}$  AICAR.

In contrast to the effects on L- $^3\text{H}$ -leucine uptake, the  $^{14}\text{C}$ -MeAIB transport in INS1E cells significantly decreased (\* $p < 0.05$ ) in the absence of D-glucose compared with 5 mM D-glucose. However, this inhibitory effect of D-glucose deprivation was prevented when AICAR was present in the D-glucose-free medium (Figure 4.4.a), increasing the  $^{14}\text{C}$ -MeAIB transport to a level similar to that seen with 5 mM D-glucose. There was therefore no significant difference between 0 and 5 mM D-glucose in the presence of AICAR (Figure 4.4.a). In L6 myoblasts, these effects on System A transport were again observed but were smaller than in INS1E cells (Figure 4.4.b). However, in L6 a small but statistically significant activation of system A by AICAR was observed at all three D-glucose concentrations, possibly because of the activation of Na,K-ATPase by AICAR that has previously been reported in L6 cells (Benziane et al. 2012) (see Discussion).

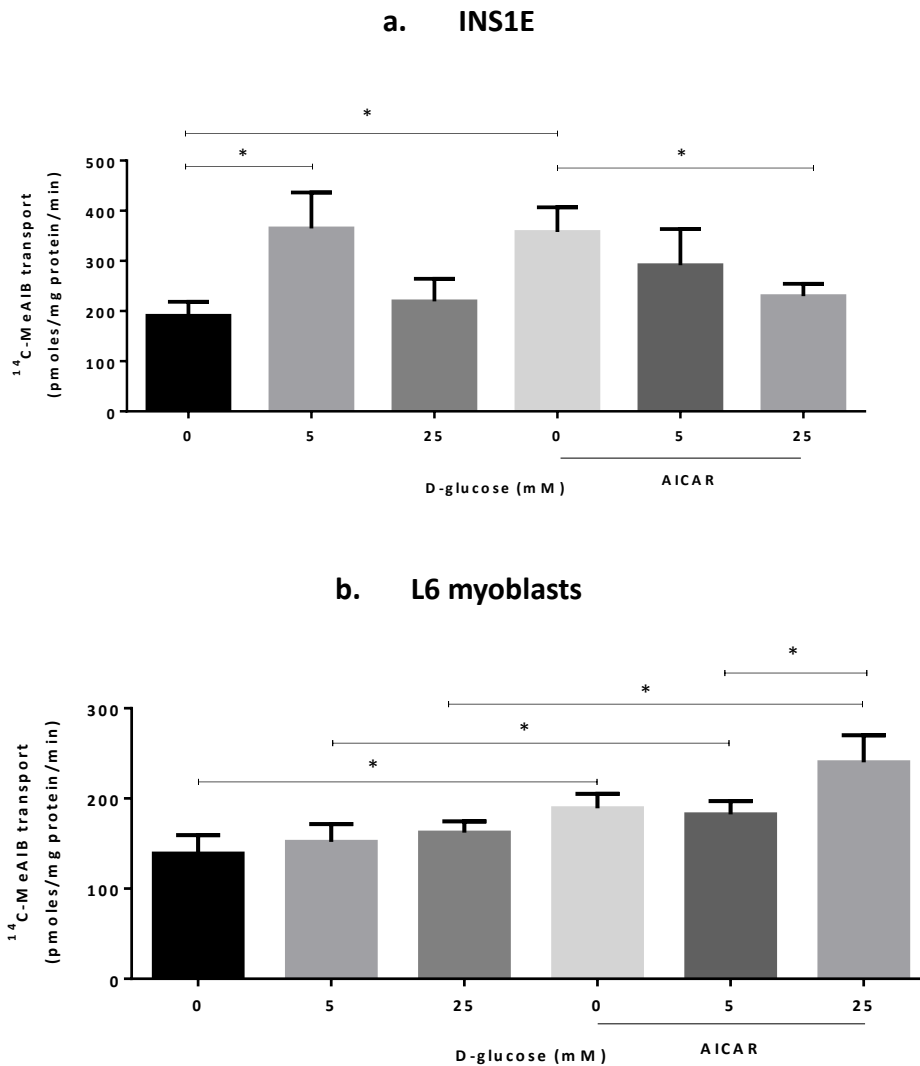


**Figure 4.4. Effect of D-glucose and AICAR in INS1E and L6 myoblasts on <sup>14</sup>C-MeAIB (System A) transport.**

<sup>14</sup>C-MeAIB uptake in INS1E cells (**a**) and L6 myoblasts (**b**) was assayed by incubating for 5 min with 50  $\mu$ M <sup>14</sup>C-MeAIB after 6 hours in DMEM containing 2 mM L-glutamine, 0.8 mM L-leucine and D-glucose (0, 5, 25 mM) in the absence or presence of 750  $\mu$ M AICAR. All transport values are expressed as picomoles per mg of protein per minute. The results presented are the mean  $\pm$  S.E.M of four independent experiments \*( $p < 0.05$ ) compared with the stated control.

#### 4.2.5. The effect of D-glucose starvation on AMPK phosphorylation in INS1E cells

To confirm the effect of D-glucose availability on the activating phosphorylation of AMPK at Thr172, INS1E cells were incubated for 3 or 6 hours with different concentrations of D-glucose (0, 5 and 25 mM) in the absence or presence of 750  $\mu$ M AICAR, followed by immuno-blotting with antibody recognising Thr172 phosphorylated AMPK- $\alpha$ . As expected, the AICAR positive control significantly activated AMPK (i.e. 2 to 20-fold increase in signal after 3 hours over 3 experiments), but this effect was transient, and was no longer statistically significant after 6 hours and the presence of AICAR at this time point did not show any significant effect (Figure 4.5). Lowering the concentration of D-glucose from 25 mM to zero significantly increased the phosphorylation of AMPK, but this only achieved statistical significance after 6 hours. This is consistent with the time course in Figure 4.1.a and implies that the AMP concentration in the cell does not immediately respond to changes in D-glucose concentration (see Discussion).

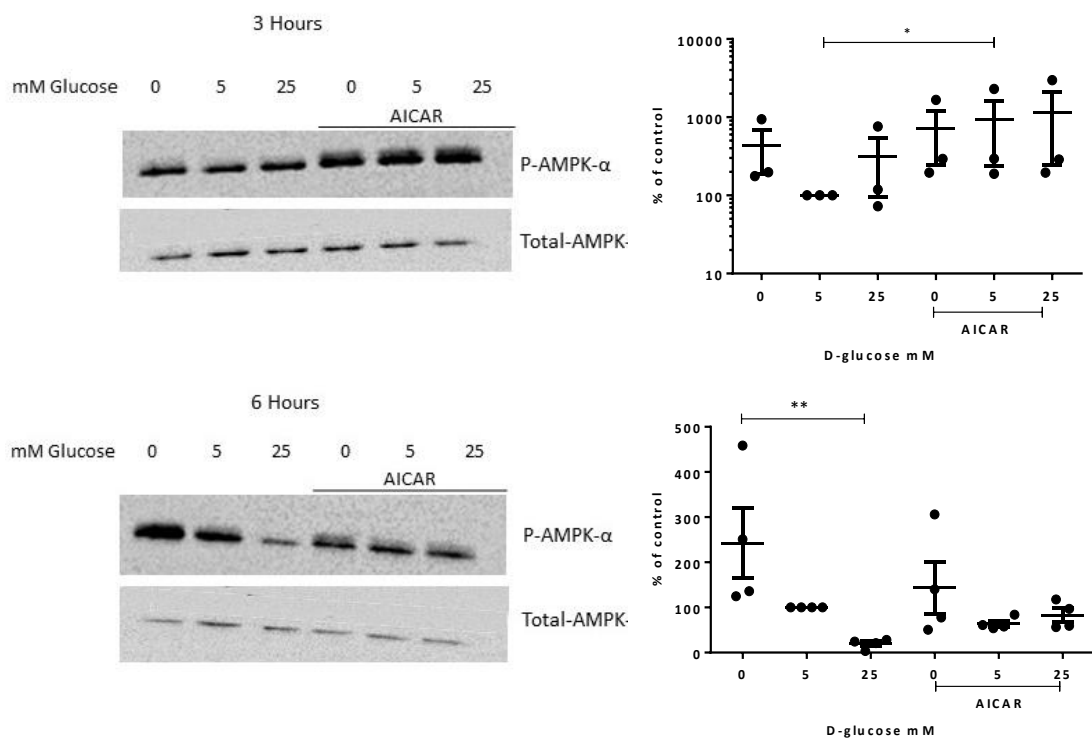


**Figure 4.5. Effect of D-glucose starvation on Thr172 AMPK phosphorylation in INS1E cells**

INS1E cells were incubated for 3 or 6 hours in DMEM containing 2 mM L-glutamine, 0.8 mM L-leucine and D-glucose (0, 5 or 25 mM) in the absence or presence of 750  $\mu$ M

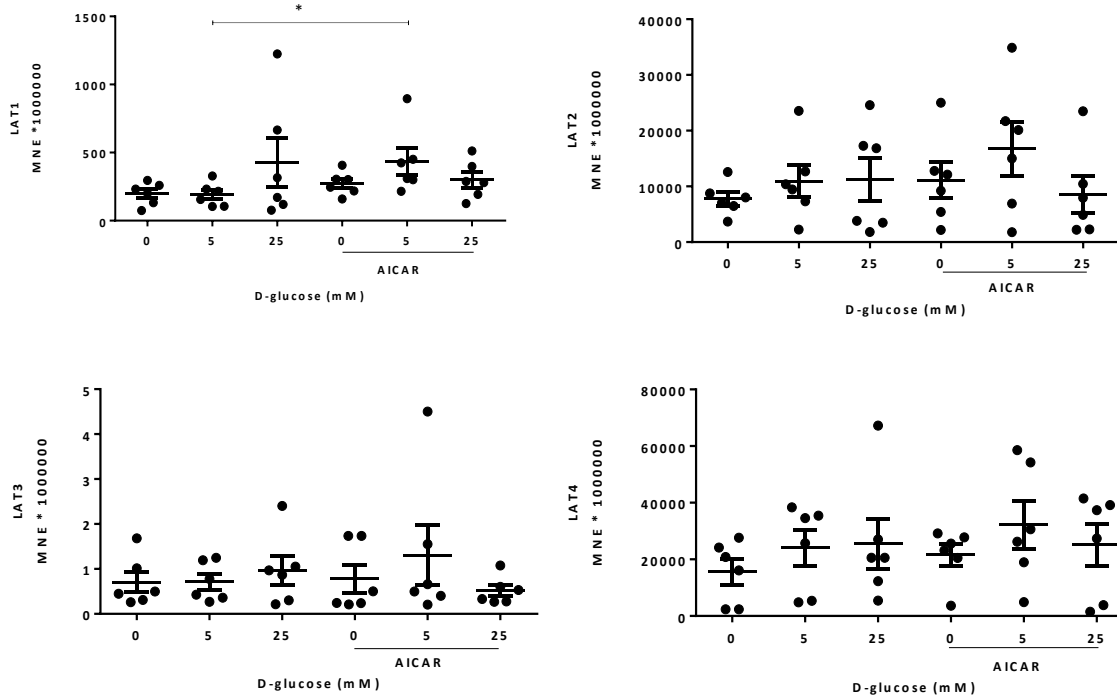
AICAR. Proteins were resolved by SDS-PAGE, and Western blotted using antisera against the proteins indicated. The data for the phospho-AMPK- $\alpha$  signal are shown as a percentage of the control value measured in the presence of 5 mM D-glucose. Data at t=3h are plotted on a logarithmic vertical scale to aid visibility. Data at t = 3 hours are from 3 independent experiments. Data at t = 6 hours are from 4 independent experiments \*(p<0.05), \*\*(p<0.01).

#### **4.2.6. The effect of 4 hours of D-glucose starvation or the activation of AMPK with AICAR on LAT1-4 mRNA expression on INS1E cells**

As the expression at mRNA level of several LAT transporter genes was detected in INS1E cells in Section 3.2.6, qRT-PCR analysis was performed on cells which had been incubated with different concentrations of D-glucose (0, 5 and 25 mM) in the absence and presence of 750  $\mu$ M AICAR, to determine whether the effects on transport observed after 6 hours of incubation might have arisen from increased transcription of LAT genes. Both 4 hour and 6 hour time points were studied because effects on mRNA expression might precede changes in LAT protein expression and transport activity, and also because AMPK activation by AICAR reached maximum before 6 hours (Figure 4.5). After 4 hours the expression of LAT1 did not show any significant change when D-glucose was removed from the medium compared to the basal conditions (5mM D-glucose). However, in the presence of AICAR there was a significant increase in the mRNA expression with 5mM D-glucose compared with the same D-glucose concentration in the absence of AICAR (Figure 4.7.a). This apparent response to AICAR but not to D-glucose deprivation is consistent with the more rapid activation of AMPK by AICAR than by D-glucose deprivation that was seen in Figure 4.5. Wide variation in the data was observed between replicate experiments and, for this reason the data for LAT1 are re-plotted in Figure 4.7.b expressed as fold-increase over the 5mM D-glucose control value.

No statistically significant changes were detected for LAT2 or LAT4. As in Section 3.2.6, very low expression of LAT3 was detected, and the results for these LAT transporters showed a variable effect (Figure 4.6).

a. mRNA expression in INS1E



Median MNE x 1000000	0 glucose	5mM glucose	25mM glucose	0 glucose + AICAR	5mM glucose + AICAR	25mM glucose + AICAR
LAT1	216	185	243	274	367	284
LAT2	7518	9915	10335	10669	17567	6408
LAT3	0	1	1	0	1	0
LAT4	18438	30105	20564	24379	28450	32387

b. INS1E LAT1 expression relative to control (5mM D-glucose)

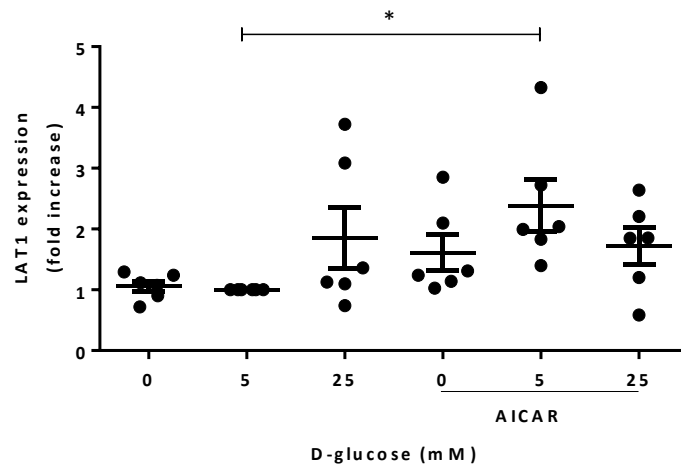


**Figure 4.6. INS1E D-glucose/AICAR effect on relative expression of system L amino acid transporters (LATs).**

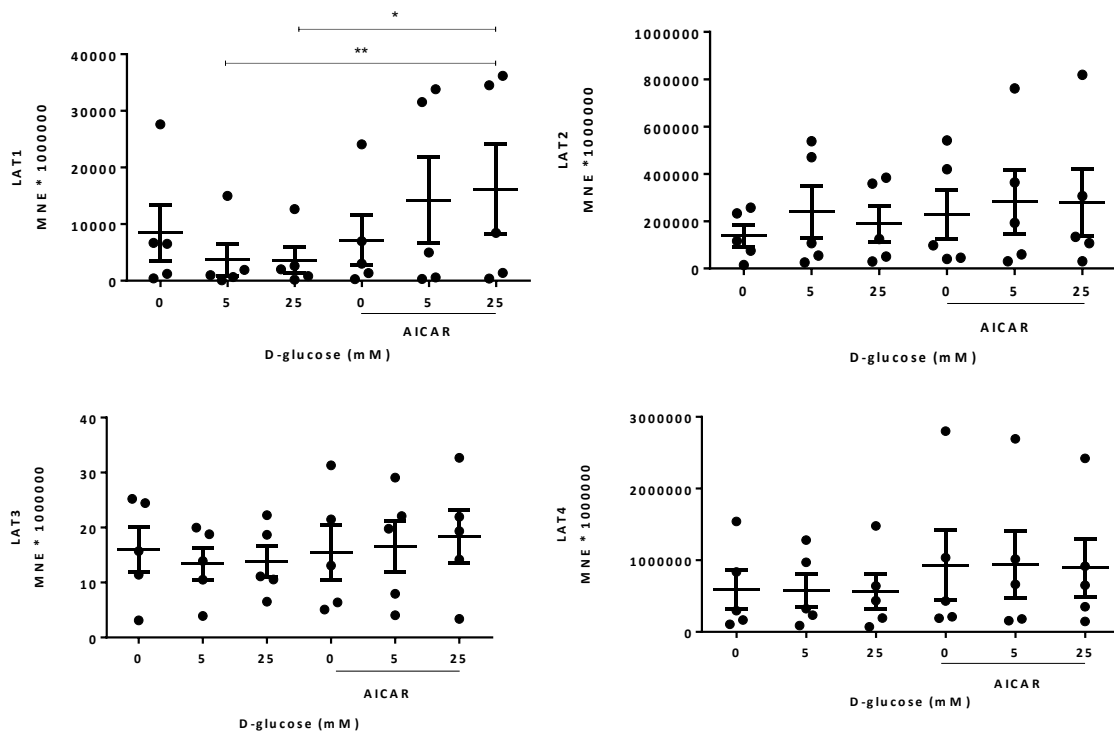
INS1E cells were incubated for 4 hours in DMEM containing 2 mM L-glutamine, 0.8 mM L-leucine and D-glucose (0, 5, 25 mM) in the absence or presence of 750  $\mu$ M AICAR. qPCR analysis was calculated as fold change in expression of the target genes (LAT1, LAT2, LAT3 and LAT4) relative to the reference gene (18S RNA). The mean normalized expression (MNE) of the target genes was calculated. Expression values were multiplied by 1000000 for clarity of presentation. The results are presented for five independent experiments. \*( $p < 0.05$ ) compared with the stated control condition.

#### 4.2.7. The effect of D-glucose starvation or the activation of AMPK with AICAR on LAT1-4 mRNA expression in INS1E cells at 6 hours

In longer incubations of 6 hours, analysis of variance on the LAT1 data still detected statistically significant elevation of LAT1 mRNA expression in the presence of AICAR in cultures with 25mM D-glucose (Figure 4.7.a). Unlike the 4 hours incubations, LAT1 expression in D-glucose-deprived cultures was higher than in control cultures with 5mM D-glucose in all 5 replicate experiments, but this did not reach statistical significance. Data for all the experiments were pooled to compare D-glucose deprivation with 5mM D-glucose in Section 4.2.10 below, showing a significant increase in LAT1 mRNA expression in the absence of D-glucose. As in the 4 hours incubations, no reproducible effects were seen on expression of LAT2, LAT3 or LAT4 (Figure 4.10.a).

Again wide variation in the data was observed between replicate experiments and, for this reason the data for LAT1 are re-plotted in Figure 4.7.b expressed as fold-increase over the 5mM D-glucose control value. The data are plotted on a logarithmic scale to make all of the replicate experiments easily visible.

a. mRNA expression in INS1E



Median MNE x 1000000	0 glucose	5mM glucose	25mM glucose	0 glucose + AICAR	5mM glucose + AICAR	25mM glucose + AICAR
LAT1	6519	998	2006	3003	4989	8443
LAT2	116092	107026	124794	97955	193297	133586
LAT3	16	14	11	13	20	19
LAT4	296836	323803	435026	431111	663556	651595

**b.INS1E LAT1 expression relative to Control (5mM D-glucose)**

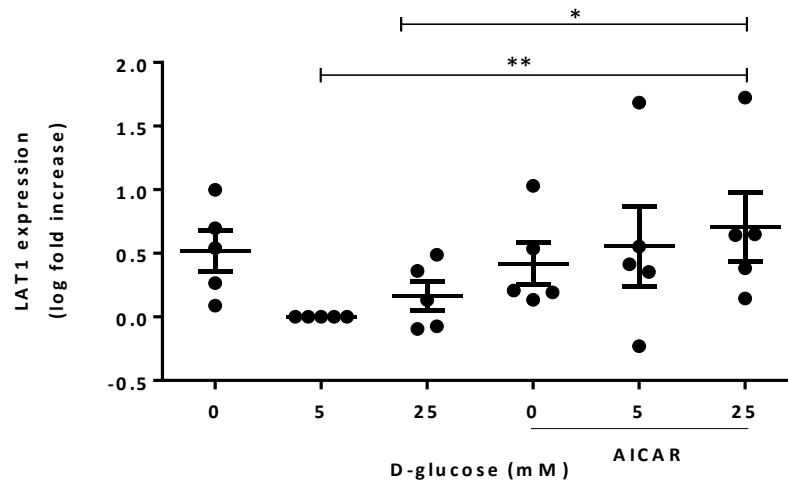


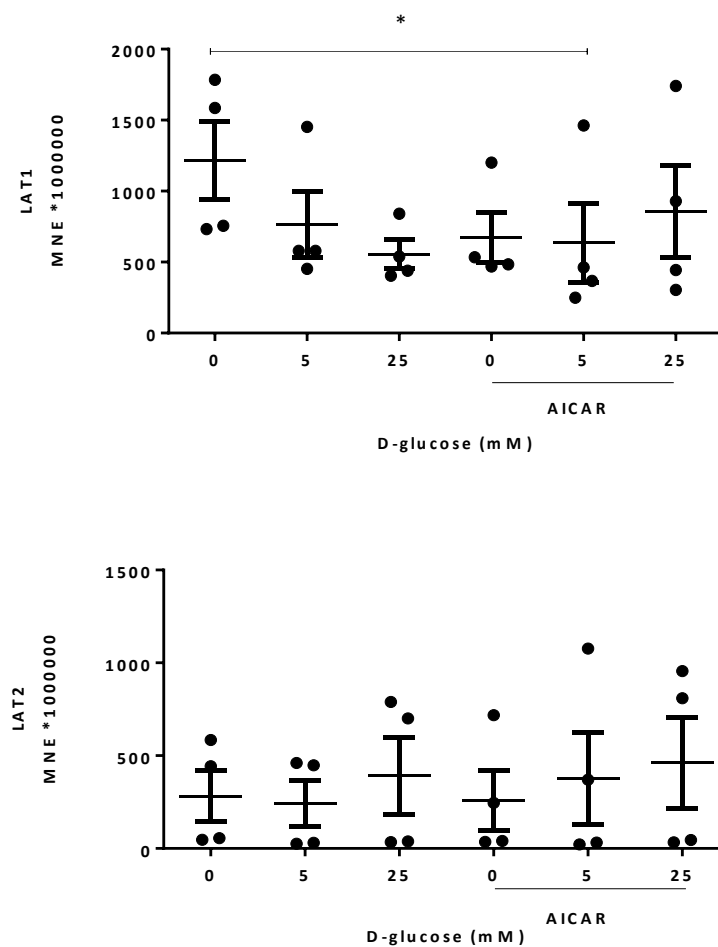
**Figure 4.7. INS1E D-glucose/AICAR effect on relative expression of system L amino acid transport (LATs).**

INS1E cells were incubated for 6 hours in DMEM containing 2 mM L-glutamine, 0.8 mM L-leucine and D-glucose (0, 5, 25 mM) in the absence or presence of 750  $\mu$ M AICAR. qPCR analysis was calculated as fold change in expression of the target genes (LAT1, LAT2, LAT3 and LAT4) relative to the reference gene (18S RNA). The mean normalized expression (MNE) of the target genes was calculated. Expression values were multiplied by 1000000 for clarity of presentation. The results are presented for five independent experiments (\* $p$ <0.05), (\*\* $p$ <0.01) compared with the stated control condition.

#### 4.2.8. The effect of 4 hours of D-glucose starvation or the activation of AMPK with AICAR on LAT1 and LAT2 mRNA expression in mouse MIN6 cells

In view of the apparent (but variable) increase in LAT1 mRNA observed in INS1E cells following D-glucose deprivation, an attempt was also made to detect this effect in another  $\beta$  cell line (mouse MIN6 cells). Using primers specific for mouse LAT1 and LAT2, relative expression was assayed by qRT-PCR after incubation of MIN6 cells with different concentrations of D-glucose (0, 5 and 25 mM) in the absence or presence of 750  $\mu$ M AICAR for 4 hours. As in INS1E cells an apparent increase in LAT1 expression was observed on D-glucose starvation, but varied widely in magnitude between replicate experiments (Figure 4.8). However, at least at this 4 hour time point, no significant effect of AICAR was observed, and this mouse model was not used for further experiments.

a. mRNA expression in MIN6



Median MNE x 1000000	0 glucose	5mM glucose	25mM glucose	0 glucose + AICAR	5mM glucose + AICAR	25mM glucose + AICAR
LAT1	1215	766	556	672	636	854
LAT2	249	240	369	143	201	428

c. MIN6 LAT1 expression relative to control (5mM D-glucose)

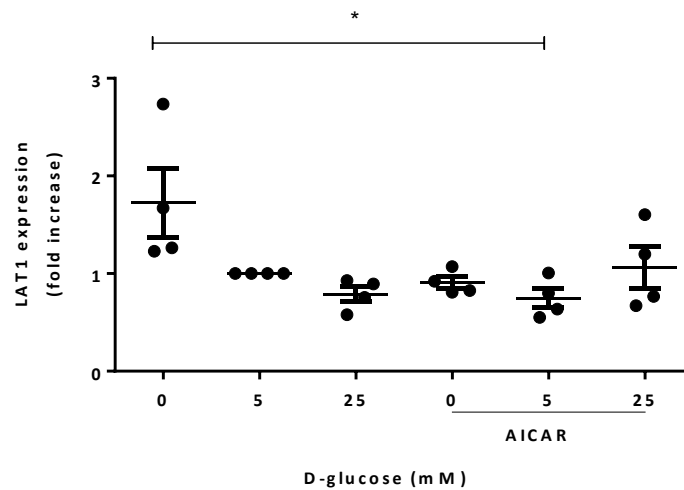


**Figure 4.8. MIN6 D-glucose/AICAR effect on relative expression of system L amino acid transporters (LATs).**

MIN6 cells were incubated for 4 hours in DMEM containing 2 mM L-glutamine, 0.8 mM L-leucine and D-glucose (0, 5, 25 mM) in the absence or presence of 750  $\mu$ M AICAR. qPCR analysis was calculated as fold change in expression of the target genes (LAT1 and LAT2) relative to the reference gene (18S RNA). The mean normalized expression (MNE) of the target genes was calculated. Expression values were multiplied by 1000000 for clarity of presentation. The results are presented for 4 independent experiments. \*( $p < 0.05$ ) compared with the stated control.

#### 4.2.9. The effect of D-glucose starvation on L-[<sup>3</sup>H]-leucine transport is not affected by blocking transcription with actinomycin-D in INS1E cells

To determine the effect of D-glucose deprivation on L-[<sup>3</sup>H]-leucine transport when transcription is blocked, INS1E cells were treated with different concentrations of D-glucose (0, 5 and 25 mM) in the absence or presence of 1 μM actinomycin-D during 6 hour incubations. Consistent with the previous experiments, the L-[<sup>3</sup>H]-leucine transport influx significantly increased with D-glucose depletion compared with normal concentration of D-glucose (5 mM). However, there was no significant blunting of this effect with the presence of actinomycin-D at these different D-glucose concentrations (Figure 4.9), suggesting that increased transcription of LAT1, leading to the variable apparent increase in LAT1 mRNA observed in Figure 4.6 (and also in Figure 4.10 below) is not required for the observed increase in L-[<sup>3</sup>H]-leucine transport.

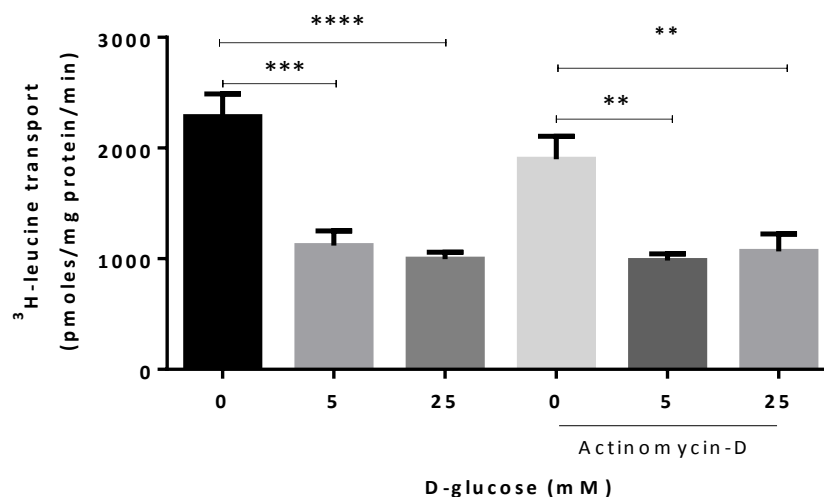


**Figure 4.9. INS1E D-glucose/actinomycin-D effect on L-[<sup>3</sup>H]-leucine transport after 6 hours incubation.**

L-[<sup>3</sup>H]-leucine uptake in INS1E cells (after incubation with 50 μM L-[<sup>3</sup>H]-leucine for 1 min) was measured after incubating for 6 hours in DMEM with different concentrations of D-glucose (0, 5 and 25 mM) in the absence or presence of 1 μM actinomycin-D. All transport values are expressed as picomoles per mg of protein per minute. The results are mean ± S.E.M of three independent experiments \*\*\*\*(p<0.0001), \*\*\*(p<0.001),\*\*(p<0.01) compared with the stated control.

#### **4.2.10. Confirming blockade of transcription with actinomycin-D**

To confirm that actinomycin-D under the conditions used in Figure 4.9 was effective in blocking transcription of LAT genes, qRT-PCR was performed with different concentrations of D-glucose (0, 5 and 25 mM) in the absence or presence of 1  $\mu$ M actinomycin-D during 6 hour incubations in INS1E cells.

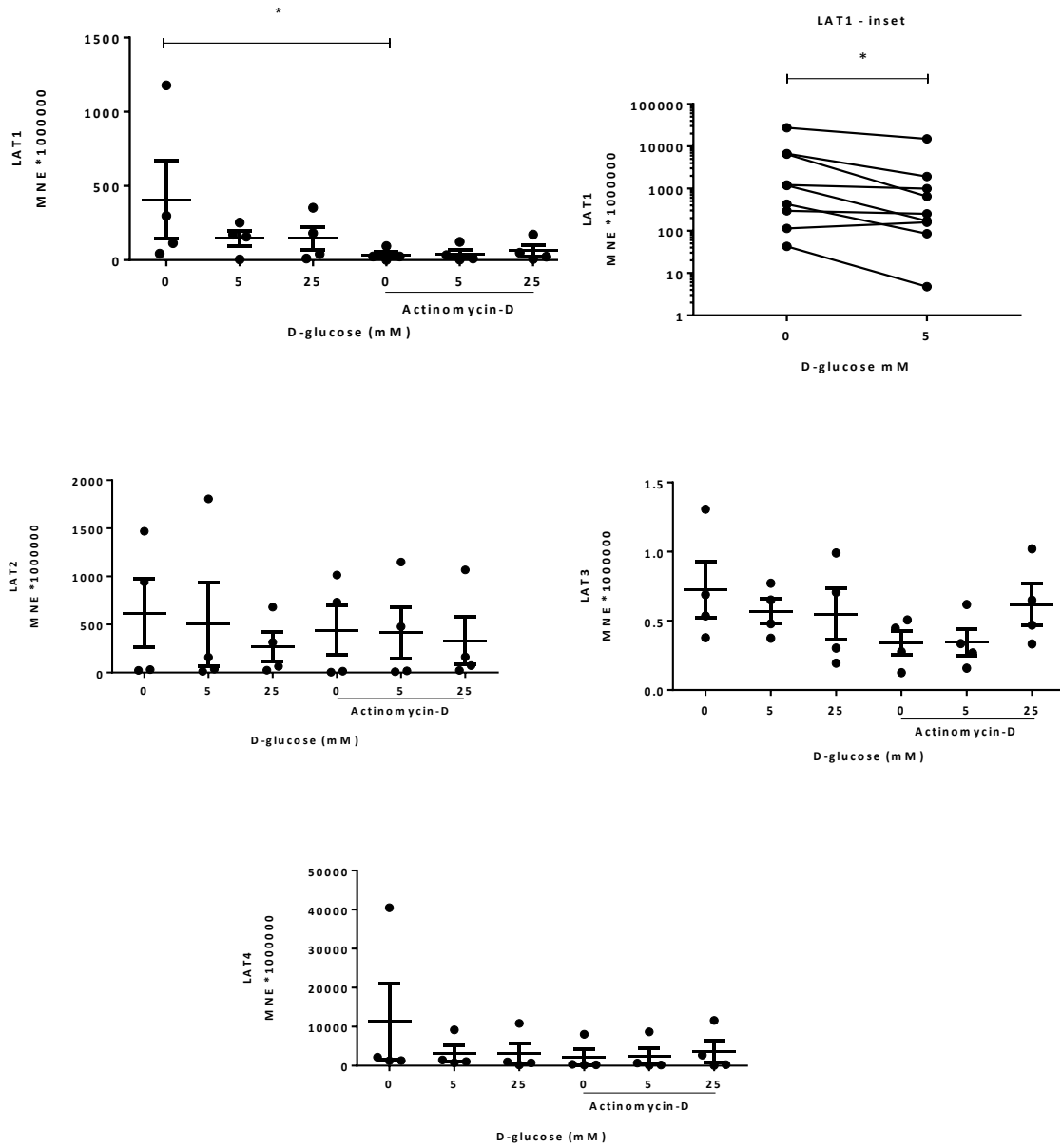
As in Figure 4.7.a, the qRT-PCR signal obtained for LAT1 varied widely between experiments (Figure 4.10.a) and the apparent increase in LAT1 mRNA expression in response to D-glucose deprivation did not reach statistical significance. (However, comparing the LAT1 signal obtained with 0 versus 5 mM D-glucose in the 9 independent experiments pooled from Figure 4.7.a and Figure 4.10.a did detect a statistically significant increase on D-glucose starvation (median 3.5-fold increase, Wilcoxon matched-pairs signed rank test,  $P < 0.05$ ). The pooled data are plotted as an inset figure in Figure 4.10.a. The LAT2, LAT3 and LAT4 mRNA expression was variable between the experiments, and LAT3 was almost undetectable (Figure 4.10.a).

The LAT1 mRNA expression was strongly inhibited by the presence of actinomycin-D, showing a statistically significant 10-fold decline in D-glucose deprived cultures in Figure 4.10.b, thus confirming the influence of the inhibitor in blocking transcription.

A possible effect of D-glucose deprivation was also found in the LAT4 mRNA expression data in Figure 4.10.a. However this was not seen in the earlier experiments (Figure 4.7.a) and no statistically significant effect was seen in the pooled data.

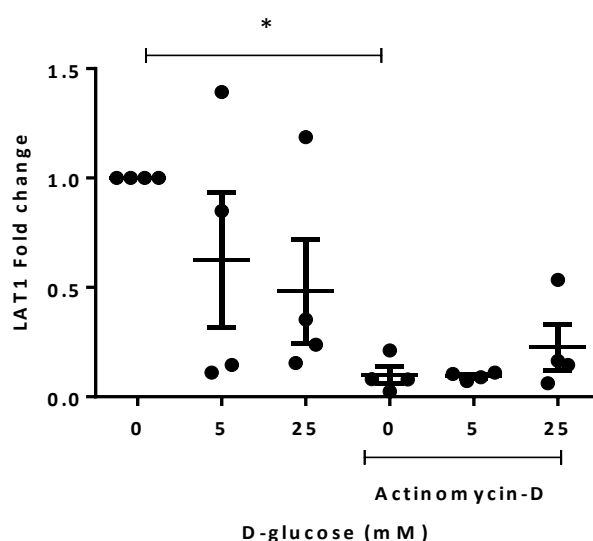
No effect of actinomycin-D was detected on the qRT-PCR signal from the 18s rRNA that was used as house-keeping gene in these experiments (data not shown). To confirm that there was also no effect of actinomycin-D on the total (largely ribosomal) concentration of RNA in these cultures, the absorbance of the RNA extracts at 260 nm was monitored and is shown in Figure 4.10.c.

a. INS1E D-glucose/actinomycin-D effect on LAT1-4 mRNA expression



Median MNE x 1000000	0 glucose	5mM glucose	25mM glucose	0 glucose + actinomycin- D	5mM glucose + actinomycin- D	25mM glucose + actinomycin- D
LAT1	206	165	111	24	22	36
LAT2	487	98	189	374	247	117
LAT3	1	1	1	0	0	1
LAT4	1760	1277	857	289	434	1490

**b. INS1E D-glucose/actinomycin-D effect on LAT1 mRNA expression (fold change)**



**c. INS1E D-glucose/actinomycin-D effect on total RNA (OD260/280)**

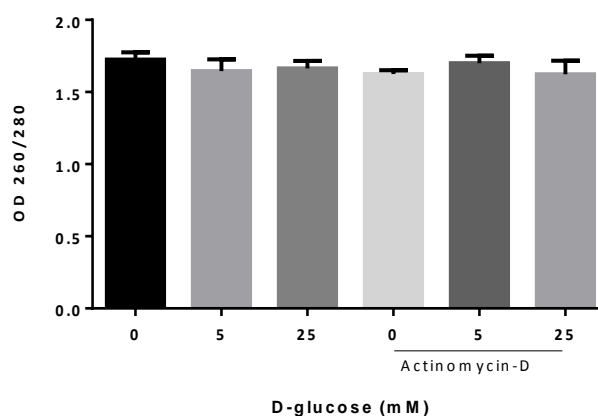


**Figure 4.10. INS1E D-glucose/actinomycin-D effect on LAT mRNA expression after 6 hours incubation.**

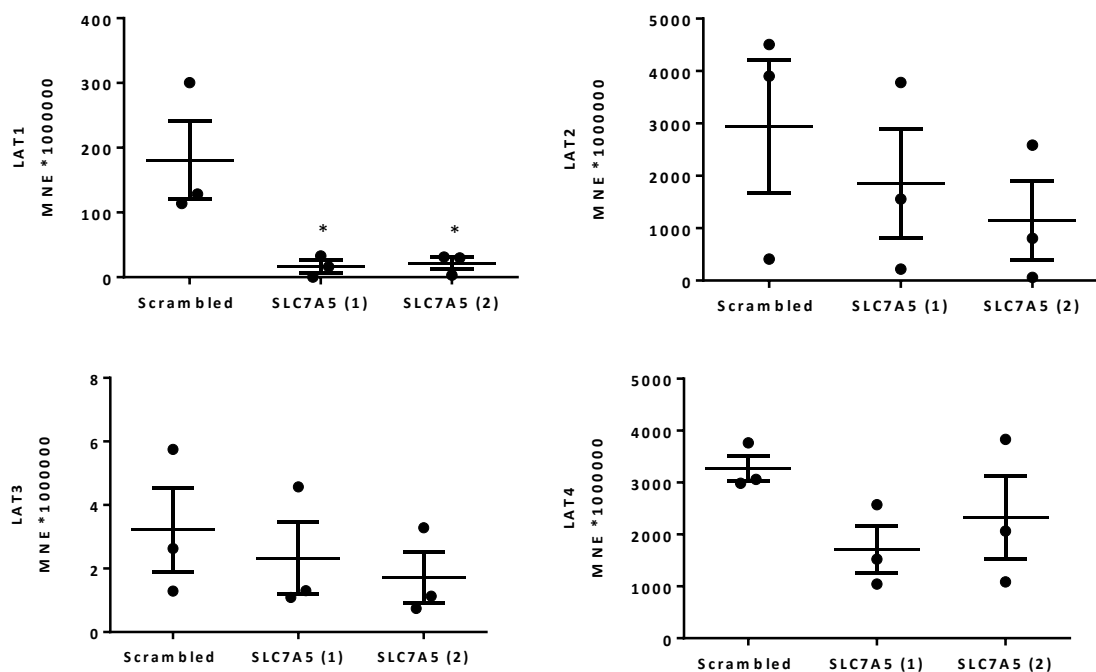
INS1E cells were incubated for 6 hours with different concentrations of D-glucose (0, 5 and 25 mM) in the presence or absence of 1  $\mu$ M actinomycin-D. cDNA was amplified by qRT-PCR using gene-specific rat primers (LAT1, LAT2, LAT3 and LAT4) and reference gene (18s rRNA). The mean normalized expression (MNE) of the target genes was calculated. In (a) expression values were multiplied by 1000000 for clarity of presentation. The results are presented for four independent experiments. Data for LAT1 from (a) are replotted in (b) as fold change relative to the values obtained in D-glucose deprived cultures. LAT1 – inset shows data from (a) pooled with data under the same conditions

from Figure 4.7.a. plotted on a logarithmic vertical scale. **(c)** Absorbance at 260 nm of Trizol RNA extracts is presented as a measure of total RNA content in the cultures. \*( $p < 0.05$ ) compared with the stated control.

#### 4.2.11. Effect of siRNA Silencing of LAT1 in Rat INS1E cells on expression of system L amino acid transporters (LATs)

As an alternative (and more selective) way to investigate the role of LAT1 mRNA expression in the regulation of L-[<sup>3</sup>H]-leucine transport, two validated small interfering RNAs (siRNAs) against LAT1(SLC7A5) designated SLC7A5 (1) (Dharmacon, L-092749-01-0005) and SLC7A5 (2) (Ambion s132356), were transfected into INS1E cells and compared with the effect of transfection of a Scrambled control siRNA. The mRNA expression of LAT1 assessed by qRT-PCR was significantly reduced by both of the two silencing siRNA preparations (Figure 4.11.a). In the same experiments no statistically significant effect was seen on the expression of the other three LATs (LAT2, LAT 3 and LAT4) (Figure 4.11.a). Expressed as a percentage of the value obtained with the Scrambled control, LAT1 siRNA decreased LAT1 mRNA expression in INS1E cells by more than 85%, confirming that both siRNA SLC7A5 (1) and SLC7A5 (2) efficiently silence LAT1 expression (Figure 4.11.b).

a. LAT1 silencing effect on mRNA expression



Median MNE x 1000000	Control	SLC7a5 (1)	SLC7a5 (2)
LAT1	300	16	30
LAT2	3900	1557	808
LAT3	3	1	1
LAT4	3062	1525	2065

**b. LAT1 silencing effect on mRNA expression expressed as a percentage of control**

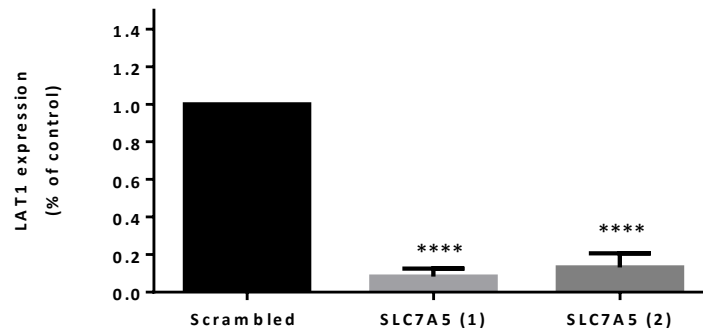


**Figure 4.11. INS1E LAT1 siRNA effect on relative expression of system L amino acid transporters (LATs).**

INS1E cells were transfected for 48 hours with siRNA against LAT1-SLC7A5 (Dharmacon (1), and Ambion (2)) or Scrambled sequence as control. qRT-PCR was then performed using gene-specific primers for LAT1, LAT2, LAT3 and LAT4, and reference gene (18s RNA). The mean normalized expression (MNE) of the target genes was calculated. Expression values were multiplied by 1000000 for clarity of presentation. In **(a)** the results are presented for three independent experiments. In **(b)** data are presented as the mean  $\pm$  S.E.M compared with the Scrambled control. \*\*\*\*( $p < 0.0001$ ), \*( $p < 0.05$ ) versus control.

#### 4.2.12. Effect of siRNA Silencing of LAT1 in Rat INS1E cells on L-[<sup>3</sup>H]-leucine transport

To further investigate the functional effect of LAT1 silencing on L-[<sup>3</sup>H]-leucine transport, siRNAs against SLC7A5 (Dharmacon, L-092749-01-0005 and Ambion s132356), were transfected into INS1E cells for 48 hours followed by assay of L-[<sup>3</sup>H]-leucine transport. Even though LAT2 and LAT4 mRNA are both strongly expressed in INS1E cells, silencing of LAT1 alone was sufficient to reduce the L-[<sup>3</sup>H]-leucine transport. With silencing siRNA SLC7A5 (2), 35% inhibition (\*p<0.05) was obtained compared with the scrambled control (Figure 4.12).

In theory, this LAT1-silencing siRNA (SLC7A5 (2)) could be used to investigate whether LAT1 is involved in the activation of L-[<sup>3</sup>H]-leucine transport that is observed in response to AICAR as in Figure 4.3.a. However, when INS1E cells were transfected with siRNA SLC7A5 (2) for 48 hours and treated with AICAR during 6 hours to assess the effect on L-[<sup>3</sup>H]-leucine transport, a technical problem was observed (Figure 4.12). In the absence of AICAR, silencing LAT1 significantly decreased the uptake of L-leucine by 33% (in agreement with Figure 4.12.a) and, as predicted, treatment with AICAR failed to give a statistically significant increase in transport in the presence of this silencing (Figure 4.12.b). However, transfection with the Scrambled siRNA control also abolished the normal stimulation of transport by AICAR (Figure 4.12.b), suggesting that the transfection agent was interfering in the experiment by blocking the action of AICAR on transport.

##### a. INS1E LAT1 siRNA effect on L-[<sup>3</sup>H]-leucine transport

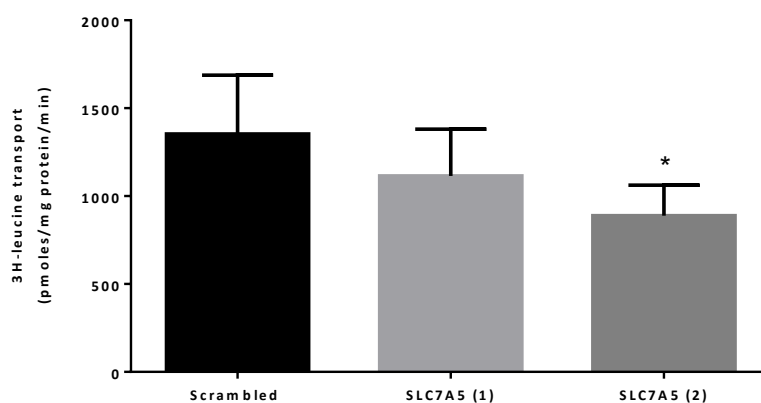


**Figure 4.12. INS1E LAT1 siRNA effect on L-[<sup>3</sup>H]-leucine transport.**

**a)** L-[<sup>3</sup>H]-leucine uptake in INS1E cells (after incubation with 50 μM L-[<sup>3</sup>H]-leucine for 1 min) after 48 hours transfection with siRNA against LAT1-SLC7A5 (Dharmacon (SLC7A5 (1)) and Ambion (SLC7A5 (2)) or Scrambled sequence as control. All transport values are expressed as picomoles per mg of protein per minute. The results are mean ± S.E.M for three independent experiments. \*(p<0.05) versus Scrambled control.

**b. INS1E LAT1 siRNA effect of AICAR on L-[<sup>3</sup>H]-leucine transport**

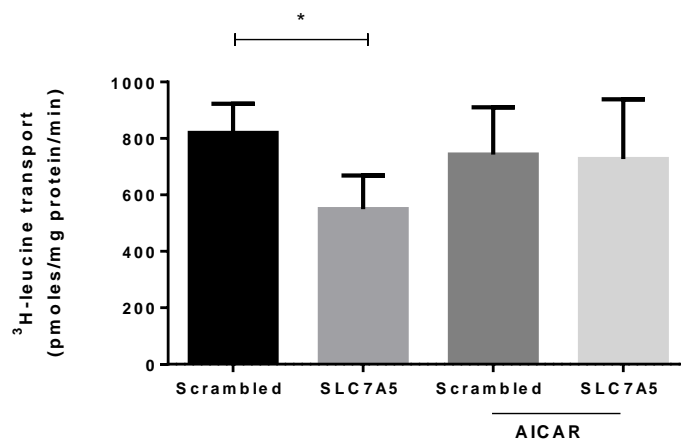


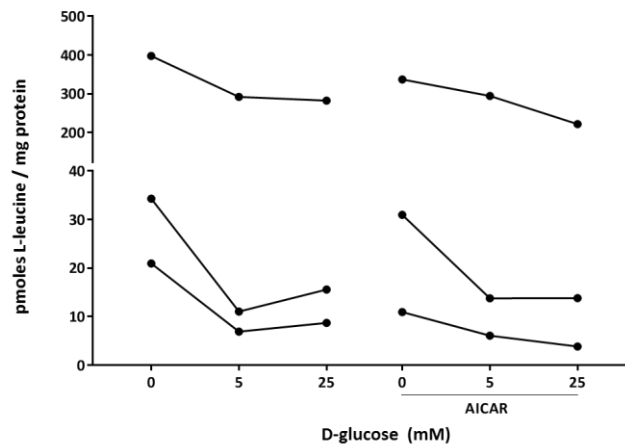
**Figure 4.12. INS1E LAT1 siRNA effect with and without AICAR on L-[<sup>3</sup>H]-leucine transport.**

**b)** L-[<sup>3</sup>H]-leucine uptake in INS1E cells (measured by incubation with 50 μM L-[<sup>3</sup>H]-leucine for 1 min) after 48 hours transfection with Ambion siRNA against LAT1-SLC7A5 or Scrambled sequence as control, and incubation with or without 750 μM AICAR for 6 hours. All transport values are expressed as picomoles per mg of protein per minute. The results are mean ± S.E.M for three independent experiments. (\*p<0.05) versus Scrambled control without AICAR.

#### **4.2.13. Effect of D-glucose withdrawal in the absence and presence of AICAR on intracellular L-leucine concentration**

Finally, an experiment was performed to investigate the correlation between the effects of D-glucose availability on intracellular signalling and L-leucine transport, and the composition of the intracellular free amino acid pool. A possible explanation for the stimulation of L-leucine transport by D-glucose deprivation is that when D-glucose supply fails, intracellular L-leucine is degraded through branched-chain keto acid dehydrogenase (BCKADH) (Harris et al. 2001) and the Krebs cycle as an alternative metabolic fuel. The resulting depletion of intracellular L-leucine may then stimulate L-leucine transport as has been seen for other amino acid transporters such as slc38a2 (SNAT2) during cellular amino acid depletion (Hyde et al. 2007). The intracellular amino acid concentrations in INS1E cells were therefore determined by HPLC (high performance liquid chromatography) after 6 hours of exposure to 0, 5 or 25 mM D-glucose with or without AICAR. However, the expected L-leucine depletion was not observed. Indeed, in spite of the wide variation in the baseline L-leucine concentration observed in the cells over the 3 experiments shown in Figure 4.13.a, D-glucose deprivation significantly increased the concentration of L-leucine. When the data were expressed as a percentage of the 5 mM D-glucose control value, an average 2.5-fold increase in cellular L-leucine concentration was observed (Figure 4.13.b). This effect was not significantly affected by the presence of AICAR (Figure 4.13).

a. Intracellular L-leucine concentration in the three independent experiments



b. Normalised data

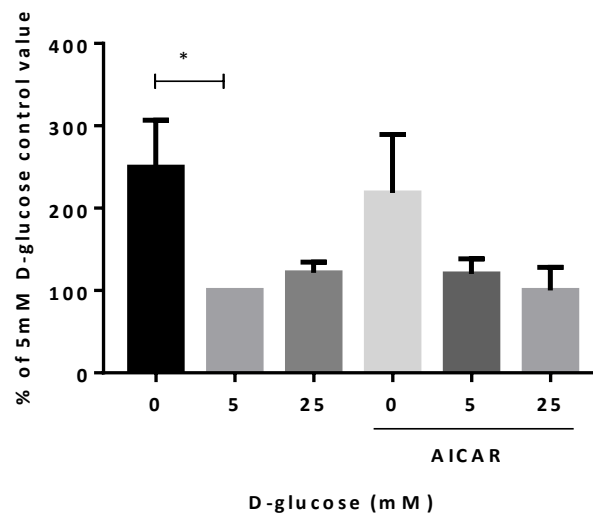


**Figure 4.13. Effect of D-glucose availability and the presence of AICAR on intracellular L-leucine concentration in INS1E cells.**

INS1E cells were incubated for 6 hours in DMEM containing 2 mM L-glutamine, 0.8 mM L-leucine and D-glucose (0, 5, 25 mM) in the absence or presence of 750 μM AICAR. The cells were then washed with isotonic saline to remove extracellular free amino acids and immediately deproteinised with perchloric acid (PCA). To separate, identify, and quantify L-leucine in the samples, the lysates in PCA were analysed by HPLC. The results are mean ± S.E.M for 3 independent experiments. (\*P<0.05) versus the control with 5 mM D-glucose.

### 4.3. Discussion

#### 4.3.1. D-glucose starvation & AICAR activate System L-[<sup>3</sup>H]-leucine transport in INS1E cells

In pancreatic  $\beta$  cells, LAT amino acid transporters are involved in the uptake of large neutral amino acids such as L-leucine to support cell growth and proliferation, and also possibly energy metabolism, because supplying amino acids to  $\beta$  cells has been shown to improve the energy status of the cell and therefore suppress the AMP-sensing kinase AMPK (Leclerc and Rutter 2004). This transport mechanism may therefore be affected by (and respond to) energy disorders such as D-glucose deprivation. The experiments in this chapter were designed to test the hypothesis that was stated in Section 1.13 of this thesis, i.e. that D-glucose deprivation, resulting in AMPK activation, stimulates or up-regulates LAT transporters resulting in an increased rate of L-leucine transport in the rat  $\beta$  cell line INS1E.

Initial experiments in INS1E to determine the effect of D-glucose starvation compared the effect of this on L-[<sup>3</sup>H]-leucine transport with control cultures supplied with 5 mM D-glucose. This demonstrated a significant increase in the transport after 5 or 6 hours (Figure 4.1.a). In contrast only a small stimulatory effect of D-glucose starvation on L-[<sup>3</sup>H]-leucine transport was seen transiently on HEK293A cells (Figure 4.1.b) and no effect on L6 myoblasts, indicating that this effect might be specific for  $\beta$  cell lines. However, similar findings to those in Figure 4.1.a have been seen with studies in retinal endothelial cells and HL60 leukaemia cells where D-glucose removal also increased L-[<sup>3</sup>H]-leucine transport or LAT1 expression, but a much longer time of D-glucose deprivation was needed than in INS1E cells (Matsuyama et al. 2012, Polet et al. 2016). The reason for this variation between cell types is unknown, but may depend on the amount of alternative fuel such as glycogen that occurs in the cells. It might be expected that ATP synthesis would start to fail (leading to a rise in AMP concentration and AMPK activation) only when glycogen is depleted. The expected effect of D-glucose availability on the activating phosphorylation of AMPK was confirmed in INS1E cells by immunoblotting at 3 and 6 hours at various D-glucose concentrations in the absence and presence of AICAR (Figure 4.5). As anticipated, AICAR significantly activated AMPK

under basal D-glucose levels at 3 hours (Figure 4.5), but D-glucose deprivation significantly increased the phosphorylation of AMPK only after 6 hours, consistent with the time need for L-[<sup>3</sup>H]-leucine transport to increase in Figure 4.1.a. This indicates that the AMP concentration does not immediately respond to changes in D-glucose concentration. A small amount of glycogen is known to occur in  $\beta$  cells, including INS1E cells, so under D-glucose deficiency, glycogenolysis may be able to maintain the rate of ATP synthesis and hence prevent the AMP concentration and AMPK activity from rising in the first 3 h (Mir-Coll et al. 2015) (Martino et al. 2012).

In contrast, the findings with high concentrations of D-glucose (25 mM) on L-[<sup>3</sup>H]-leucine transport were variable between batches of cells (compare Figures 4.1.a, 4.2 and 4.3.a). This was possibly happening because high concentrations of (osmotically active) D-glucose cause a variable stimulation of insulin secretion (Hohmeier et al. 2000) which activates mTORC1, activating in turn LAT1 transporters (Milkereit et al. 2015). To test the effect of D-glucose concentration on L-[<sup>3</sup>H]-leucine transport when the insulin secretion is blocked, nifedipine was used with different concentrations of D-glucose in INS1E cells (Figure 4.2). There was no significant effect of nifedipine on L-[<sup>3</sup>H]-leucine transport with 25 mM D-glucose, suggesting that the effect of autocrine insulin was negligible. However, D-glucose starvation in the presence of nifedipine, significantly increased L-[<sup>3</sup>H]-leucine transport, increasing the stimulatory effect of the absence of D-glucose on L-leucine transport, indicating that there may be involved a calcium-dependent process other than insulin secretion. A chronic (10 hour) increase in intracellular calcium has been shown to blunt AMPK activation in C2C12 myotubes (Park et al. 2013). Therefore if AMPK is involved in activating L-[<sup>3</sup>H]-leucine transport in D-glucose-deprived cells, this may explain why chronic incubation with a calcium channel blocker amplified the effect of D-glucose deprivation in Figure 4.2

To test more directly the idea that, under D-glucose deprivation, INS1E cells may reduce their energy status sensed by AMP-activated kinase (AMPK) which might then be responsible for the significant increase in L-[<sup>3</sup>H]-leucine transport, the AMPK analogue AICAR was used in INS1E cells under different concentrations of D-glucose (Figure 4.3.a). The presence of AICAR exhibited a high stimulatory effect on L-[<sup>3</sup>H]-leucine transport in

INS1E cells with 5 mM D-glucose. However, AICAR did not show any further increase with D-glucose deprivation, suggesting that the AICAR and D-glucose deprivation effects are not additive and may act through the same pathway (i.e. AMPK). With the cell types tested here, this effect was confined to INS1E cells as there was no effect found in the presence of AICAR on non-transfected HEK293A cells (Figure 4.3.b) nor L6 myoblasts (Figure 4.3.c). The reason for this is unknown, but might arise from differences in the L-leucine transporter proteins that are most strongly expressed in these cell types.

#### **4.3.2. Effects of D-glucose starvation and AICAR on L-leucine transport are not accompanied by stimulation of System A**

LAT transporters such as LAT1 are passive exchangers of neutral amino acids such as L-leucine across the plasma membrane in exchange for some intracellular amino acids (Zheng et al. 2016). This transport process can lead to active transport (i.e. pumping) of L-leucine into cells- by coupling to active System A transporters (Figure 1.12) to control the intracellular concentration of L-leucine (Baird et al. 2009, Evans et al. 2007).

In T-lymphocytes the expression of System A transporters of the SLC38 gene family can be up-regulated following D-glucose starvation and, in AMPK knock-out mice, the expression of these transporters is reported to be blunted (Blagih et al. 2015). However, in that study the activity of System A transporters was not measured. To investigate whether the D-glucose deprivation-induced and AICAR-induced increase in L-leucine transport in the present study was accompanied by stimulation of System A amino acid transport activity to drive active L-leucine pumping into the cells, <sup>14</sup>C-MeAIB transport (an indicator of System A activity) was measured in INS1E cells and L6 myoblasts under different concentrations of D-glucose with AICAR (Figure 4.4). Contrary to what was found on L-[<sup>3</sup>H]-leucine uptake, the <sup>14</sup>C-MeAIB transport significantly decreased in INS1E cells under D-glucose starvation, but this inhibitory effect was stopped by the presence of AICAR (Figure 4.4.a). To a smaller extent these effects were also found in L6 myoblasts where System A activity showed a small but statistically significant increase in the presence of AICAR (Figure 4.4.b).

System A transporters use the Na<sup>+</sup> gradient across the plasma membrane to drive active transport of amino acids and this Na<sup>+</sup> gradient is maintained by the hydrolysis of ATP by

Na<sup>+</sup>/K<sup>+</sup>-ATPase (Figure 1.12). The Na<sup>+</sup>/K<sup>+</sup>-ATPase pumps sodium out of cells in exchange for potassium: this is a highly ATP-consuming process and uses mainly ATP produced from D-glucose by glycolysis in the cytosol (Sepp et al. 2014). D-glucose deprivation would therefore be expected to inhibit Na<sup>+</sup>/K<sup>+</sup>-ATPase and this may explain the impaired System A activity in D-glucose deprived cells in Figure 4.4. However, AMPK is a key sensor to maintain cellular energy and is activated by D-glucose deprivation or any stress that may increase the intracellular AMP:ATP ratio (Hardie 2003). AMPK activation can activate Na<sup>+</sup>/K<sup>+</sup>-ATPase, and activation of Na<sup>+</sup>/K<sup>+</sup>-ATPase by AICAR has been reported in L6 cells (Benziane et al. 2012). This effect of AICAR may explain the increased System A activity observed with AICAR in Figure 4.4.

#### **4.3.3. The LAT1 transport activation under D-glucose removal is accompanied by increased expression of LAT1 mRNA but not the mRNA for other LATs**

Once it was confirmed that there was a stimulatory effect of D-glucose deprivation and AICAR on the L-leucine transport in INS1E cells, it was necessary to check whether there was an increase in the transcription of LAT genes at 4 and 6 hours to see whether an effect on mRNA expression (possibly leading to increased transporter protein expression) might explain the increased transport activity. At 4 hours, the relative expression of LAT1 under conditions of D-glucose deprivation did not show significant changes. However, LAT1 mRNA expression did increase in the presence of AICAR under normal D-glucose conditions (Figure 4.6.b). In a longer incubation (t = 6h), all experiments on D-glucose-deprived cultures showed higher amounts of LAT1 mRNA compared with normal (5mM D-glucose) conditions, and pooled data from 9 experiments did show a statistically significant 3.5-fold increase in LAT1 mRNA expression (Figure 4.7.b and Figure 4.10.a - inset). This time dependence in the induction of LAT1 expression with a more rapid effect with AICAR than under D-glucose deprivation is consistent with Figure 4.5 where the activation of AMPK by AICAR was more rapid than the D-glucose deprivation. In contrast, both 4 and 6 hour incubations revealed no reproducible effects on expression of LAT2, LAT3 or LAT4.

With the aim of comparing the effect of D-glucose deprivation in LAT1 mRNA relative expression in INS1E cells with another  $\beta$  cell line, mouse MIN6 cells were cultured 4

hours under the same conditions to perform qRT-PCR using specific primers for mouse LAT1 and LAT2. In MIN6 as in INS1E cells, an increase in LAT1 expression was found under D-glucose deprivation, but between the 4 replicate experiments the values were variable (Figure 4.8); and (unlike INS1E) no effect was observed with AICAR. The reason for this difference is unknown, but might mean that the time course of AMPK activation by AICAR in MIN6 is different from that in INS1E. MIN6 culture yield was significantly lower than for INS1E and this could be explained because MIN6 cells are not just  $\beta$  cells. It has been previously demonstrated that MIN6 cells are tumor derived cells that are able to secrete islet hormones such as insulin, glucagon, somatostatin and ghrelin (Nakashima, 2009).

#### **4.3.4. Blockade of transcription with actinomycin-D may slightly blunt the stimulated L-[<sup>3</sup>H]-leucine transport effect of D-glucose starvation but does not abolish it**

To determine the effect of D-glucose deprivation on L-[<sup>3</sup>H]-leucine transport when the apparent transcriptional effect on LAT1 is blocked, INS1E cells were cultured with the same concentrations of D-glucose used before, in the absence or presence of the transcription blocker actinomycin-D during 6 hours. Consistent with the previous experiments, D-glucose depletion significantly increased the L-[<sup>3</sup>H]-leucine transport influx. However, there was no significant blunting of this effect in the presence of actinomycin-D (Figure 4.9). These findings suggest that the increased L-[<sup>3</sup>H]-leucine transport is not exclusively due to increased LAT1 transcription, and that additional effects may be involved e.g. translocation of LAT1 to the plasma membrane activated by AMPK – analogous to the translocation of GLUT glucose transporters stimulated by AMPK in skeletal muscle cells (Park et al. 2009). Investigating this requires an experimental model for labelling (tagging) LAT proteins such as LAT1 and investigating their expression and location in a model cell. Such experiments are the subject of Chapter 5 in this thesis.

To confirm the effectiveness of actinomycin-D in blocking transcription of LAT genes, qRT-PCR was performed under the same D-glucose concentrations in the absence or presence of actinomycin-D. The results obtained for LAT1 mRNA expression in the

absence of actinomycin-D were again very variable, but there was an apparent increase in LAT1 mRNA expression in response to D-glucose starvation, and the LAT1 mRNA expression was strongly inhibited with actinomycin-D, presenting a 10-fold decline in D-glucose deprived cultures (Figure 4.10). This confirmed that actinomycin-D was effective in blocking transcription, and that the lack of effect of actinomycin-D on L-[<sup>3</sup>H]-leucine transport in Figure 4.9 did not arise simply because insufficient actinomycin-D had entered the cells.

#### **4.3.5. siRNA silencing can suppress LAT1 mRNA expression in INS1E, and this can blunt basal (unstimulated) L-[<sup>3</sup>H]-leucine transport**

Through this entire chapter, the importance of energy status in regulating L-leucine transporters in INS1E cells has been studied, and accompanying effects on LAT1 mRNA expression were shown. However the functional importance of LAT1 in relation with L-leucine transport under D-glucose deprivation in  $\beta$  cells was not entirely clear. For example, as LAT4 mRNA was found to be very strongly expressed in these cells, it might be argued that all of the L-[<sup>3</sup>H]-leucine transport that was measured in these experiments was occurring through LAT4 transporter proteins rather than through LAT1. To explore the functional contribution of LAT1 in L-leucine transport in INS1E cells, the effects of silencing LAT1 expression with small interfering RNAs (siRNA) in the regulation of L-[<sup>3</sup>H]-leucine transport were measured.

INS1E cells were transfected with two validated LAT1 siRNA preparations and scrambled control. The LAT1 mRNA expression was inhibited with both siRNAs used in the transfection (Figure 4.11.a) and, expressed as a percentage of the control, the LAT1 siRNA significantly reduced the LAT1 mRNA expression by more than 85% (Figure 4.11.b), confirming the efficiency of the LAT1 silencers. As expected, there was no statistically significant effect on the mRNA expression of the other LATs.

To further investigate the functional effect of this silencing of LAT1 on the L-leucine transport, the same siRNAs were used to transfect INS1E cells for L-[<sup>3</sup>H]-leucine uptake studies. Silencing LAT1 inhibited the L-[<sup>3</sup>H]-leucine transport by 35% with one of the silencers (Figure 4.12.a). It is important that cultures transfected with the scrambled siRNA preparation should be used as the control in these transport experiments (rather

than non-transfected cultures) because it has been reported that short double-stranded RNAs can have significant non-specific stimulatory effects on amino acid transporters (Liong and Lappas 2017).

The LAT1 silencing transport data in Figure 4.12.a suggest that, in spite of its strong expression at mRNA level in INS1E cells, the LAT1 transporter is probably not the only contributor to L-[<sup>3</sup>H]-leucine transport. This conclusion is also supported by experiments with the selective LAT substrate  $\alpha$ -methyl tyrosine which competitively blocks L-leucine transport thus inhibiting mTORC1 signalling in INS1E cells (in an experiment similar to that performed with BCH in Figure 3.1.b) (Cheng 2013), even though  $\alpha$ -methyl tyrosine is not a substrate for LAT1 (Bodoy et al. 2013).

#### **4.3.6. Intracellular concentrations of L-leucine increased under D-glucose deprivation**

A possible explanation for the increased L-leucine transport that was observed here under D-glucose-free conditions is that in the absence of D-glucose, L-leucine influx is up-regulated to provide L-leucine as a fuel to replace D-glucose. This would be consistent with the observation that, even in the presence of D-glucose, an amino acid supplement (including L-leucine) significantly suppresses AMPK activation in MIN6 b-cells (Leclerc and Rutter 2004). Intracellular L-leucine can be degraded through branched-chain keto acid dehydrogenase (BCKADH) (Harris et al. 2001) and the Krebs cycle as an alternative metabolic fuel in mammalian cells, suggesting that, if this explanation is correct, D-glucose starvation should stimulate the depletion of L-leucine inside the cells, possibly leading to a compensatory increase in L-leucine transport into the cell.

To test this explanation, the intracellular L-leucine concentration in INS1E cells under D-glucose deprivation and in the presence of AICAR was measured by HPLC. Surprisingly, the L-leucine concentration under D-glucose deprivation significantly increased compared with that under normal (5 mM) D-glucose conditions (Figure 4.13.b). This accumulation of free L-leucine in the cells is not consistent with the idea that enhanced consumption of intracellular L-leucine is driving the observed changes in L-leucine transport. An alternative explanation for these findings is that the D-glucose starvation

is inhibiting global protein synthesis (but not protein degradation), leading to intracellular accumulation of L-leucine derived from proteins, and this alternative is discussed in more detail in Chapter 6.

This effect on the L-leucine concentration was not observed however in the presence of AICAR (Figure 4.13.a), possibly as a consequence of the faster (but transient) AMPK response to AICAR that was seen in Figure 4.5.

#### **4.4. Conclusion**

The magnitude of the stimulatory effect on L-[<sup>3</sup>H]-leucine transport in INS1E cells (i.e. approximately 70% increase) that was observed after 6 hours of D-glucose starvation or 0.75mM AICAR treatment in this chapter is similar in magnitude to the well-documented stimulatory effect of AMPK activation or of AICAR treatment on glucose transport that has previously been described in skeletal muscle cells (- for example the ~ 80% increase in 2-deoxyglucose transport that is observed in L6 skeletal muscle cells in response to AICAR (Turban et al. 2012)). The AMPK effect on GLUT transporters is partly transcriptional and partly a result of GLUT protein translocation to the plasma membrane (Park et al. 2009). The observation here that this L-leucine transport effect is accompanied by increased LAT1 mRNA expression, but that blockade of LAT1 transcription with actinomycin-D does not prevent the increase in L-[<sup>3</sup>H]-leucine transport, also suggests that a post-transcriptional protein translocation to the plasma membrane may be required. Testing this possibility using an experimental model involving cloning and expression of a tagged LAT1 protein in transfected HEK293A cells, and investigating the factors affecting the location of this tagged LAT1 protein in the cells, are the subject of the next chapter.

### 5.1. Introduction

Previously in Chapter 4 it was demonstrated that the increase in L-[<sup>3</sup>H]-leucine transport in D-glucose-deprived INS1E cells is accompanied by a statistically significant but variable increase in LAT1 mRNA, but that blocking LAT1 transcription with actinomycin-D showed that the effect on transport is not linked to increased LAT1 transcription and additional effects such as translocation of LAT1 to the plasma membrane activated by AMPK may be involved. Furthermore, (at least under basal unstimulated conditions) silencing LAT1 expression with small interfering RNAs (siRNA) significantly reduced the L-[<sup>3</sup>H]-leucine transport and LAT1 mRNA expression. This novel finding suggested that there may be an important role for LAT1 in the L-leucine uptake in INS1E  $\beta$  cells and that it may respond to AMPK and changes in the energy status of the cells. However, investigating further the idea that AMPK can bring about translocation of LAT1 proteins from an intracellular pool to the plasma membrane (as previously shown for GLUT transporters in muscle and heart (Luiken et al. 2015)) requires an experimental model in which LAT1 proteins can be tagged with a probe that makes them easy to visualise and track within a cell.

To assess the functional relevance of increased LAT1 expression and the requirement for CD98, the following strategy was used. Human LAT1 (SLC5A7) and CD98 (SLC3A2) cDNA was cloned into eGFP and FLAG expression vectors respectively and confirmed by sequencing as described in Sections 2.4 to 2.6. eGFP tagged LAT1 was then expressed in HEK293A cells (a more readily transfected cell line than INS1E) and expression of the LAT1-eGFP fusion protein was confirmed in the cell by fluorescence microscopy. Once the transfection efficiency was confirmed, transport assays were performed to see whether LAT1 and CD98 transfection could increase L-[<sup>3</sup>H]-leucine transport in HEK293A cells. To further investigate the effect on the cells with increased expression of LAT1 under conditions of increased AMPK activity, HEK293A transfected cells were treated with AICAR and the effect on LAT1-eGFP distribution in the cells was assessed by fluorescence microscopy to see whether the fluorescent fusion protein moved to a more peripheral location in the cells associated with the plasma membrane.

## 5.2. Results

### 5.2.1. Efficiency of transfection in HEK293A cells

To confirm the efficiency of the transfection, HEK293A cells were transfected with empty eGFP vector (Figure 5.1.a); or LAT1-eGFP plasmid at concentrations varying from 0.3 to 2.5  $\mu\text{g}$  per 35 mm culture well (Figure 5.1b to d) and examined 48 h post-transfection under fluorescence microscopy. With the empty vector, a uniform diffuse fluorescence was observed in the cells, consistent with the expected expression of free soluble eGFP protein in the cytosol. However, transfection with the LAT1-eGFP construct led to a less even distribution of fluorescence within the cells, more consistent with expression of a membrane protein. At lower plasmid concentrations, the cells remained flattened and adherent on the culture well (Figure 5.1.b, c and d). However, cells transfected with a higher concentration of the LAT1-eGFP plasmid (Figure 5.1.e) sometimes showed rounding of some of the cells and poor adherence suggesting some level of toxicity. For this reason 0.6  $\mu\text{g}$  DNA per well was chosen to be the optimal plasmid concentration for the transfection, achieving the strongest expression judged from fluorescent intensity, without significant loss of adherence.

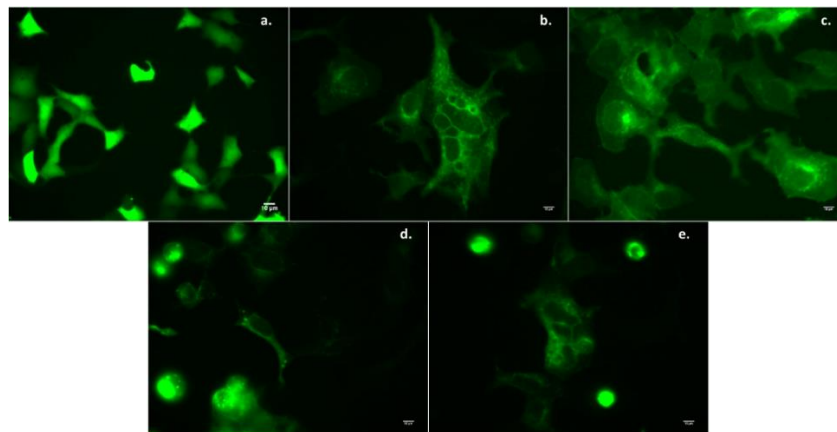


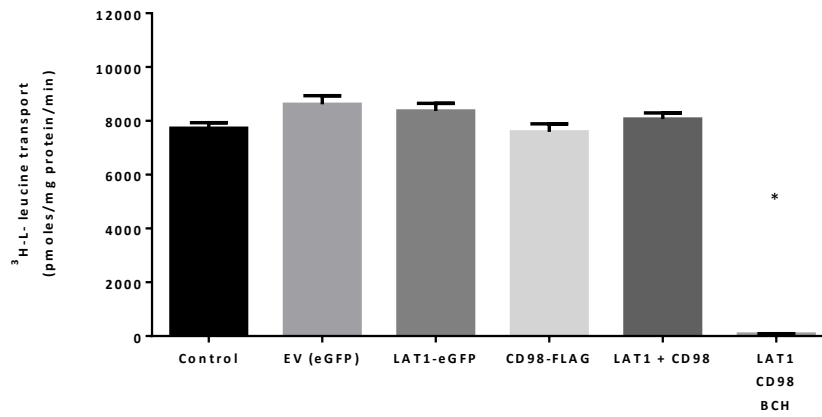
**Figure 5.1. Efficiency of transfection in HEK293A cells**

HEK293A cells examined 48 h post-transfection with LAT1-eGFP under fluorescence microscopy (Excitation max 488 nm; Emission max 509 nm). Transfection efficiency was monitored using the following concentrations of plasmid DNA per 35 mm culture well: **a)** Empty vector 0.6  $\mu\text{g}$  DNA; and for LAT1-eGFP plasmid **b)** 0.3  $\mu\text{g}$  DNA, **c)** 0.6  $\mu\text{g}$  DNA, **d)** 1.5  $\mu\text{g}$  DNA, **e)** 2.5  $\mu\text{g}$  DNA.

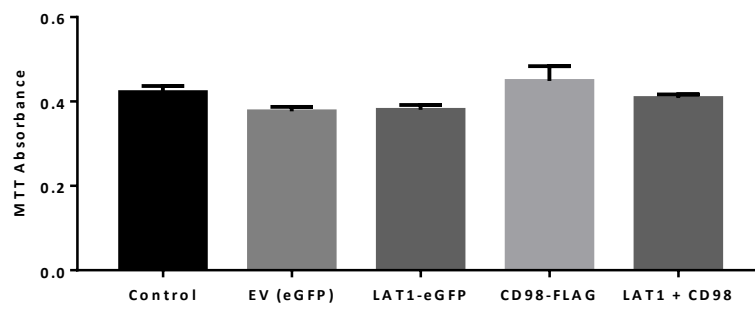
### **5.2.2. The effect of LAT1 or CD98 cDNA constructs on L-[<sup>3</sup>H]-leucine transport in HEK293A cells**

To determine the functional effect of overexpressing LAT1 in HEK293A, cells were transfected with LAT1-eGFP or empty vector (EV) and L-[<sup>3</sup>H]-leucine transport activity was measured. Basal L-leucine transport rate was very high in HEK293A cells (about 4 times higher than in INS1E cells – see Figure 4.2.1) and this basal activity was abolished by incubation with 10mM BCH, confirming that the transport assay was working and was detecting a form of System L. i.e. expression of endogenous system L (LAT) transporters in these cells (Figure 5.2.a). In spite of clear expression of LAT1-eGFP demonstrated by fluorescence microscopy (Figure 5.1), no significant increase in transport above baseline was seen when the cells were transfected with LAT1 constructs: the L-[<sup>3</sup>H]-leucine transport activity in LAT1-eGFP transfected cells was no higher than in the empty vector-transfected cells. A possible requirement for additional CD98 was also tested by transfecting with the same amount of a plasmid encoding FLAG-tagged CD98. However, neither the CD98 plasmid nor CD98 transfection on top of LAT1-eGFP transfection had any effect on transport (Figure 5.2.a) i.e. CD98 expression was apparently not a limiting factor. These transfections also had no significant effect on cell viability assessed by MTT assay (Figure 5.2.b). In lysates from parallel cultures Western blotting with anti-GFP antibody was also performed to confirm the molecular weight of the expressed free eGFP in the empty vector-transfected cultures and the eGFP-tagged fusion protein in the LAT1-eGFP transfected cultures (Figure 5.2.c).

**a. HEK293A LAT1/CD98 transfection effect on L-[<sup>3</sup>H]-L-leucine transport**



**b. HEK293A LAT1/CD98 transfection effect on cell viability**



**c. Western blotting with anti-GFP antibody on lysates from HEK293A cells transfected with LAT1-eGFP and/or CD98-FLAG**

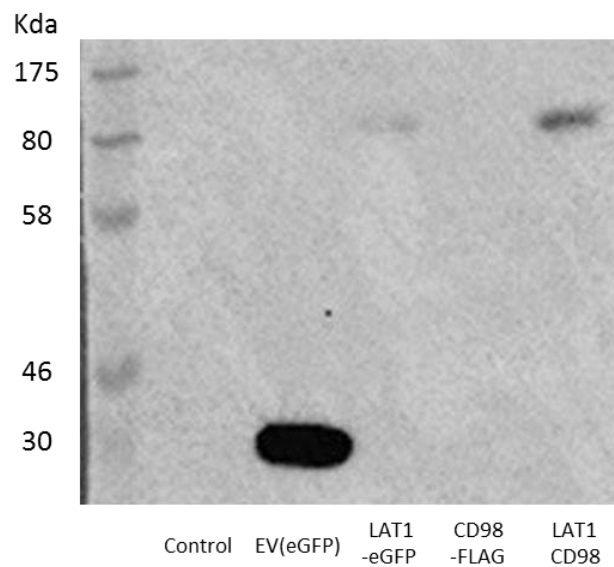


**Figure 5.2. Effect of transfection with LAT1-eGFP and CD98-FLAG on L-[<sup>3</sup>H]-leucine transport and cell viability in HEK293A cells.**

(a) L-[<sup>3</sup>H]-leucine uptake in HEK293A cells was measured by incubation with 50  $\mu$ M L-[<sup>3</sup>H]-leucine for 1 min at 48 hours post-transfection with 0.6  $\mu$ g of LAT1-eGFP or CD98-FLAG cDNA in plasmid, or 0.6  $\mu$ g of empty vector control plasmid (EV) per 35mm culture well. All transport values are expressed as picomoles per mg of protein per minute. The concentration of the transport inhibitor BCH in the medium was 10mM. The results are mean  $\pm$  S.E.M for three independent experiments. \*(p<0.02) compared with all other conditions. **(b)** Cell viability was assessed in parallel with (a) at 48 hours post-transfection by incubating with MTT (3-(4,5-Dimethylthiazol-2-yl)-2,5-diphenyltetrazolium bromide) at 2mg/ml in DMEM for 1 h at 37°C under 5% CO<sub>2</sub> in the dark, followed by measurement of absorbance at 520nm. **(c)** Detection of eGFP-tagged proteins in lysates from cells cultured in parallel with (a). Proteins were resolved by SDS-PAGE, and Western blotted using anti-GFP antibody.

### 5.2.3. Effect of AICAR on HEK293A cells overexpressing LAT1-eGFP

To determine if the LAT1-eGFP overexpression could give a statistically significant increase in L-[<sup>3</sup>H]-leucine transport in HEK293A cells when transfection was followed by incubation in the presence of AICAR; 48 hours post-transfection HEK293A cells overexpressing LAT1-eGFP were incubated during 3 hours in DMEM (5mM glucose) in the absence and presence of 750  $\mu$ M AICAR. A 3 hour incubation was chosen because the only previous statistically significant stimulation of L-[<sup>3</sup>H]-leucine transport by energy stress in these cells had been observed at this time point in Figure 4.2.1.b.

Transfection with LAT1-eGFP increased L-[<sup>3</sup>H]-leucine transport by 12% when compared to the untransfected control but, as in Figure 5.2.a above, this apparent stimulation did not reach statistical significance ( $p=0.348$ ). Similarly no increase was observed when non-transfected control cultures were incubated in the presence of AICAR alone (Figure 5.3) – consistent with the lack of effect of AICAR previously seen in Figure 4.3.b. Transfection with empty vector alone gave a small (4.0%) and statistically insignificant stimulation relative to the non-transfected control both in Figure 5.3 and in the earlier experiment in Figure 5.2.a. A small but statistically significant stimulation of transport (9.7% increase relative to the non-transfected control,  $P<0.05$ ) was observed when cells transfected with Empty Vector were incubated with AICAR. However, the clearest statistically significant stimulation of transport (24% relative to non-transfected controls) was observed only when LAT1-eGFP transfection was combined with AICAR ( $P<0.01$ , Figure 5.3).

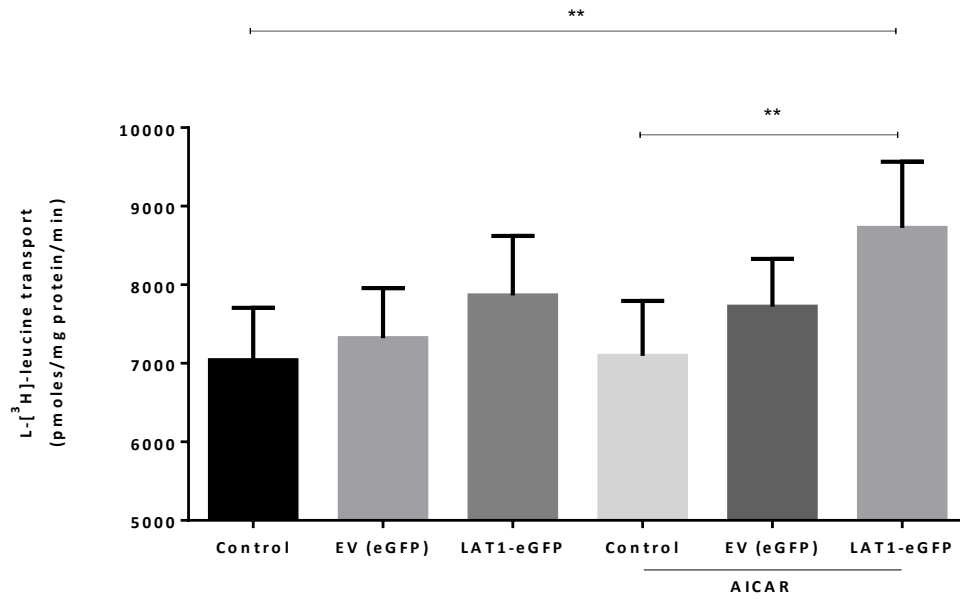


**Figure 5.3. Effect of AICAR on L-[<sup>3</sup>H]-leucine transport in HEK293A cells overexpressing LAT1-eGFP.**

HEK293A cells were transfected with 0.6  $\mu$ g of LAT1-eGFP or CD98-FLAG cDNA in plasmid, or 0.6  $\mu$ g of empty vector control plasmid (EV) per 35mm culture well. Starting 48 hours post-transfection, the cells were incubated with 750  $\mu$ M AICAR for 3 hours. L-[<sup>3</sup>H]-leucine uptake was then measured by incubation with 50  $\mu$ M L-[<sup>3</sup>H]-leucine for 1 min. All transport values are expressed as picomoles per mg of protein per minute. The results are mean  $\pm$  S.E.M of four independent experiments. (\*\* $p$ <0.01, \* $P$ <0.05) compared with the stated control.

#### 5.2.4. AICAR effect on the localisation of LAT1-eGFP in HEK293A cells

To investigate whether the apparent combined effect of AICAR and LAT1-eGFP transfection in Figure 5.3 might be associated with LAT1-eGFP re-distribution, for example net movement of the fusion protein in response to AICAR to a peripheral location which is more associated with the plasma membrane, fluorescence images were examined from LAT1-eGFP transfected cells incubated as in Figure 5.3 with and without AICAR. No obvious effect of AICAR was seen on the fluorescence distribution (Figure 5.4). It was noticed however that, in both AICAR treated and control cultures, the LAT1-eGFP images showed an apparent spectrum of sub-cellular LAT1-eGFP distribution where the fluorescence in some of them seemed to be concentrated near the centre of the cell (Figure 5.5 – images 1-2), whereas in some others it appeared to be spread more diffusely around the cell (Figure 5.5 – images 3-7), while in others the distribution of the fluorescence was almost entirely peripheral and located in bright focal or punctate structures (Figure 5.5 – image 8).

To see whether there was any AICAR effect on the distribution of the LAT1-eGFP expressed in HEK293A cells, images of cells expressing LAT1-eGFP were examined from 3 independent experiments. In total 282 cells were examined after incubation under control conditions without AICAR, and 306 cells after incubation for 3 hours with 750 $\mu$ M AICAR. The cells were scored (according to the localisation of the LAT1-eGFP in the cells) on a scale from 1 to 8 by a blinded observer, using the 8 specimen images in Figure 5.5.a as a calibration scale.

The resulting counts are shown in the Figure 5.5.b. If AICAR causes net movement of LAT1-eGFP towards more peripheral sites, the score with AICAR would be expected to increase. In fact the opposite trend was observed, with a small apparent AICAR-induced shift towards lower score i.e. away from peripheral bright focal structures (Score 8) towards more diffuse or centrally located fluorescence (Score 1-7).

Average Control score: – Mean 5.805; Median 6; Mode 6

Average AICAR score: - Mean 5.569; Median 6; Mode 6

This apparent shift in the average score fell just short of statistical significance (Mann Whitney U test,  $P=0.059$ ).

In view of this borderline significant result, the frequency of the scores was also examined, comparing the number of cells scored as 1 to 7 with the number scored as 8 (Figure 5.5.b and c). Again a marginally significant effect was detected (Fisher's exact test –  $P=0.023$ ), suggesting that some association of the LAT1-eGFP localisation occurs with the presence or absence of AICAR.

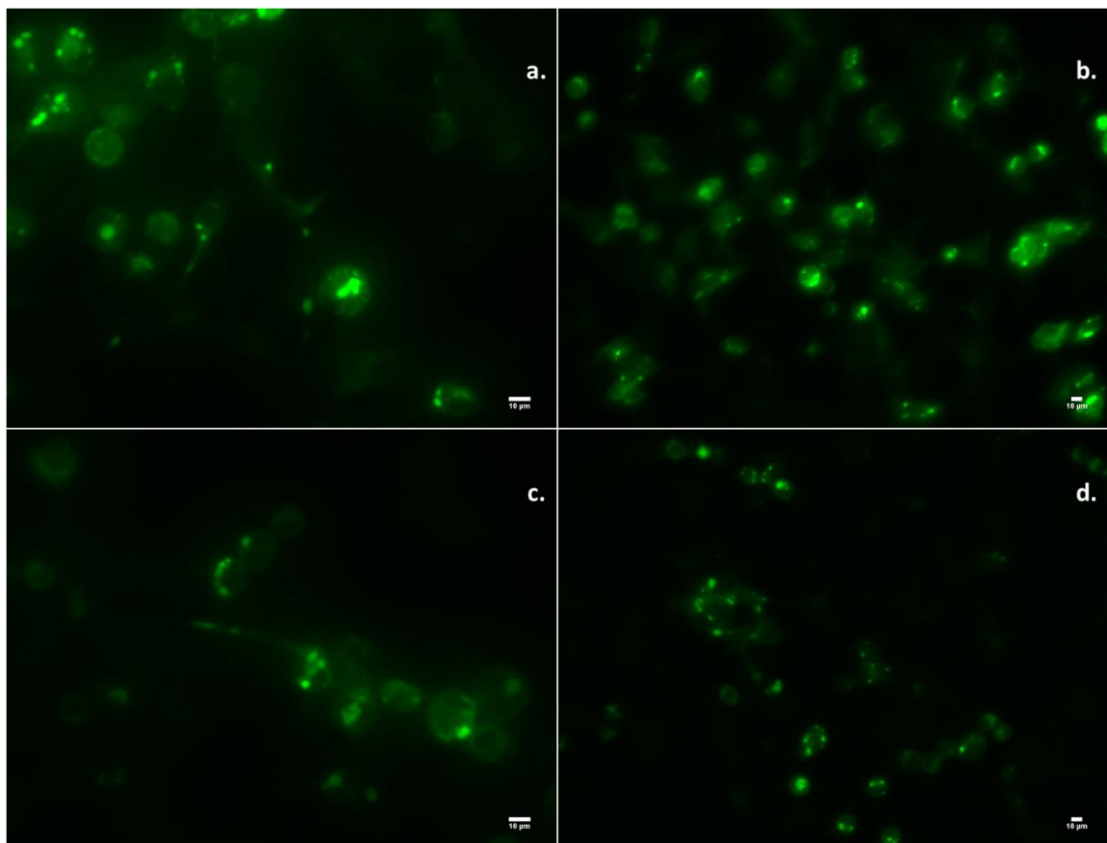
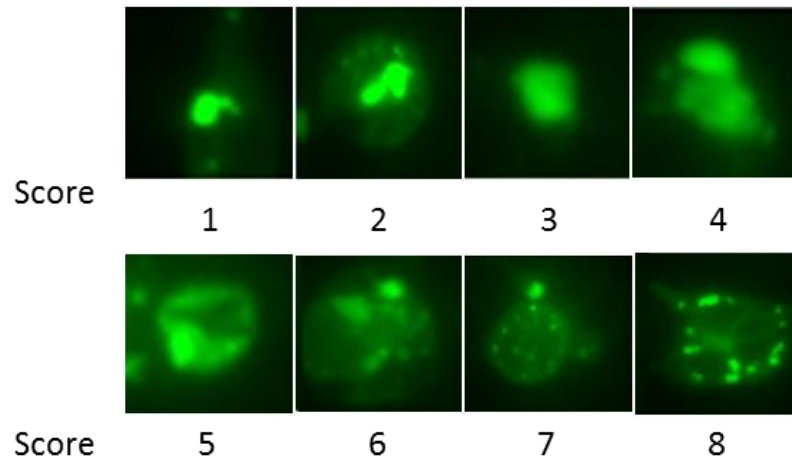


**Figure 5.4. Effect of AICAR on fluorescence images of HEK293A cells overexpressing LAT1-eGFP**

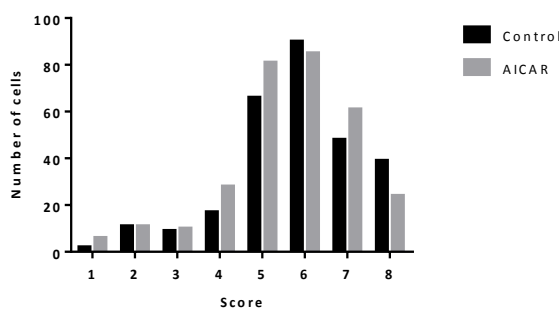
HEK293A cells were transfected with 0.6 μg of LAT1-eGFP cDNA in plasmid per 35mm culture well. Starting 48 hours post-transfection, the cells were incubated with 750 μM AICAR for 3 hours. **a)** and **b)** LAT1-eGFP; **c)** and **d)** LAT1-eGFP + 750 μM AICAR.

### 5.2.5. Analysis of the effect of AICAR on the localisation of LAT1-eGFP fluorescence

#### a. Effect of AICAR on the localisation of LAT1-eGFP fluorescence



#### b. Cell counts for all 8 score categories



#### c. Cell counts with pooling of data from cells scored 1 – 7

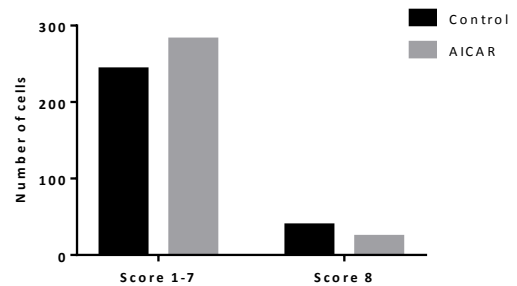


**Figure 5.5. Analysis of the effect of AICAR on the localisation of LAT1-eGFP fluorescence in HEK293A cells.**

Cells were transfected and incubated as stated in Figure 5.4. The images show the range of patterns of fluorescence observed, varying from centrally located (Score 1) to peripheral and punctate (Score 8). Images of HEK293A cells pooled from 3 independent experiments were examined: 282 cells under control conditions, and 306 cells with AICAR. A blinded score between 1 and 8 was given to each cell in accordance with the localisation of the fluorescence in the cell **(a)**. Cell counts are displayed **(b)** for all 8 score categories and **(c)** with pooling of data from cells scored 1 – 7. Statistical analysis is explained in the text.

### 5.3. Discussion

In order to visualize the effect of transfecting with increasing concentrations of LAT1-eGFP cDNA, HEK293A cells were transfected with from 0.3 to 2.5  $\mu\text{g}$  per 35 mm culture well and examined under fluorescence microscopy. Empty vector transfected cells expressed a uniform diffuse fluorescence, consistent with a free eGFP protein in the cytosol. However, LAT1-eGFP showed a more limited intracellular distribution of the fluorescence, consistent with the LAT1 localization in membranes as expected from the physiological roles of this transporter. Cells transfected at the lower LAT1-eGFP plasmid concentrations still showed normal cell distribution and adhesion to the culture plate and were therefore thought to be suitable for further experiments (Figure 5.1). The MTT assay showed no effect of the plasmid on cell viability (Figure 5.2.b). Furthermore the anti-GFP Western blot in Figure 5.2c confirmed that empty vector transfection leads to expression of free eGFP (with a molecular weight of about 29kDa) and LAT1-eGFP transfection leads to expression of an eGFP-tagged fusion protein of about the expected size (i.e.  $29 + 55 = 84\text{kDa}$ ).

Once the optimal concentration of the plasmid had been established, the functional relevance of LAT1 overexpression and the effect of CD98 co-expression on the transport activity was examined. In HEK293A cells, LAT1 or LAT1/CD98 co-expression showed no significant increase in transport compared with basal levels. However, a technical problem in these experiments was that HEK293A cells have a very high basal L-[ $^3\text{H}$ ]-leucine transport rate which was inhibited by BCH, and which was consistent with the expression of high System L activity (Figure 5.2.a). This basal System L transport activity was around 4 times higher in HEK293A cells compared with INS1E cells (Figure 4.2.1) and may explain why an earlier report of transient transfection with LAT1 and/or CD98 cDNA did not use HEK293 cells (Campbell and Thompson 2001). In that study it was found that, in mouse hepatocytes, to increase L-[ $^3\text{H}$ ]-leucine transport it was sufficient to transfect with LAT1 cDNA, but in mouse fibroblasts it was necessary to co-transfect with both LAT1 and CD98 cDNA. In the present study, transfection with LAT1 cDNA had little effect on L-[ $^3\text{H}$ ]-leucine transport, and this was not enhanced by co-transfection

with the CD98-FLAG construct that was tested here (Figure 5.2.a).

The only apparent effect of CD98 co-transfection that was observed is shown in the anti-eGFP Western blot in Figure 5.2c in which the LAT1-eGFP band observed seemed more intense when the LAT1-eGFP was co-transfected with CD98. The reason for this is unknown, and needs to be confirmed with a rigorous loading control, but might arise because increased expression of the full LAT1-CD98 heterodimer protects the LAT1-eGFP protein from attack by proteases in the cell lysate. However, as CD98 co-expression had no obvious effect on transport in Figure 5.2.a, no further CD98 co-transfection experiments were performed.

To evaluate the effect of AMPK activation combined with LAT1 overexpression in the L-[<sup>3</sup>H]-leucine transport, HEK293A cells were transfected with LAT1-eGFP and treated with AICAR. The transfection with LAT1-eGFP slightly increased L-[<sup>3</sup>H]-leucine transport but this effect was not significant. The presence of AICAR significantly increased the L-[<sup>3</sup>H]-leucine transport in the empty vector compared with the control and there was a further increase with the overexpression of LAT1, reaching 24% above baseline in spite of the very high basal transport activity in these cells (Figure 5.3).

This stimulation of L-[<sup>3</sup>H]-leucine transport that was seen on combining AICAR stimulation with LAT1-eGFP transfection could not arise from an increase in LAT1 transcription of the sort that was observed in Chapter 4, because the cells were transfected only with a LAT1 cDNA construct that lacked the promoter region of the human LAT1 gene. This could not therefore be activated by AMPK-dependent transcription factors like CREB (Thomson et al. 2008) and HNF4a (Hong et al. 2003) that are shown at the bottom of Figure 1.9.

The images from the fluorescence microscope from LAT1-eGFP transfected cells (with or without the presence of AICAR) seemed to have an apparent pattern of localisation where the distribution of the fluorescence in some images was concentrated in the centre of the cell, but in others it was more diffuse or even entirely peripheral (images

1 to 8 in Figure 5.5.a). The reason for this variation in the pattern of fluorescence is unknown, but presumably some cells took up the LAT1-eGFP cDNA early in the 24h transfection period (images 7-8) and some late in the 24h period (images 1-2) so that the latter show newly synthesised LAT1-eGFP which is still mainly perinuclear – i.e. in the endoplasmic reticulum or Golgi regions of the cell.

The aim of these experiments was to assess whether the presence of AICAR in LAT1-eGFP transfected cells has an effect in the localisation of the fluorescence such as re-distribution to a peripheral location near the plasma membrane. AICAR was found for the first time to have some association with the LAT1-eGFP localisation (Figure 5.4), but it was the opposite of what was expected, with AICAR treatment being associated with fewer cells with peripheral fluorescence of the sort that is shown in image 8 in Figure 5.5.a.

#### **5.4. Conclusion**

Even though a combination of AMPK activation by AICAR with LAT1-eGFP transfection in HEK293A cells gave a statistically significant 24% stimulation of L-[<sup>3</sup>H]-leucine transport, analysis of fluorescence images of LAT1-eGFP location in the cells failed to support a simple 2-pool model in which AICAR stimulated movement of LAT1-eGFP from an intracellular pool to a peripheral plasma membrane pool. This simple 2-pool model also did not explain why much of the more peripheral LAT1-eGFP fluorescence in many of the cells was found in focal or punctate structures. A more detailed model which may explain these problems, and all of the other main experimental observations from this project, is therefore needed. This model is discussed in the final chapter of this thesis.

### 6.1. Biological significance of these findings

The data presented in Chapter 4 of this thesis suggest that D-glucose starvation and AMPK activation in INS1E cells lead to a previously undescribed stimulation of L-leucine transport which is similar in magnitude to that previously described for glucose transport in response to AMPK activation in muscle. Like the glucose transport effect, this effect on L-leucine transport seemed to have two components – an increase in LAT1 mRNA (which was shown by actinomycin-D inhibition not to be required for the increase in transport), and a separate non-transcriptional contribution. This second contribution was modelled in HEK293A cells in Chapter 5 by stimulating the cells with the AMPK agonist AICAR after transfecting with a LAT1 cDNA construct that lacked the promoter region of the human LAT1 gene and so could not be activated by transcription factors that increased LAT1 mRNA expression in INS1E cells. In spite of the high basal rate of L-leucine transport in HEK293A cells, a stimulation of the transport was seen, but this was only statistically significant when LAT1 transfection was combined with AICAR stimulation, and this may have been accompanied by some AICAR-dependent redistribution of the eGFP-tagged LAT1 fusion protein within the cells.

The only previously described report of an AMPK effect on LAT1 transporters was a study in which AMPK seemed to inhibit LAT1. The protein kinase YAP1 is reported indirectly to up-regulate LAT1 in hepatocellular carcinoma (Park et al. 2016) and AMPK has been shown to inhibit YAP1 (Mo et al. 2015). However these effects only occur in rapidly proliferating cells, which is a very different situation from the serum-free non-proliferating INS1E cultures that were used here (see also Section 6.6).

As discussed in Chapter 4, a possible driving force for this stimulation of L-leucine transport in D-glucose-starved cells or cells with activated AMPK is that intracellular L-leucine has been depleted because it has been consumed as a fuel (Harris et al. 2001) and LAT1 then up-regulates in response to this to bring more L-leucine into the cells. However, direct measurement of intracellular free L-leucine by HPLC failed to detect this expected depletion: indeed an increase was observed in D-glucose-starved cells.

This increase is unlikely to arise from increased active transport of L-leucine into the cells as a result of the coupling between System A and System L transporters that was shown in Figure 1.12, because direct measurement of System A transport activity in the D-glucose-starved cells (Chapter 4) showed that this activity had declined, thus removing the driving force for active L-leucine accumulation inside the cells. Some other form of active Na<sup>+</sup>-dependent L-leucine transport might explain the increase in intracellular L-leucine concentration (e.g. up-regulation of B<sup>0</sup>AT1 (Section 1.10.3.2)) but this also seems unlikely because D-glucose starvation leading to Na<sup>+</sup>,K<sup>+</sup>-ATPase inhibition as discussed in Chapter 4 would reduce the Na<sup>+</sup> gradient that drives such transporters.

This suggests therefore that the up-regulation of L-leucine transport demonstrated in Chapter 4 might arise in some other way. A possible explanation may come from the apparent compartmentation of LAT1 observed in the fluorescence localisation experiments in Chapter 5.

## **6.2. Studies of LAT1-eGFP location do not support a simple two-pool model of LAT1 distribution**

The hypothesis that was used in the design of the experiment on localisation of LAT1-eGFP in Chapter 5 made the assumption that the transporter occurs in 2 pools comprising:

- Pool 1. Intracellular newly synthesised LAT1-eGFP in the peri-nuclear endoplasmic reticulum/Golgi region of the cell (i.e. with a central location within the cell)
- Pool 2. Peripherally located more diffuse LAT1-eGFP which will include the plasma membrane (transporting) pool that is detected in L-[<sup>3</sup>H]-leucine transport experiments.

In moving from Pool 1 to Pool 2, the arbitrary scoring system that was assigned to the cells in Chapter 5 should therefore show an increase in the score from 1 towards 8 if AICAR is driving more of the proteins into the peripheral plasma membrane

(transporting) pool. In practice it was found however that there was a small (but marginally statistically significant) shift in the opposite direction, apparently at the expense of some form of organelle pool near the plasma membrane that was observed to be strongly expressing fluorescent LAT1-eGFP in some of the cells.

From this, it seems likely that a significant 3rd pool of LAT1 exists. So a possible interpretation of the experiment in Figure 5.5 is that in response to AICAR, Pool 2 (i.e. the transporting pool) is recruiting LAT1 at the expense of this additional Pool 3.

The nature of this third pool is unknown. It might be a pool of membrane vesicles carrying LAT1 from the Golgi to the plasma membrane, or endocytic vesicles (endosomes) withdrawing LAT1 from the plasma membrane. However, these fluorescent structures seem too large to be explained entirely by such vesicles. As HEK293 cell diameter is typically  $\sim 20 \mu\text{m}$ , many of these features shown in images 7 and 8 of Figure 5.5 seem to be  $\sim 0.1 - 1 \mu\text{m}$  in diameter. This size is more consistent with lysosomes (Bionumbers 2011).

In principle there are 2 ways that LAT1 could be incorporated into the endolysosomal compartment:

- By fusion of lysosomes with endosomes internalising LAT1 from the plasma membrane pool of LAT1
- By the recently described association of LAT1 with its binding partner LAPTM4b on lysosomes (see Figure 1.10 and Figure 6.1) (Milkereit et al. 2015).

In future experiments it would therefore be interesting to perform co-localisation experiments to examine whether LAT1-eGFP co-localises with lysosomal markers as described in a recent study (Rebsamen et al. 2015) in which another amino acid transporter (SLC38A9) was shown to be expressed on lysosomes in HeLa cells by its co-localisation with lysosomal markers, giving a punctate fluorescence from GFP-tagged SLC38A9 which was a little like that seen for LAT1-eGFP in Figure 5.5 images 7 and 8.

It has also recently been shown that AMPK (and its upstream kinase LKB1) localise to lysosomes (C-S Zhang et al. 2017) (Figure 6.1). The LAT1-lysosome association discussed above has been shown to assist mTORC1 activation, probably by transporting L-leucine into the lysosome (Milkereit et al. 2015). An important possibility to be investigated in future work is therefore that activated lysosomal AMPK (in addition to its inhibitory phosphorylating effect on mTORC1 (Figure 1.9)) also causes dissociation of LAT1 from the lysosome, thus further inhibiting translation/protein synthesis and reducing ATP utilisation under conditions of energy depletion. If the dissociated lysosomal LAT1 moves to the plasma membrane (Pool 2 in Figure 6.1), the apparent rise in plasma membrane L-leucine transport observed on AMPK activation in INS1E cells in Chapter 4, and the smaller apparent effect of AICAR in LAT1-transfected HEK293A cells in Chapter 5 might be just an accidental consequence of the need to remove LAT1 from the lysosome under conditions of energy stress.

However, this does not explain:

- a) Why D-glucose deprivation and AICAR also increased LAT1 mRNA in INS1E cells (Chapter 4)
- b) Why D-glucose deprivation and AICAR had no significant effect on L-leucine transport in other cells such as the L6 myoblasts in Chapter 4.

This suggests that the activation of the plasma membrane (transporting) pool of LAT1 in INS1E cells might have some biological function of its own.

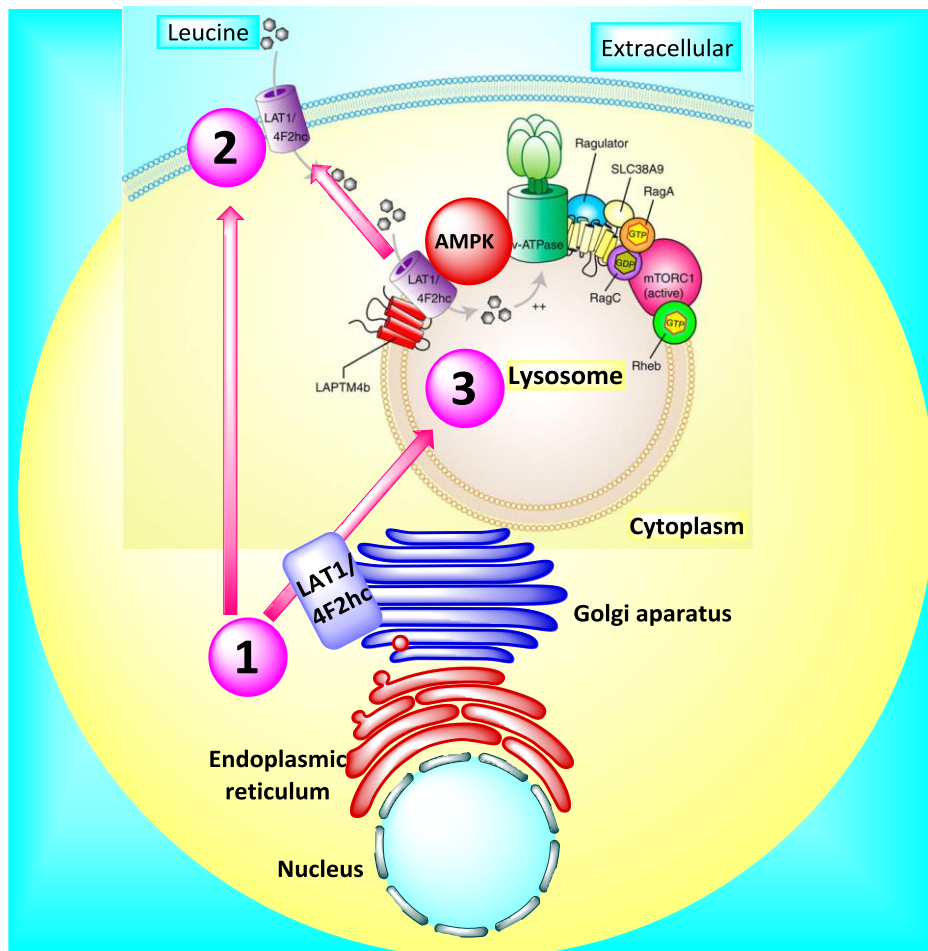


**Figure 6.1. Distribution of LAT1(SLC7A5)/4F2hc(SLC3A2) into 3 pools**

Adapted from Milkereit et al., 2015 (Milkereit et al. 2015). Schematic diagram showing hypothetical distribution of LAT1(SLC7A5)/4F2hc(SLC3A2) into 3 pools ((1) newly synthesised in the ER/Golgi); (2) performing transport across the plasma membrane; (3) the lysosomal pool) and their relation to AMPK and mTORC1.

### 6.3. Does LAT1 up-regulation in energy-depleted cells drive influx or efflux of L-leucine from the cell?

It has been known for many years that when energy supply fails in mammalian cells, the translation and overall synthesis of many of the cell's proteins is decreased to save energy (Byfield et al. 2005). Glucose starvation in mammalian cells is one such stimulus for global inhibition of translation and protein synthesis (de Haro et al. 1996). In part the cell does this by activating AMPK, which inhibits mTORC1 as described in Section 1.6 and Figure 1.8. If protein synthesis from free amino acids decreases but protein degradation continues, by definition the size of the free amino acid pool must initially increase. For that reason, shutting down protein synthesis in mammalian cells (for

example with translation inhibitors such cycloheximide or puromycin) raises the concentration of most of the free amino acids in the cell (Iiboshi et al. 1999, Manchester 1970), including L-leucine. In INS1E cells in the present study such a rise in the cellular L-leucine concentration was seen by HPLC after 6 hours of D-glucose–starvation (Fig 4.13).

However, even though the decrease in protein synthesis in energy depleted cells may reduce the rate of ATP consumption, the resulting rise in concentration of free amino acids such as L-leucine may cause problems if the increase becomes too large. Two possible problems are:

- 1) Excess L-leucine entering lysosomes through LAT1 may activate mTORC1 which may re-activate translation and hence increase ATP consumption.
- 2) High concentrations of certain free amino acids (including L-leucine) are toxic. A toxic effect of L-leucine has been described in detail in brain astrocytes where it impairs energy metabolism (Yudkoff et al. 2005) which would be a problem if it occurred in D-glucose-starved INS1E cells. In addition to glucotoxicity and lipotoxicity (Section 1.1.5) it has also been suggested that so-called “aminoacidotoxicity” might contribute to  $\beta$  cell damage in T2DM and it has been shown *in vitro* in INS1E cells and in isolated mouse islets that a high concentration of L-leucine does cause such damage even in the absence of D-glucose starvation (Liu et al. 2012).

A possible way to minimise both of these two problems caused by excess L-leucine may therefore be for LAT1 to be translocated out of lysosomes and into the plasma membrane where it could perform additional amino acid exchange (including L-leucine *efflux* from the cell), thus limiting the rise in the intracellular L-leucine concentration. This seems consistent with the changes in L-leucine transporter activity, LAT1 expression and sub-cellular LAT1-eGFP location that were observed in Chapters 4 and 5. It is also consistent with the observed inhibition of System A transporter activity under these conditions (Figure 4.4.a) which would inhibit active pumping of L-leucine into the cell through the System A – System L coupling mechanism shown in Figure 1.12.

However, if carrying excess intracellular amino acid out of the cell under these conditions is the biological role of the up-regulation of LAT1 in glucose-deprived INS1E cells, it still remains unclear whether LAT1 is responding directly to AMPK activation or to the rise in the intracellular amino acid concentration.

The idea that an important biological role of LAT1 may be to carry excess amino acid out of the cell is also supported by the kinetic properties of the transporter. It was noted in Chapter 1 that the  $K_m$  on LAT1 for L-leucine efflux from the cytosol is estimated to be greater than the  $K_m$  on LAT1 for L-leucine influx from the extracellular fluid (see Section 1.10.1.1). This is consistent with the idea that LAT1 may serve partly to carry efflux of potentially toxic excess amino acids from the cytosol when their concentration rises above the efflux  $K_m$ .

If the rise in L-leucine transporter activity in the plasma membrane in Chapters 4 and 5 serves to carry excess L-leucine out of the cell on the LAT/4F2hc exchanger, L-leucine efflux must be occurring in exchange for entry of another System L amino acid. This is most likely to be L-glutamine which was the most abundant amino acid in the incubation medium in the experiments in this thesis, is the most abundant amino acid in extracellular fluid *in vivo*, and can safely accumulate to high concentrations inside cells without toxic effects (for example  $\sim 10$ -50 times the extracellular concentration in skeletal muscle cells) (Evans et al. 2007).

#### **6.4. Future experiments to confirm and extend these findings**

The assays of System L transporter activity in this thesis measured only the initial (1 minute) rate of influx of L-[ $^3\text{H}$ ]-leucine from the extracellular medium into the cells. This was done because initial rate gives a measure of the activity of the plasma membrane transporters without any significant contribution from intracellular metabolism of the L-[ $^3\text{H}$ ]-leucine. Confirmation that this assay measures mainly transport and not metabolism (i.e. that the rate of [ $^3\text{H}$ ] uptake is limited by transporters in the plasma membrane) was obtained by showing that uptake was strongly inhibited with BCH (Figure 3.3 and Figure 5.2), which inhibits System L transporters but has no known effect on intracellular L-leucine metabolism.

To confirm directly the suggestion in Section 6.3 that AMPK activation promotes L-leucine efflux on LAT1, it would be helpful also to assay System L transporter activity in the efflux direction (i.e. the rate of transfer of L-[<sup>3</sup>H]-leucine from pre-labelled cells into the extracellular medium). However, this cannot be done in intact cells because most of the intracellular <sup>3</sup>H label would be in the form of intracellular metabolites of L-leucine (mainly proteins). The mathematical description of this rate of efflux is complex because it depends strongly on intracellular metabolism of the <sup>3</sup>H label (Kemp et al. 1988) and is nothing like the simple Michaelis Menten equation that was used to fit the transport curve for L-[<sup>3</sup>H]-leucine influx that was shown in Figure 3.4. The efflux rate of System L amino acids such as L-leucine or L-phenylalanine from pre-labelled cells is a measure of protein degradation rate, not a measure of the plasma membrane efflux transport rate, and it has been widely used to study overall protein degradation rate in cultured cells (Evans et al. 2008).

For this reason, in future experiments, use of a series of selective small molecule inhibitors may be a simpler and more direct way to test the model that was proposed in Section 6.3 and in Figure 6.1 i.e. that LAT1 is upregulated by AMPK-dependent translocation of LAT1 to the plasma membrane where it carries out L-leucine efflux. If this explanation is correct, the stimulatory effect of D-glucose deprivation on L-[<sup>3</sup>H]-leucine transport in Chapter 4 should be blocked with an AMPK inhibitor such as Compound C. (However, care is needed in the use of Compound C as it has been shown to have several other targets apart from AMPK) (Jin et al. 2009, Liu et al. 2014, Saito et al. 2012). In addition, the effects of AICAR on L-leucine transport in Chapters 4 and 5 should be blocked by cytoskeleton disrupting drugs such as cytochalasins and colchicine which have been shown previously to block the up-regulation or down-regulation of GLUT glucose transporters that occurs by translocation to or from the plasma membrane in mammalian cells (Foley et al. 2011). Most relevant of all, blockade of the expected L-leucine efflux in D-glucose deprived cells by inhibition of the up-regulated LATs with BCH should further elevate intracellular L-leucine beyond the high level shown in Figure 4.13 and, if L-leucine toxicity is important, this should lower cell viability.

## 6.5. Relevance of these findings to $\beta$ cell function and glucotoxicity in T2DM

The effects of D-glucose deprivation that are described in Chapter 4 of this thesis lead to AMPK activation, increased L-leucine transport at the plasma membrane and high intracellular L-leucine concentration. It has been observed previously that elevation of the extracellular D-glucose concentration to a value like that seen in blood plasma in T2DM has the opposite effect on AMPK i.e. it significantly decreases AMPK activation judged from its phosphorylation (Leclerc and Rutter 2004), and this was confirmed in this thesis by incubation of INS1E cells for 6 hours in medium with 25mM D-glucose in Figure 4.5. It would therefore be expected that this AMPK inhibition would decrease L-[<sup>3</sup>H]-leucine transport into the cell to a value below that seen with 5mM D-glucose. If this occurred *in vivo* during the rise in plasma D-glucose and D-leucine concentration that follows a meal, this might have the undesirable effect of blunting the stimulatory effect of L-leucine on insulin secretion (Section 1.3). However, no significant decrease in L-leucine transport was observed with 25mM D-glucose (Figure 4.2, 4.3 and 4.9), indeed in some experiments this high D-glucose concentration increased L-[<sup>3</sup>H]-leucine transport (Figure 4.1.a), suggesting that, in addition to signalling by inhibiting AMPK, high D-glucose concentration also exerts an opposing stimulatory effect on L-leucine transport which is variable in magnitude. The osmotic effect caused by the high concentrations of D-glucose, is characterized by the increase in demand of  $\beta$  cells to synthesise and secrete insulin to maintain blood D-glucose levels. In T2D the chronic inflammation caused by oxidative stress is responsible for the insulin resistance and later T2D. The nifedipine experiment in Figure 4.2 suggested that insulin secretion from INS1E cells induced by high D-glucose concentration, leading to an autocrine insulin stimulation of mTORC1 (which is a known stimulator of LAT1) (Liu et al. 2004) was not the cause of this opposing effect. Whether high D-glucose leads to mTORC1 stimulation by some alternative pathway in INSE remains to be determined.

In future therefore it would be of interest to characterise further these two apparent opposing effects of high D-glucose on L-leucine transport in INS1E cells by examining whether high D-glucose can:

- a) Reproducibly inhibit L-leucine transport via AMPK inhibition if any hypothetical stimulation of transport by mTORC1 is inhibited with Rapamycin
- b) Reproducibly stimulate L-leucine transport if the D-glucose signal through AMPK is inhibited with Compound C (or more selectively with AMPK siRNA silencing).

To assess *in vivo* whether such effects of D-glucose or T2DM on  $\beta$  cell L-leucine transport, cell mass or toxicity are mediated by LAT1 (SLC7A5), the role of SLC7A5 would need to be assessed by tissue-specific knock-out of SLC7A5 in  $\beta$  cells in a transgenic mouse. Generation of a transgenic mouse containing both SLC7A5-Flox and Cre transgenes to achieve tissue-specific knockout of SLC7A5 expression has already been achieved in tissues such as skeletal muscle (Poncet et al. 2014). Using a similar Cre-loxP system, tissue-specific knockout of the insulin receptor in pancreatic  $\beta$  cells has been used to determine the functional role of insulin signalling in these cells *in vivo*. This showed a selective loss of insulin secretion in the resultant mice, and a progressive impairment of glucose tolerance (Kulkarni et al. 1999). This work demonstrates the up-regulation of LAT1 by AMPK and it may be feasible in the near future to generate a  $\beta$  cell specific SLC7A5 knock-out mouse to confirm the effect of D-glucose deprivation in  $\beta$  cell LAT1 activity of knock-out mouse.

A further possible link between this thesis and diabetes mellitus is endoplasmic reticulum stress (ERS) which is thought to contribute to  $\beta$  cell dysfunction (Fonseca et al. 2011). ERS arises (at least partly) from the effects of high D-glucose concentration in diabetes, and triggers the so-called “unfolded protein response” in which the cell shuts down protein synthesis to limit the amount of mis-folded protein that accumulates in the endoplasmic reticulum. As with the impairment of protein synthesis caused by D-glucose deprivation in Section 6.3, this ERS-induced impairment of protein synthesis should lead to accumulation of intracellular amino acids, including L-leucine, to which the cells may again respond by up-regulating LAT1. A recent preliminary report in the *db/db* diabetic mouse has shown that increased LAT1 expression correlates with the progression of disease, and that imposing ERS on  $\beta$  cells does give the expected increase in LAT1 expression (Ratnam et al. 2016).

## **6.6. Possible relevance to cancer**

As was noted in section 1.12, in hypoxic tumours in non-small cell lung cancer patients, the expression of LAT1 protein has been shown to correlate with expression of markers of hypoxia, suggesting that hypoxia (and probably anaerobic glycolysis leading to D-glucose depletion) may lead to up-regulation of LAT1 expression. As in the D-glucose deprivation experiments in this thesis, this leads to the question of whether this up-regulation has any important biological function in the tumour cells. In some tumours hypoxia leads to activation of AMPK (Zadra et al. 2015), which may contribute to the LAT1 up-regulation as in the D-glucose-deprived INS1E insulinoma studied here. It is not obvious how an increase in L-leucine influx would benefit hypoxic tumour cells, which could not oxidise L-leucine as a fuel under hypoxic conditions and might have limited protein synthesis under conditions of AMPK activation. However, LAT1 may be required in hypoxic tumours (with impaired protein synthesis and resulting amino acid accumulation) to perform L-leucine efflux to avoid L-leucine-induced toxicity as discussed in Section 6.3 above. Blockade of such efflux leading to amino acid toxicity might therefore be a potential target for chemotherapy, and might contribute to the reported therapeutic effect of novel anti-LAT1 anti-cancer drugs such as KMH-233 (Huttunen et al. 2016).

## **6.7. Conclusion**

This thesis has provided for the first time evidence that the well characterised up-regulation of solute carriers by AMPK, that has previously been described for GLUT D-glucose transporters in muscle, may also occur for LAT1(SLC7A5)/4F2hc(SLC3A2) amino acid transporters in the INS1E insulinoma  $\beta$  cell line. Like the GLUT effect, the effect of D-glucose starvation and of AMPK activation on LAT1 may involve both increased transcription of LAT1 mRNA and a post-transcriptional effect possibly involving redistribution of LAT1 proteins within the cell. However, while the effect of low energy state on LAT1 seems to be significant in INS1E cells, the effect of D-glucose excess and its relevance to T2DM remains to be determined.

## References

---

- Abe, H., Uchida, T., Mizukami, H., Komiya, K., Koike, M., Shigihara, N., Toyofuku, Y., Ogihara, T., Uchiyama, Y., Yagihashi, S., Fujitani, Y. and Watada, H. (2013) Exendin-4 Improves  $\beta$ -Cell Function in Autophagy-Deficient  $\beta$ -Cells. *Endocrinology*, Volume 154(Issue 12).
- Ackermann, A. M. and Gannon, M. (2007) Molecular regulation of pancreatic beta-cell mass development, maintenance, and expansion. *J Mol Endocrinol*, 38(1-2), pp. 193-206.
- Altman, J. K., Szilard, A., Goussetis, D. J., Sassano, A., Colamonici, M., Gounaris, E., Frankfurt, O., Giles, F. J., Eklund, E. A., Beauchamp, E. M. and Plataniias, L. C. (2014) Autophagy Is a Survival Mechanism of Acute Myelogenous Leukemia Precursors during Dual mTORC2/mTORC1 Targeting. *Clinical Cancer Research*, 20(9), pp. 2400-2409.
- Altshuler, D., Hirschhorn, J. N., Klannemark, M., Lindgren, C. M., Vohl, M.-C., Nemesh, J., Lane, C. R., Schaffner, S. F., Bolk, S., Brewer, C., Tuomi, T., Gaudet, D., Hudson, T. J., Daly, M., Groop, L. and Lander, E. S. (2000) The common PPAR  $\gamma$  Pro12Ala polymorphism is associated with decreased risk of type 2 diabetes. *nature genetics volume 26*
- Ashcroft, F. and Rorsman, P. (2004) Type 2 diabetes mellitus: not quite exciting enough? *Human molecular genetics*, 13(suppl 1), pp. R21-R31.
- Ashcroft, F. M. (2005) ATP-sensitive potassium channelopathies: focus on insulin secretion. *The Journal of clinical investigation*, 115(8), pp. 2047-2058.
- Association, A. D. (2014) Diagnosis and Classification of Diabetes Mellitus. *Diabetes Care Volume 37*(Supplement 1).
- Atkinson, M. A., Eisenbarth, G. S. and Michels, A. W. (2014) Type 1 diabetes. *The Lancet*, 383(9911), pp. 69-82.
- Averous, J., Lambert-Langlais, S., Carraro, V., Gourbeyre, O., Parry, L., B'Chir, W., Muranishi, Y., Jousse, C., Bruhat, A. and Maurin, A.-C. (2014) Requirement for lysosomal localization of mTOR for its activation differs between leucine and other amino acids. *Cellular signalling*, 26(9), pp. 1918-1927.
- Babu, E., Kanai, Y., Chairoungdua, A., Kim, D. K., Iribe, Y., Tangtrongsup, S., Jutabha, P., Li, Y., Ahmed, N. and Sakamoto, S. (2003) Identification of a novel system L amino acid transporter structurally distinct from heterodimeric amino acid transporters. *Journal of Biological Chemistry*, 278(44), pp. 43838-43845.
- Baird, F. E., Bett, K. J., MacLean, C., Tee, A. R., Hundal, H. S. and Taylor, P. M. (2009) Tertiary active transport of amino acids reconstituted by coexpression of System A and L transporters in *Xenopus* oocytes. *Am J Physiol Endocrinol Metab*, 297(3), pp. E822-9.
- Balcazar M, N. and Aguilar de P, C. (2012) Role of AKT/mTORC1 pathway in pancreatic  $\beta$ -cell proliferation. *Colombia Médica*, 43(3), pp. 235-243.
- Bar-Peled, L. and Sabatini, D. M. (2014) Regulation of mTORC1 by amino acids. *Trends in cell biology*, 24(7), pp. 400-406.
- Bardeesy, N. and DePinho, R. A. (2002) Pancreatic cancer biology and genetics. *Nature Reviews Cancer*, 2(12), pp. 897-909.
- Bartolome, A. and Guillen, C. (2014) Role of the Mammalian Target of Rapamycin (mTOR) Complexes in

Pancreatic b-Cell Mass Regulation. *Vitamins & Hormones, Volume 95*, pp. 425–469.

- Benziane, B., Björnholm, M., Pirkmajer, S., Austin, R. L., Kotova, O., Viollet, B., Zierath, J. R. and Chibalin, A. V. (2012) Activation of AMP-activated protein kinase stimulates Na<sup>+</sup>, K<sup>+</sup>-ATPase activity in skeletal muscle cells. *Journal of Biological Chemistry*, 287(28), pp. 23451-23463.
- Bertran, J., Werner, A., Moore, M. L., Stange, G., Markovich, D., Biber, J., Testar, X., Zorzano, A., Palacin, M. and Murer, H. (1992) Expression cloning of a cDNA from rabbit kidney cortex that induces a single transport system for cystine and dibasic and neutral amino acids. *Proceedings of the National Academy of Sciences*, 89(12), pp. 5601-5605.
- Bhaskar, P. T. and Hay., N. (2007) The Two TORCs and Akt. *Dev. Cell Vol. 12*( Issue 4), pp. 487–502.
- Bionumbers (2011) *Lysosome diameter*, Available:  
<http://bionumbers.hms.harvard.edu/bionumber.aspx?id=106072>.
- Blagih, J., Coulombe, F., Vincent, E. E., Dupuy, F., Galicia-Vázquez, G., Yurchenko, E., Raissi, T. C., van der Windt, G. J., Viollet, B. and Pearce, E. L. (2015) The energy sensor AMPK regulates T cell metabolic adaptation and effector responses in vivo. *Immunity*, 42(1), pp. 41-54.
- Blandino-Rosano, M., Angela Y. Chen, Joshua O. Scheys, Emily U. Alejandro, Aaron P. Gould, Tatyana Taranukha, Lynda Elghazi, Corentin Cras-Méneur and Bernal-Mizrachi., E. (2012) mTORC1 signaling and regulation of pancreatic  $\beta$ -cell mass. *Cell Cycle* 11:10, pp. 1892-1902.
- Boado, R. J., Li, J. Y., Tsukamoto, H. and Pardridge, W. M. (2003) Hypoxia induces de-stabilization of the LAT1 large neutral amino acid transporter mRNA in brain capillary endothelial cells. *Journal of neurochemistry*, 85(4), pp. 1037-1042.
- Bodoy, S., Fotiadis, D., Stoeger, C., Kanai, Y. and Palacín, M. (2013) The small SLC43 family: facilitator system I amino acid transporters and the orphan EEG1. *Molecular aspects of medicine*, 34(2), pp. 638-645.
- Borack Michael and Rasmussen., B. (2014) Leucine activation of mTORC1 in skeletal muscle cells is inhibited by the lysosomotropic agent chloroquine. *The FASEB Journal*
- Boron, W. F. and Boulpaep, E. L. (2016) *Medical physiology*, Elsevier Health Sciences.
- Bouwens, L. and Rومان, I. (2005) Regulation of pancreatic beta-cell mass. *Physiol Rev*, 85(4), pp. 1255-70.
- Bröer, A., Wagner, C. A., Florian, L. and Bröer, S. (2000) The heterodimeric amino acid transporter 4F2hc/y<sup>+</sup> LAT2 mediates arginine efflux in exchange with glutamine. *Biochemical Journal*, 349(3), pp. 787-795.
- Bröer, S. (2009) The role of the neutral amino acid transporter BOAT1 (SLC6A19) in Hartnup disorder and protein nutrition. *IUBMB life*, 61(6), pp. 591-599.
- Brownie, A. C. a. K., J.C. (1999) *Churchill's Mastery of Medicine: Biochemistry*, Churchill Livingstone.
- Byfield, M. P., Murray, J. T. and Backer, J. M. (2005) hVps34 is a nutrient-regulated lipid kinase required for activation of p70 S6 kinase. *J Biol Chem*, 280(38), pp. 33076-82.
- Campbell, W. A. and Thompson, N. L. (2001) Overexpression of LAT1/CD98 light chain is sufficient to increase system L-amino acid transport activity in mouse hepatocytes but not fibroblasts. *J Biol Chem*, 276(20), pp. 16877-84.

- Cawston, E. E. a. M., L.J. (2010) Therapeutic potential for novel drugs targeting the type 1 cholecystokinin receptor. *Br J Pharmacol*, 159(5), pp. 1009-21.
- Chan, J. e. a. (2013) Failure of the adaptive unfolded protein response in islets of obese mice is linked with abnormalities in  $\beta$ -cell gene expression and progression to diabetes. *Diabetes*, 62(5), pp. 1557-68.
- Chand, A. L. and Legge, M. (2011) Amino acid transport system L activity in developing mouse ovarian follicles. *Hum Reprod*, 26(11), pp. 3102-8.
- Cheng, Q. (2013) *The role of system L amino acid transporters in pancreatic  $\beta$ -cells* Unpublished MPhil, University of Leicester.
- Cheng, Q., Beltran, V. D., Chan, S. M., Brown, J. R., Bevington, A. and Herbert, T. P. (2016) System-L amino acid transporters play a key role in pancreatic  $\beta$ -cell signalling and function. *Journal of molecular endocrinology*, 56(3), pp. 175-187.
- Cheng, Q., Shah, N., Bröer, A., Fairweather, S., Jiang, Y., Schmoll, D., Corry, B. and Bröer, S. (2017) Identification of novel inhibitors of the amino acid transporter B0AT1 (SLC6A19), a potential target to induce protein restriction and to treat type 2 diabetes. *British Journal of Pharmacology*.
- Chungchunlam, S., Henare, S., Ganesh, S. and Moughan, P. (2015) Dietary whey protein influences plasma satiety-related hormones and plasma amino acids in normal-weight adult women. *European journal of clinical nutrition*, 69(2), pp. 179-186.
- Closs, E., Boissel, J.-P., Habermeier, A. and Rotmann, A. (2006) Structure and function of cationic amino acid transporters (CATs). *The Journal of membrane biology*, 213(2), pp. 67-77.
- Colas, C., Ung, P. M.-U. and Schlessinger, A. (2016) SLC transporters: structure, function, and drug discovery. *MedChemComm*, 7(6), pp. 1069-1081.
- Correia, M., Neves-Petersen, M. T., Jeppesen, P. B., Gregersen, S. and Petersen, S. B. (2012) UV-light exposure of insulin: pharmaceutical implications upon covalent insulin dityrosine dimerization and disulphide bond photolysis. *PLoS one*, 7(12), pp. e50733.
- Daneman, D. (2006) Type 1 diabetes. *The Lancet*, 367(9513), pp. 847-858.
- de Haro, C., Mendez, R. and Santoyo, J. (1996) The eIF-2 $\alpha$  kinases and the control of protein synthesis. *FASEB J*, 10(12), pp. 1378-87.
- Del Prato, S. (2009) Role of glucotoxicity and lipotoxicity in the pathophysiology of Type 2 diabetes mellitus and emerging treatment strategies. *Diabetic Medicine*, 26(12), pp. 1185-1192.
- Deves, R. and Boyd, C. (1998) Transporters for cationic amino acids in animal cells: discovery, structure, and function. *Physiological reviews*, 78(2), pp. 487-545.
- Dhawan, D. and Padh, H. (2016) Genetic variations in TCF7L2 influence therapeutic response to sulfonylureas in Indian diabetics. *Diabetes Research and Clinical Practice*, 121, pp. 35-40.
- Dibble, C. C. and Cantley, L. C. (2015) Regulation of mTORC1 by PI3K signaling. *Trends in cell biology*, 25(9), pp. 545-555.
- Dickens, D., Webb, S. D., Antonyuk, S., Giannoudis, A., Owen, A., Rädisch, S., Hasnain, S. S. and Pirmohamed, M. (2013) Transport of gabapentin by LAT1 (SLC7A5). *Biochemical pharmacology*, 85(11), pp. 1672-1683.

- Dodd, K. M. and Tee, A. R. (2012) Leucine and mTORC1: a complex relationship. *Am J Physiol Endocrinol Metab*, 302(11), pp. E1329-42.
- Dolgodilina, E., Imobersteg, S., Laczko, E., Welt, T., Verrey, F. and Makrides, V. (2016) Brain interstitial fluid glutamine homeostasis is controlled by blood–brain barrier SLC7A5/LAT1 amino acid transporter. *Journal of Cerebral Blood Flow & Metabolism*, 36(11), pp. 1929-1941.
- El-Assaad, W., Buteau, J., Peyot, M.-L., Nolan, C., Roduit, R., Hardy, S., Joly, E., Dbaibo, G., Rosenberg, L. and Prentki, M. (2003) Saturated fatty acids synergize with elevated glucose to cause pancreatic  $\beta$ -cell death. *Endocrinology*, 144(9), pp. 4154-4163.
- Evans, Nasim, Z., Brown, J., Butler, H., Kauser, S., Varoqui, H., Erickson, J. D., Herbert, T. P. and Bevington, A. (2007) Acidosis-sensing glutamine pump SNAT2 determines amino acid levels and mammalian target of rapamycin signalling to protein synthesis in L6 muscle cells. *Journal of the American Society of Nephrology*, 18(5), pp. 1426-1436.
- Evans, Nasim, Z., Brown, J., Clapp, E., Amin, A., Yang, B., Herbert, T. P. and Bevington, A. (2008) Inhibition of SNAT2 by metabolic acidosis enhances proteolysis in skeletal muscle. *J Am Soc Nephrol*, 19(11), pp. 2119-29.
- Evans, K., Nasim, Z., Brown, J., Butler, H., Kauser, S., Varoqui, H., Erickson, J. D., Herbert, T. P. and Bevington, A. (2007) Acidosis-sensing glutamine pump SNAT2 determines amino acid levels and mammalian target of rapamycin signalling to protein synthesis in L6 muscle cells. *J Am Soc Nephrol*, 18(5), pp. 1426-36.
- Fahien, L. A. and MacDonald, M. J. (2011) The complex mechanism of glutamate dehydrogenase in insulin secretion. *Diabetes*, 60(10), pp. 2450-2454.
- Foley, K., Boguslavsky, S. and Klip, A. (2011) Endocytosis, recycling, and regulated exocytosis of glucose transporter 4. *Biochemistry*, 50(15), pp. 3048-61.
- Fonseca, S. G., Gromada, J. and Urano, F. (2011) Endoplasmic reticulum stress and pancreatic beta-cell death. *Trends Endocrinol Metab*, 22(7), pp. 266-74.
- Fotiadis, D., Kanai, Y. and Palacín, M. (2013) The SLC3 and SLC7 families of amino acid transporters. *Molecular aspects of medicine*, 34(2), pp. 139-158.
- Fox, H. L. e. a. (1998) Amino acid effects on translational repressor 4E-BP1 are mediated primarily by L-leucine in isolated adipocyteS. *Am J Physiol*.
- Freudenberg, A., Petzke, K. J. and Klaus, S. (2012) Comparison of high-protein diets and leucine supplementation in the prevention of metabolic syndrome and related disorders in mice. *The Journal of nutritional biochemistry*, 23(11), pp. 1524-1530.
- Fukumoto, S., Hanazono, K., Komatsu, T., Ueno, H., Kadosawa, T., Iwano, H. and Uchide, T. (2013) L-type amino acid transporter 1 (LAT1): A new therapeutic target for canine mammary gland tumour. *The Veterinary Journal*, 198(1), pp. 164-169.
- Fukushima, D., Doi, H., Fukushima, K., Katsura, K., Ogawa, N., Sekiguchi, S., Fujimori, K., Sato, A., Satomi, S. and Ishida, K. (2010) Glutamate exocrine dynamics augmented by plasma glutamine and the distribution of amino acid transporters of the rats pancreas. *Journal of Physiology and Pharmacology*, 61(3), pp. 265.
- Gaw, A. (2008) *Clinical biochemistry: an illustrated colour text*, Elsevier Health Sciences.
- Ginion, A., Auquier, J., Benton, C. R., Mouton, C., Vanoverschelde, J.-L., Hue, L., Horman, S., Beauloye, C.

- and Bertrand, L. (2011) Inhibition of the mTOR/p70S6K pathway is not involved in the insulin-sensitizing effect of AMPK on cardiac glucose uptake. *American Journal of Physiology-Heart and Circulatory Physiology*, pp. ajpheart. 00986.2010.
- Gloyn, A. L., Weedon, M. N., Owen, K. R., Turner, M. J., Knight, B. A., Hitman, G., Walker, M., Levy, J. C., Sampson, M. and Halford, S. (2003) Large-scale association studies of variants in genes encoding the pancreatic  $\beta$ -cell KATP channel subunits Kir6. 2 (KCNJ11) and SUR1 (ABCC8) confirm that the KCNJ11 E23K variant is associated with type 2 diabetes. *Diabetes*, 52(2), pp. 568-572.
- Gong, L., Goswami, S., Giacomini, K. M., Altman, R. B. and Klein, T. E. (2012) Metformin pathways: pharmacokinetics and pharmacodynamics. *Pharmacogenetics and genomics*, 22(11), pp. 820.
- Gran, P. and Cameron-Smith, D. (2011) The actions of exogenous leucine on mTOR signalling and amino acid transporters in human myotubes. *BMC physiology*, 11(1), pp. 10.
- Grundy, S. M. (2012) Pre-diabetes, metabolic syndrome, and cardiovascular risk. *Journal of the American College of Cardiology*, 59(7), pp. 635-643.
- Guan, Y., Yan, L., Liu, X., Zhu, X., Wang, S. and Chen, L. (2016) Correlation of the TCF7L2 (rs7903146) polymorphism with an enhanced risk of type 2 diabetes mellitus: a meta-analysis. *Genetics and molecular research: GMR*, 15(3).
- Guertin, D. A. a. S., D.M. (2007 ) Defining the role of mTOR in cancer. *Cancer Cell*, 12(1), pp. 9-22.
- Hardie, D. G. (2003) Minireview: the AMP-activated protein kinase cascade: the key sensor of cellular energy status. *Endocrinology*, 144(12), pp. 5179-5183.
- Hardie, D. G. (2011) AMP-activated protein kinase: an energy sensor that regulates all aspects of cell function. *Genes Dev*, 25(18), pp. 1895-908.
- Harris, R. A., Kobayashi, R., Murakami, T. and Shimomura, Y. (2001) Regulation of branched-chain  $\alpha$ -keto acid dehydrogenase kinase expression in rat liver. *The Journal of nutrition*, 131(3), pp. 841S-845S.
- Hayashi, K. and Anzai, N. (2017) Novel therapeutic approaches targeting L-type amino acid transporters for cancer treatment. *World J Gastrointest Oncol*, 9(1), pp. 21-29.
- Hohmeier, H. E., Mulder, H., Chen, G., Henkel-Rieger, R., Prentki, M. and Newgard, C. B. (2000) Isolation of INS-1-derived cell lines with robust ATP-sensitive K<sup>+</sup> channel-dependent and-independent glucose-stimulated insulin secretion. *Diabetes*, 49(3), pp. 424-430.
- Hong, Y. H., Varanasi, U. S., Yang, W. and Leff, T. (2003) AMP-activated protein kinase regulates HNF4 $\alpha$  transcriptional activity by inhibiting dimer formation and decreasing protein stability. *J Biol Chem*, 278(30), pp. 27495-501.
- Hristova, M., Rocha - Ferreira, E., Fontana, X., Thei, L., Buckle, R., Christou, M., Hompoonsup, S., Gostelow, N., Raivich, G. and Peebles, D. (2016) Inhibition of Signal Transducer and Activator of Transcription 3 (STAT3) reduces neonatal hypoxic - ischaemic brain damage. *Journal of neurochemistry*, 136(5), pp. 981-994.
- Hundal, H. S. and Taylor, P. M. (2009) Amino acid transceptors: gate keepers of nutrient exchange and regulators of nutrient signaling. *American Journal of Physiology-Endocrinology and Metabolism*, 296(4), pp. E603-E613.
- Huttunen, K. M., Gynther, M., Huttunen, J., Puris, E., Spicer, J. A. and Denny, W. A. (2016) A Selective and Slowly Reversible Inhibitor of I-Type Amino Acid Transporter 1 (LAT1) Potentiates Antiproliferative Drug Efficacy in Cancer Cells. *Journal of medicinal chemistry*, 59(12), pp. 5740-

5751.

- Hyde, P. and Hundal, H. (2003 ) Amino acid transporters: roles in amino acid sensing and signalling in animal cells *Biochem. J.*, 373(1–18).
- Hyde, R., Cwiklinski, E. L., MacAulay, K., Taylor, P. M. and Hundal, H. S. (2007) Distinct sensor pathways in the hierarchical control of SNAT2, a putative amino acid transceptor, by amino acid availability. *Journal of Biological Chemistry*, 282(27), pp. 19788-19798.
- Iiboshi, Y., Papst, P. J., Kawasome, H., Hosoi, H., Abraham, R. T., Houghton, P. J. and Terada, N. (1999) Amino acid-dependent control of p70(s6k). Involvement of tRNA aminoacylation in the regulation. *J Biol Chem*, 274(2), pp. 1092-9.
- Inoki, K., Li, Y., Xu, T. and Guan, K.-L. (2003) Rheb GTPase is a direct target of TSC2 GAP activity and regulates mTOR signaling. *Genes & development*, 17(15), pp. 1829-1834.
- Ishihara, H., Asano, T., Tsukuda, K., Katagiri, H., Inukai, K., Anai, M., Kikuchi, M., Yazaki, Y., Miyazaki, J.-I. and Oka, Y. (1993) Pancreatic beta cell line MIN6 exhibits characteristics of glucose metabolism and glucose-stimulated insulin secretion similar to those of normal islets. *Diabetologia*, 36(11), pp. 1139-1145.
- Ishizuka, Y., Kakiya, N., Nawa, H. and Takei, N. (2008) Leucine induces phosphorylation and activation of p70S6K in cortical neurons via the system L amino acid transporter. *J Neurochem*, 106(2), pp. 934-42.
- Islam, M. S. (2010) *The islets of langerhans*, Springer.
- Janpipatkul, K., Suksen, K., Borwornpinyo, S., Jearawiriyapaisarn, N., Hongeng, S., Piyachaturawat, P. and Chairoungdua, A. (2014) Downregulation of LAT1 expression suppresses cholangiocarcinoma cell invasion and migration. *Cellular signalling*, 26(8), pp. 1668-1679.
- Jewell, J. L., Kim, Y. C., Russell, R. C., Yu, F.-X., Park, H. W., Plouffe, S. W., Tagliabracci, V. S. and Guan, K.-L. (2015) Differential regulation of mTORC1 by leucine and glutamine. *Science*, 347(6218), pp. 194-198.
- Jewell, J. L., Russell, R. C. and Guan, K. L. (2013) Amino acid signalling upstream of mTOR. *Nature Reviews Molecular Cell Biology*, 14(3), pp. 133-139.
- Jiang, Y., Rose, A. J., Sijmonsma, T. P., Bröer, A., Pfenninger, A., Herzig, S., Schmoll, D. and Bröer, S. (2015) Mice lacking neutral amino acid transporter B 0 AT1 (Slc6a19) have elevated levels of FGF21 and GLP-1 and improved glycaemic control. *Molecular metabolism*, 4(5), pp. 406-417.
- Jin, J., Mullen, T. D., Hou, Q., Bielawski, J., Bielawska, A., Zhang, X., Obeid, L. M., Hannun, Y. A. and Hsu, Y. T. (2009) AMPK inhibitor Compound C stimulates ceramide production and promotes Bax redistribution and apoptosis in MCF7 breast carcinoma cells. *J Lipid Res*, 50(12), pp. 2389-97.
- Joslin, E. P. and Kahn, C. R. (2005) *Joslin's Diabetes Mellitus: Edited by C. Ronald Kahn...[et Al.]*, Lippincott Williams & Wilkins.
- Kaira, K., Oriuchi, N., Takahashi, T., Nakagawa, K., Ohde, Y., Okumura, T., Murakami, H., Shukuya, T., Kenmotsu, H. and Naito, T. (2011) LAT1 expression is closely associated with hypoxic markers and mTOR in resected non-small cell lung cancer. *Am J Transl Res*, 3(5), pp. 468-478.
- Kanai, Y., Fukasawa, Y., Cha, S. H., Segawa, H., Chairoungdua, A., Kim, D. K., Matsuo, H., Kim, J. Y., Miyamoto, K.-i. and Takeda, E. (2000) Transport properties of a system y+ L neutral and basic amino acid transporter insights into the mechanisms of substrate recognition. *Journal of*

*Biological Chemistry*, 275(27), pp. 20787-20793.

- Kemp, G. J., Bevington, A. and Russell, R. G. (1988) Theoretical interpretation of isotope labelling experiments in cells in which the label is chemically incorporated: the example of orthophosphate. *J Theor Biol*, 134(3), pp. 351-64.
- Killian, D. M. and Chikhale, P. J. (2001) Predominant functional activity of the large, neutral amino acid transporter (LAT1) isoform at the cerebrovasculature. *Neuroscience letters*, 306(1), pp. 1-4.
- Kim, C.-H., Kyung Jin Park, Jung Rim Park, Yoshikatsu Kanai, Hitoshi Endou, Park, J.-C. and Kim, D. K. (2006) The RNA Interference of Amino Acid Transporter LAT1 Inhibits the Growth of KB Human Oral Cancer Cells. *ANTICANCER RESEARCH* 26, pp. 2943-2948.
- Kim, J., Kundu, M., Viollet, B. and Guan, K.-L. (2011) AMPK and mTOR regulate autophagy through direct phosphorylation of Ulk1. *Nature cell biology*, 13(2), pp. 132-141.
- Kim, W., Fiori, J. L., Shin, Y.-K., Okun, E., Kim, J. S., Rapp, P. R. and Egan, J. M. (2014) Pancreatic polypeptide inhibits somatostatin secretion. *FEBS letters*, 588(17), pp. 3233-3239.
- Klok, M., Jakobsdottir, S. and Drent, M. (2007) The role of leptin and ghrelin in the regulation of food intake and body weight in humans: a review. *Obesity reviews*, 8(1), pp. 21-34.
- Kulkarni, R. N., Brüning, J. C., Winnay, J. N., Postic, C., Magnuson, M. A. and Kahn, C. R. (1999) Tissue-Specific Knockout of the Insulin Receptor in Pancreatic  $\beta$  Cells Creates an Insulin Secretory Defect Similar to that in Type 2 Diabetes. *Cell*, 96 pp. 329-339.
- Kurth-Kraczek, E. J., Hirshman, M. F., Goodyear, L. J. and Winder, W. W. (1999) 5'AMP-activated protein kinase activation causes GLUT4 translocation in skeletal muscle. *Diabetes*, 48(8), pp. 1667-1671.
- Laplante, M. a. S., D.M. (2012 ) mTOR signaling in growth control and disease. *Cell*, 13;149(2), pp. 274-93.
- Leclerc, I. and Rutter, G. A. (2004) AMP-activated protein kinase: a new beta-cell glucose sensor? Regulation by amino acids and calcium ions. *Diabetes*, 53(suppl 3), pp. S67-S74.
- Li, Y.-y., Wang, L.-s., Lu, X.-z., Yang, Z.-j., Wang, X.-m., Zhou, C.-w., Xu, J., Qian, Y. and Chen, A.-l. (2013) CDKAL1 gene rs7756992 A/G polymorphism and type 2 diabetes mellitus: a meta-analysis of 62,567 subjects. *Scientific reports*, 3, pp. 3131.
- Lieberthal, W. a. L., J.S ( 2009) The Role of the Mammalian Target Of Rapamycin (mTOR) in Renal Disease. *J Am Soc Nephrol* 20, pp. 2493–2502.
- Limon, J. J. and Fruman, D. A. (2007) Akt and mTOR in B cell activation and differentiation. *PI3K signalling*, pp. 6.
- Lin, L., Yee, S. W., Kim, R. B. and Giacomini, K. M. (2015) SLC transporters as therapeutic targets: emerging opportunities. *Nature reviews Drug discovery*, 14(8), pp. 543-560.
- Liong, S. and Lappas, M. (2017) Lipopolysaccharide and double stranded viral RNA mediate insulin resistance and increase system a amino acid transport in human trophoblast cells in vitro. *Placenta*, 51, pp. 18-27.
- Liu, X., Chhipa, R. R., Nakano, I. and Dasgupta, B. (2014) The AMPK inhibitor compound C is a potent AMPK-independent anti glioma agent. *Mol Cancer Ther*, 13(3), pp. 596-605.
- Liu, X. M., Reyna, S. V., Ensenat, D., Peyton, K. J., Wang, H., Schafer, A. I. and Durante, W. (2004) Platelet-

- derived growth factor stimulates LAT1 gene expression in vascular smooth muscle: role in cell growth. *FASEB J*, 18(6), pp. 768-70.
- Liu, Z., Jeppesen, P. B., Gregersen, S., Larsen, L. B. and Hermansen, K. (2012) Chronic exposure to leucine in vitro induces beta-cell dysfunction in INS-1E cells and mouse islets. *J Endocrinol*, 215(1), pp. 79-88.
- Lowry, O. H., Rosebrough, N. J., Farr, A. L. and Randall, R. J. (1951) Protein measurement with the Folin phenol reagent. *J Biol Chem*, 193(1), pp. 265-75.
- Luiken, J. J., Glatz, J. F. and Neumann, D. (2015) Cardiac contraction-induced GLUT4 translocation requires dual signaling input. *Trends Endocrinol Metab*, 26(8), pp. 404-10.
- Lynch, C. J. and Adams, S. H. (2014) Branched-chain amino acids in metabolic signalling and insulin resistance. *Nature Reviews Endocrinology*, 10(12), pp. 723-736.
- MacDonald, M. J., Hasan, N. M. and Longacre, M. J. (2008) Studies with leucine,  $\beta$ -hydroxybutyrate and ATP citrate lyase-deficient beta cells support the acetoacetate pathway of insulin secretion. *Biochimica et Biophysica Acta (BBA)-General Subjects*, 1780(7), pp. 966-972.
- Mainous, A. G., Tanner, R. J., Jo, A. and Anton, S. D. (2016) Prevalence of prediabetes and abdominal obesity among healthy-weight adults: 18-Year trend. *The Annals of Family Medicine*, 14(4), pp. 304-310.
- Makrides, V., Camargo, S. M. and Verrey, F. (2014) Transport of amino acids in the kidney. *Compr Physiol*, 4(1), pp. 367-403.
- Manchester, K. L. (1970) The control by insulin of amino acid accumulation in muscle. *Biochem J*, 117(3), pp. 457-65.
- Mani, B. K. and Zigman, J. M. (2015) A Strong Stomach for Somatostatin. *Endocrinology*, 156(11), pp. 3876-3879.
- Manning, B. D. and Cantley, L. C. (2007) AKT/PKB signaling: navigating downstream. *Cell*, 129(7), pp. 1261-1274.
- Marlon, E. (2013) Beta cell dysfunction and insulin resistance. *Front. Endocrinol*, 4, pp. 37.
- Martino, L., Masini, M., Novelli, M., Befly, P., Bugliani, M., Marselli, L., Masiello, P., Marchetti, P. and Tata, V. D. (2012) Palmitate Activates Autophagy in INS-1E b-Cells and in Isolated Rat and Human Pancreatic Islets. *Volume 7*(Issue 5).
- Mastroberardino, L., Spindler, B., Pfeiffer, R., Skelly, P. J., Loffing, J., Shoemaker, C. B. and Verrey, F. (1998) Amino-acid transport by heterodimers of 4F2hc/CD98 and members of a permease family. *Nature*, 395(6699), pp. 288-291.
- Matsuyama, R., Tomi, M., Akanuma, S., Tabuchi, A., Kubo, Y., Tachikawa, M. and Hosoya, K. (2012) Up-regulation of L-type amino acid transporter 1 (LAT1) in cultured rat retinal capillary endothelial cells in response to glucose deprivation. *Drug Metab Pharmacokinet*, 27(3), pp. 317-24.
- McCarthy, M. I. (2010) Genomics, type 2 diabetes, and obesity. *New England Journal of Medicine*, 363(24), pp. 2339-2350.
- Meier, C., Ristic, Z., Klauser, S. and Verrey, F. (2002) Activation of system L heterodimeric amino acid exchangers by intracellular substrates. *The EMBO journal*, 21(4), pp. 580-589.

- Metzgar, R. S., Hollingsworth, M. A. and Kaufman, B. (1993) Pancreatic mucins. *The Pancreas: Biology, Pathology, and Disease*, pp. 351-367.
- Mihaylova, M. M. and Shaw, R. J. (2011) The AMPK signalling pathway coordinates cell growth, autophagy and metabolism. *Nature cell biology*, 13(9), pp. 1016-1023.
- Milkereit, R., Persaud, A., Vanoaica, L., Guetg, A., Verrey, F. and Rotin, D. (2015) LAPT4b recruits the LAT1-4F2hc Leu transporter to lysosomes and promotes mTORC1 activation. *Nature communications*, 6.
- Mir-Coll, J., Duran, J., Slebe, F., García-Rocha, M., Gomis, R., Gasa, R. and Guinovart, J. J. (2015) Genetic models rule out a major role of beta cell glycogen in the control of glucose homeostasis. *Diabetologia*.
- Mo, J.-S., Meng, Z., Kim, Y. C., Park, H. W., Hansen, C. G., Kim, S., Lim, D.-S. and Guan, K.-L. (2015) Cellular energy stress induces AMPK-mediated regulation of YAP and the Hippo pathway. *Nature cell biology*, 17(4), pp. 500-510.
- Moberg, M., Apró, W., Ekblom, B., van Hall, G., Holmberg, H.-C. and Blomstrand, E. (2016) Activation of mTORC1 by leucine is potentiated by branched-chain amino acids and even more so by essential amino acids following resistance exercise. *American Journal of Physiology-Cell Physiology*, 310(11), pp. C874-C884.
- Nakada, N., Mikami, T., Hana, K., Ichinoe, M., Yanagisawa, N., Yoshida, T., Endou, H. and Okayasu, I. (2014) Unique and selective expression of L-amino acid transporter 1 in human tissue as well as being an aspect of oncofetal protein. *Histology and histopathology*, 29(2), pp. 217-227.
- Nicklin, P., Bergman, P., Zhang, B., Triantafellow, E., Wang, H., Nyfeler, B., Yang, H., Hild, M., Kung, C. and Wilson, C. (2009) Bidirectional transport of amino acids regulates mTOR and autophagy. *Cell*, 136(3), pp. 521-534.
- O'Rahilly, S. (2009) Human genetics illuminates the paths to metabolic disease. *Nature*, 462(7271), pp. 307.
- Pan, M. and Stevens, B. R. (1995) Differentiation- and protein kinase C-dependent regulation of alanine transport via system B. *Journal of Biological Chemistry*, 270(8), pp. 3582-3587.
- Park, S., Scheffler, T., Gunawan, A., Shi, H., Zeng, C., Hannon, K., Grant, A. and Gerrard, D. (2009) Chronic elevated calcium blocks AMPK-induced GLUT-4 expression in skeletal muscle. *American Journal of Physiology-Cell Physiology*, 296(1), pp. C106-C115.
- Park, S., Scheffler, T. L., Rossie, S. S. and Gerrard, D. E. (2013) AMPK activity is regulated by calcium-mediated protein phosphatase 2A activity. *Cell Calcium*, 53(3), pp. 217-223.
- Park, Y. Y., Sohn, B. H., Johnson, R. L., Kang, M. H., Kim, S. B., Shim, J. J., Mangala, L. S., Kim, J. H., Yoo, J. E. and Rodriguez - Aguayo, C. (2016) Yes - associated protein 1 and transcriptional coactivator with PDZ - binding motif activate the mammalian target of rapamycin complex 1 pathway by regulating amino acid transporters in hepatocellular carcinoma. *Hepatology*, 63(1), pp. 159-172.
- Pineda, M., Fernández, E., Torrents, D., Estévez, R., López, C., Camps, M., Lloberas, J., Zorzano, A. and Palacín, M. (1999) Identification of a membrane protein, LAT-2, that co-expresses with 4F2 heavy chain, an L-type amino acid transport activity with broad specificity for small and large zwitterionic amino acids. *Journal of Biological Chemistry*, 274(28), pp. 19738-19744.
- Polet, F., Martherus, R., Corbet, C., Pinto, A. and Feron, O. (2016) Inhibition of glucose metabolism prevents glycosylation of the glutamine transporter ASCT2 and promotes compensatory LAT1

- upregulation in leukemia cells. *Oncotarget*, 7(29), pp. 46371-46383.
- Poncet, N., Mitchell, F. E., Ibrahim, A. F., McGuire, V. A., English, G., Arthur, J. S., Shi, Y. B. and Taylor, P. M. (2014) The catalytic subunit of the system L1 amino acid transporter (slc7a5) facilitates nutrient signalling in mouse skeletal muscle. *PLoS one*, 9(2), pp. e89547.
- Prentki, M. and Nolan, C. J. (2006) Islet beta cell failure in type 2 diabetes. *J Clin Invest*, 116(7), pp. 1802-12.
- Proud, C. G. (2007) Amino acids and mTOR signalling in anabolic function. *Biochemical Society Transactions Volume 35*(part 5).
- Puertollano, R. (2014) mTOR and lysosome regulation. *F1000prime reports*, 6.
- Rachdi, L., Balcazar, N., Osorio-Duque, F., Elghazi, L., Weiss, A., Gould, A., Chang-Chen, K. J., Gambello, M. J. and Bernal-Mizrachi, E. (2008) Disruption of Tsc2 in pancreatic  $\beta$  cells induces  $\beta$  cell mass expansion and improved glucose tolerance in a TORC1-dependent manner. *Proceedings of the National Academy of Sciences*, 105(27), pp. 9250-9255.
- Ratnam, C., Chan, S., Laybutt, R. and Herbert, T. P. (2016) Investigating the role of the System-L amino acid transporter LAT1 in the development of pancreatic beta-cell dysfunction and type 2 diabetes. *Abstracts of Australian Diabetes Society and the Australian Diabetes Educators Association Annual Scientific Meeting*.
- Rebsamen, M., Pochini, L., Stasyk, T., de Araújo, M. E., Galluccio, M., Kandasamy, R. K., Snijder, B., Fauster, A., Rudashevskaya, E. L. and Bruckner, M. (2015) SLC38A9 is a component of the lysosomal amino acid sensing machinery that controls mTORC1. *Nature*, 519(7544), pp. 477-481.
- Reig, N., Chillarón, J., Bartoccioni, P., Fernández, E., Bendahan, A., Zorzano, A., Kanner, B., Palacín, M. and Bertran, J. (2002) The light subunit of system bo,+ is fully functional in the absence of the heavy subunit. *The EMBO journal*, 21(18), pp. 4906-4914.
- Rosario, F. J., Kanai, Y., Powell, T. L. and Jansson, T. (2013) Mammalian target of rapamycin signalling modulates amino acid uptake by regulating transporter cell surface abundance in primary human trophoblast cells. *J Physiol*, 591(3), pp. 609-25.
- Ruderman, N. B., Carling, D., Prentki, M. and Cacicedo, J. M. (2013) AMPK, insulin resistance, and the metabolic syndrome. *The Journal of clinical investigation*, 123(7), pp. 2764-2772.
- Rutter, G. A. (2001) Nutrient–secretion coupling in the pancreatic islet  $\beta$  -cell: recent advances. *Molecular aspects of medicine*, 22(6), pp. 247-284.
- Saito, S., Furuno, A., Sakurai, J., Park, H. R., Shin-ya, K. and Tomida, A. (2012) Compound C prevents the unfolded protein response during glucose deprivation through a mechanism independent of AMPK and BMP signaling. *PLoS one*, 7(9), pp. e45845.
- Samama, P., Rumennik, L. and Grippo, J. F. (2003) The melanocortin receptor MCR4 controls fat consumption. *Regulatory peptides*, 113(1), pp. 85-88.
- Schlienger, J.-L. (2013) Type 2 diabetes complications. *Presse medicale (Paris, France: 1983)*, 42(5), pp. 839-848.
- Sengupta, S. e. a. (2010 ) Regulation of the mTOR complex 1 pathway by nutrients, growth factors, and stress *Mol Cell*, 22;40(2), pp. 310-22.
- Sepp, M., Sokolova, N., Jugai, S., Mandel, M., Peterson, P. and Vendelin, M. (2014) Tight coupling of

- Na<sup>+</sup>/K<sup>+</sup>-ATPase with glycolysis demonstrated in permeabilized rat cardiomyocytes. *PLoS one*, 9(6), pp. e99413.
- Shah, O. J. e. a. (2004 ) Inappropriate activation of the TSC/Rheb/mTOR/S6K cassette induces IRS1/2 depletion, insulin resistance, and cell survival deficiencies. *Curr Biol*, 21:14(18), pp. 1650-6.
- Simon, P. (2003) Q-Gene: processing quantitative real-time RT-PCR data. *Bioinformatics*, 19(11), pp. 1439-40.
- Spaight, C., Gross, J., Horsch, A. and Puder, J. (2016) Gestational Diabetes Mellitus. in *Novelties in Diabetes*: Karger Publishers. pp. 163-178.
- Stretton, C., Hoffmann, T. M., Munson, M. J., Prescott, A., Taylor, P. M., Ganley, I. G. and Hundal, H. S. (2015) GSK3-mediated raptor phosphorylation supports amino-acid-dependent mTORC1-directed signalling. *Biochemical Journal*, 470(2), pp. 207-221.
- Strowski, M., Parmar, R., Blake, A. and Schaeffer, J. (2000) Somatostatin Inhibits Insulin and Glucagon Secretion via Two Receptor Subtypes: An in Vitro Study of Pancreatic Islets from Somatostatin Receptor 2 Knockout Mice 1. *Endocrinology*, 141(1), pp. 111-117.
- Stumvoll, M., Goldstein, B. J. and van Haefen, T. W. (2005) Type 2 diabetes: principles of pathogenesis and therapy. *The Lancet*, 365(9467), pp. 1333-1346.
- Talchai, C. e. a. (2012 ) Pancreatic  $\beta$  cell dedifferentiation as a mechanism of diabetic  $\beta$  cell failure. *Cell*, 14;150(6), pp. 1223-34. .
- Taylor, P. M. (2014) Role of amino acid transporters in amino acid sensing. *Am J Clin Nutr*, 99(1), pp. 223S-230S.
- Thompson, W. A. C. a. N. L. (2001) Overexpression of LAT1/CD98 Light Chain Is Sufficient to Increase System L-Amino Acid Transport Activity in Mouse Hepatocytes but Not Fibroblasts. *THE JOURNAL OF BIOLOGICAL CHEMISTRY*, Vol. 276, No. 20, ,(Issue of May 18), pp. 16877-16884.
- Thomson, D. M., Herway, S. T., Fillmore, N., Kim, H., Brown, J. D., Barrow, J. R. and Winder, W. W. (2008) AMP-activated protein kinase phosphorylates transcription factors of the CREB family. *J Appl Physiol* (1985), 104(2), pp. 429-38.
- Thorens, B. (2015) GLUT2, glucose sensing and glucose homeostasis. *Diabetologia*, 58(2), pp. 221-232.
- Turban, S., Stretton, C., Drouin, O., Green, C. J., Watson, M. L., Gray, A., Ross, F., Lantier, L., Viollet, B., Hardie, D. G., Marette, A. and Hundal, H. S. (2012) Defining the contribution of AMP-activated protein kinase (AMPK) and protein kinase C (PKC) in regulation of glucose uptake by metformin in skeletal muscle cells. *J Biol Chem*, 287(24), pp. 20088-99.
- Walker, D. K., Drummond, M. J., Dickinson, J. M., Borack, M. S., Jennings, K., Volpi, E. and Rasmussen, B. B. (2014) Insulin increases mRNA abundance of the amino acid transporter SLC7A5/LAT1 via an mTORC1-dependent mechanism in skeletal muscle cells. *Physiol Rep*, 2(3), pp. e00238.
- Wang, Q. and Holst, J. (2015) L-type amino acid transport and cancer: targeting the mTORC1 pathway to inhibit neoplasia. *American journal of cancer research*, 5(4), pp. 1281.
- Wang, S., Tsun, Z.-Y., Wolfson, R. L., Shen, K., Wyant, G. A., Plovanich, M. E., Yuan, E. D., Jones, T. D., Chantranupong, L. and Comb, W. (2015) Lysosomal amino acid transporter SLC38A9 signals arginine sufficiency to mTORC1. *Science*, 347(6218), pp. 188-194.
- Wang, X. and Proud, C. G. (2009) Nutrient control of TORC1, a cell-cycle regulator. *Trends Cell Biol*, 19(6),

pp. 260-7.

- Whiting, D. R., Guariguata, L., Weil, C. and Shaw, J. (2011) IDF diabetes atlas: global estimates of the prevalence of diabetes for 2011 and 2030. *Diabetes research and clinical practice*, 94(3), pp. 311-321.
- WHO (2016) Global report on diabetes.
- Widdows, K. L., Panitchob, N., Crocker, I. P., Please, C. P., Hanson, M. A., Sibley, C. P., Johnstone, E. D., Sengers, B. G., Lewis, R. M. and Glazier, J. D. (2015) Integration of computational modeling with membrane transport studies reveals new insights into amino acid exchange transport mechanisms. *Faseb J*, 29(6), pp. 2583-94.
- Wierup, N., Sundler, F. and Heller, R. (2014) The islet ghrelin cell. *Journal of molecular endocrinology*, 52(1), pp. R35-49.
- Williams, G. and Pickup, J. (1999) Handbook of diabetes 2nd. *Blackwell science*, 8, pp. 53-158.
- Xie, J. and Herbert, T. P. (2012) The role of mammalian target of rapamycin (mTOR) in the regulation of pancreatic beta-cell mass: implications in the development of type-2 diabetes. *Cell Mol Life Sci*, 69(8), pp. 1289-304.
- Yada, T., Damdindorj, B., Rita, R., Kurashina, T., Ando, A., Taguchi, M., Koizumi, M., Sone, H., Nakata, M. and Kakei, M. (2014) Ghrelin signalling in  $\beta$  - cells regulates insulin secretion and blood glucose. *Diabetes, Obesity and Metabolism*, 16(S1), pp. 111-117.
- Yang, J., Chi, Y., Burkhardt, B. R., Guan, Y. and Wolf, B. A. (2010) Leucine metabolism in regulation of insulin secretion from pancreatic beta cells. *Nutr Rev*, 68(5), pp. 270-9.
- Yang, J., Wong, R. K., Park, M., Wu, J., Cook, J. R., York, D. A., Deng, S., Markmann, J., Najj, A. and Wolf, B. A. (2006) Leucine regulation of glucokinase and ATP synthase sensitizes glucose-induced insulin secretion in pancreatic  $\beta$  -cells. *Diabetes*, 55(1), pp. 193-201.
- Yao, K., Duan, Y., Tan, B., Hou, Y., Wu, G. and Yin, Y. (2016) Leucine in Obesity: Therapeutic Prospects. *Trends in pharmacological sciences*.
- Yoon, M.-S., Son, K., Arauz, E., Han, J. M., Kim, S. and Chen, J. (2016) Leucyl-tRNA synthetase activates Vps34 in amino acid-sensing mTORC1 signaling. *Cell reports*, 16(6), pp. 1510-1517.
- Yuan, T., Rafizadeh, S., Gorrepati, K. D. D., Lupse, B., Oberholzer, J., Maedler, K. and Ardestani, A. (2016) Reciprocal regulation of mTOR complexes in pancreatic islets from humans with type 2 diabetes. *Diabetologia*, pp. 1-11.
- Yudkoff, M., Daikhin, Y., Nissim, I., Horyn, O., Luhovyy, B., Lazarow, A. and Nissim, I. (2005) Brain amino acid requirements and toxicity: the example of leucine. *J Nutr*, 135(6 Suppl), pp. 1531S-8S.
- Zadra, G., Batista, J. L. and Loda, M. (2015) Dissecting the Dual Role of AMPK in Cancer: From Experimental to Human Studies. *Mol Cancer Res*, 13(7), pp. 1059-72.
- Zhang, C.-S., Li, M. and Lin, S.-C. (2017) Chapter Twenty-Seven-Methods to Study Lysosomal AMPK Activation. *Methods in Enzymology*, 587, pp. 465-480.
- Zhang, S., Zeng, X., Ren, M., Mao, X. and Qiao, S. (2017) Novel metabolic and physiological functions of branched chain amino acids: a review. *Journal of Animal Science and Biotechnology*, 8(1), pp. 10.
- Zhang, X., Tang, N., Hadden, T. J. and Rishi, A. K. (2011) Akt, FoxO and regulation of apoptosis. *Biochimica*

*et Biophysica Acta (BBA)-Molecular Cell Research*, 1813(11), pp. 1978-1986.

- Zheng, D., MacLean, P. S., Pohnert, S. C., Knight, J. B., Olson, A. L., Winder, W. W. and Dohm, G. L. (2001) Regulation of muscle GLUT-4 transcription by AMP-activated protein kinase. *Journal of Applied Physiology*, 91(3), pp. 1073-1083.
- Zheng, L., Zhang, W., Zhou, Y., Li, F., Wei, H. and Peng, J. (2016) Recent Advances in Understanding Amino Acid Sensing Mechanisms that Regulate mTORC1. *International Journal of Molecular Sciences*, 17(10), pp. 1636.
- Zhou, H. a. H., S. (2011 ) Role of mTOR signaling in tumor cell motility, invasion and metastasis. *Curr Protein Pept Sci*, 2(1), pp. 30-42.
- Zoncu, R., Efeyan, A. and Sabatini, D. M. (2011) mTOR: from growth signal integration to cancer, diabetes and ageing. *Nat Rev Mol Cell Biol*, 12(1), pp. 21-35.

**Appendix 1. DNA sequencing confirmation of the LAT1-eGFP cDNA construct**

NNNNNNNNNNNNNNNNNNCGCCNNTGCTCNCNTGGTGGNNNNNNNGTGGATCCCGGGCCCGCGG  
TACCGTCGACTGCATGAATTCTGTCTCCTGGGGGACCACCTGCATGAGCTTCTGACACAGGACGGTCGTG  
GAGAAGATGCCCTGGAGGAGCCACTTGGGCTTGTTTTTCCACCAGACCCCGAAGAAGTAGACGGGCAG  
CCCGCTGAGGATGATGGTGAAGCCGATGCCACACTCCACGGGTGTCTTCCAGAAGGAGACGGCGATCA  
GGAAGAGGCAGGCCAGGATGAAGAACACAGGCAGGGCCAGGTTACCTTGATGGGCCGCTCAAGCTC  
AGGCTTTCTGTGGCGCAGCCAGATCATGCCGATGATGGCCAGGGCCACGCAGAGCCAGTTGAAGAAGC  
TGAAGAAGTTGATGACGGAGAAGATGTCCTTGGAGAAGGCGTAGAGCAGCGTCATCACACACGTGAAC  
ACGAGGGACGGCACGGGGGTGAGGAGCTGTGGGTGGATCATGGAGAGGATGGAGGGCAGGTGGCCT  
TCCCGGGACCCACGAAGAAGAGCCTGGAGGATGTGAACAGGGACCCATTGACGGAGCCGAAGCAGG  
ACAGGCCACGAAGACGGGGATGATCCAGGACATGACGCCAGGTGATAGTTCCCGAAGTCCACGGCC  
ACGGCCTCGGACGACAGCATCTGCTCGGTGGACAGGGTGGTGAAGTAGGCCAGGTTGGTCAGCACGTA  
CACCAGCGTCACGATGGGCAGGGAGATGATGATGGCCAGGGGCAGGTTTCTGTANGGGTTGATCATTTC  
CTCTGTGACGAAATCAAGTAATCCATCCTCCATANGCAAAGAGGCCGCTGTATAATGCCAGCACAATGT  
TCCCCACATCCAGTTTGGTGCCTTCAAATGANAAGTTGGGATCTANATTGGACACNACACCCTTCCCGAT  
CTGGNCGAAGCCCAGCANNNTGATCNNNNNNNGGGCCAGGAGCTTGGNGGCGGCAAANNATCCNGGN  
CCNGGNNGGCGGNCNTTACGCTGNANCANTTACGGCNGTGNNCAGCANCACNNNNANNNNGNC  
CACNANCNNNNNCCTCCNNNNGGNNNNNNNGNGNNNNANNNNNNNNNANNNNGNNNGNN  
NNNNANNNNNNNNNANNTACNNNNNANNCNGNNNANGNNNNNNANNNNNNNNNNNNGN  
NNNNNNNNNNNNNNCCNNCNNNNNNNNNNNGNNNNNN

## Appendix 2. DMEM preparation without L-leucine, L-glutamine and D-glucose

COMPONENT	g/L	
<b>Inorganic salts</b>		
CaCl <sub>2</sub>	0.2	
Fe(NO <sub>3</sub> ) <sub>3</sub> • 9H <sub>2</sub> O	0.0001	
MgSO <sub>4</sub>	0.09767	
KCl	0.4	Dissolved in H <sub>2</sub> O
NaHCO <sub>3</sub>	3.7	
NaCl	6.4	
NaH <sub>2</sub> PO <sub>4</sub>	0.109	
<b>Amino acids</b>		
L-histidine • HCL • H <sub>2</sub> O	0.042	
L-methionine	0.03	Dissolved in 1M HCl
L-tryptophan	0.016	
L-tyrosine • 2Na • 2H <sub>2</sub> O	0.10379	
L-isoleucine	0.105	Disolved in H <sub>2</sub> O
L-phenilalanine	0.066	
L-arginine • HCl	0.084	
L-cysteine • 2HCl	0.0626	
Glycine	0.03	
L-Lysine • HCl	0.146	Dissolved in H <sub>2</sub> O
L-serine	0.042	
L-threonine	0.095	
L-valine	0.094	
<b>Vitamins</b>		
100x MEM vitamins (Ref M6895 Sigma)	10ml per L	
<b>Others</b>		
Penicillin-Streptomycin (10,000 U/mL) (Ref 15140122 Gibco)	10ml per L	
Phenol red	0.0159 g/L	

### Appendix 3. Lysis buffer for preparation of cell lysates for Western blotting

Final concentration	Reagent
1 %	Triton X – 100
50 mM	NaF or Na Fluoride
50 mM	Tris-HCl pH 7.5
1 mM	Na <sub>3</sub> VO <sub>4</sub> or Na Orthovanadate
10 mM	$\beta$ -glycerophosphate
1 mM	EGTA
1 mM	EDTA pH 8
0.2 mM	PMSF
1 mM	Benzamidine
1 $\mu$ g/ml	Pepstatin
1 $\mu$ g/ml	Leupeptin
0.1%	$\beta$ -mercaptoethanol